Liquid Chromatography coupled to Isotope Ratio Mass Spectrometry of Selected Polar Compounds

Dissertation

zur Erlangung des akademischen Grades eines
Doktors der Naturwissenschaften
– Dr. rer. nat. –

vorgelegt von

Dorothea Marzena Kujawinski

geboren in Karlshorst (Polen)

Instrumentelle Analytische Chemie
der
Universität Duisburg-Essen

2014

Die vorliegende Arbeit wurde im Zeitraum von März 2009 bis Juni 2014 im Arbeitskreis von Prof. Dr. Torsten Schmidt am Institut für Instrumentelle Analytische Chemie der Universität Duisburg-Essen durchgeführt.

Tag der Disputation: 12.11.2014

Gutachter:	Prof. Dr. Torsten C. Schmidt
	Prof. Dr. Oliver J. Schmitz
Vorsitzender:	Prof. Dr. Mathias Ulbricht

Summary

The analysis of light stable isotopes of organic compounds is nowadays a common tool in almost all fields of science. Geochemistry, archeology, product authenticity and ecology are only a few examples of the applicability of isotope ratio mass spectrometry. In this context it can answer questions regarding the botanical or synthetical origin of a sample constituent or help to reveal reaction mechanisms.

However, due to several instrumental challenges there is still a need for analytical methods to determine compound-specific isotope ratios of thermolabile and non-volatile substances. Hence, many compound classes have not yet been studied using isotope ratio techniques.

Thus, the work presented herewith focuses on the development of liquid chromatographic methods which can be used in combination with isotope ratio mass spectrometry. As analytes several sulfonamide drugs, trimethoprim and the herbicide glyphosate along with its metabolite aminomethylphosphonic acid were chosen. The developed methods were used to study environmentally relevant degradation mechanisms of these compounds.

In the first part of the work, a high temperature liquid chromatography method was developed for the analysis of sulfadiazine, sulfathiazole, sulfametazine, sulfamethoxazole and trimethoprim. By the application of a high temperature gradient to a pure aqueous eluent for separation, all these compounds were fully resolved from each other on an octadecyl stationary phase. The lowest amounts necessary for a precise carbon isotopic analysis varied between 0.3 to 0.5 µg on column depending on the investigated substance. A repeatable offset of isotope ratios of 1.6 to 3.6 ‰ on the δ-scale has been observed and a careful investigation revealed an incomplete conversion of the analytes to the measured gas CO_2 causing this offset. Additionally, it could be shown that the observed offsets could be corrected to obtain unbiased isotopic signatures.

The applicability of the method was shown by the analysis of pharmaceutical products containing trimethoprim and sulfamethoxazole and direct photolysis of sulfamethoxazole. It was shown that the isotopic fractionation of this important degradation process is very low, slightly above the overall analytical precision, and is probably based on a secondary inverse isotope effect.

The other compounds studied in this work were glyphosate, one of the most widely used herbicides world-wide and its metabolite aminomethylphosphonic acid. For the analysis of these compounds ion exchange and reversed phase chromatography on a porous graphitic carbon column were investigated. The latter separation mode yielded the best separation of glyphosate and aminomethylphosphonic acid. Fractionation factors for the chromatographic separation could be calculated and it was shown that a carbon isotope effect associated with anion exchange is not detectable, while in contrast a carbon isotope substitution produces a very small but observable secondary isotope effect in the cation exchange of an amine group. Since these fractionation factors are very small, it can be concluded, that adsorption of glyphosate to soil resulting from van der Waals interactions and ion exchange will not change its carbon isotope ratio significantly.

One of the developed methods, a reversed-phase chromatography on porous graphitic carbon, was used to study the isotopic fractionation of the degradation of glyphosate by manganese

dioxide. The observed fractionation factor of about -3.5 ‰ was too big to originate from adsorption to the mineral surface. It was concluded that two reaction pathways lead to the cleavage of glyphosate and the observed isotope effect is a sum of both. A comparison with the calculated maximum isotope effect (Streitwieser limit) showed that other factors than zero point energy differences, such as differences in symmetry and mass moments of inertia, govern the isotopic fractionation of this reaction. Since there was no change in $\delta^{13}C$ values of AMPA, it was concluded that the origin of this unspecific degradation product in the environment may be traced in future.

Therefore, the last chapter of this work aimed to develop a method to determine position specific carbon isotope ratios of glyphosate, as this is a requisite in tracing the origin of AMPA. Besides, such a method might be useful for product authenticity control of glyphosate herbicide formulations. Two approaches, nuclear magnetic spectroscopy and an enzymatic cleavage followed by liquid chromatography isotope ratio mass spectrometry of the fragments, were chosen. However, it was not possible to determine accurate and precise carbon isotope ratios mainly due to non-linear response in nuclear magnetic resonance spectroscopy and unfavorable reaction conditions for the enzymatic cleavage.

The chromatographic methods developed in this work enabled new insights on reaction pathways of glyphosate and sulfamethoxazole and will certainly be used in further investigations on these substances. But there is still work necessary to extend the application field of LC-IRMS to other important compounds and elements.

Zusammenfassung

Heutzutage ist die Analyse von Stabilisotopenverhältnissen organischer Stoffe in fast allen Forschungsgebieten vertreten. Einige Beispiele dafür sind Geochemie, Archäologie, Ökologie sowie die Produktauthentifizierung.

Durch die Isotopenverhältnismassenspektrometrie können wirtschaftlich bedeutende Fragen der botanischen oder synthetischen Herkunft eines Produktes beantwortet werden. Zudem ist es unter anderem möglich, Reaktionsmechanismen zu identifizieren. Aufgrund instrumenteller Anforderungen gibt es trotz der vielseitigen Anwendungsmöglichkeiten nur wenige flüssigchromatographische Methoden, um komponentenspezifische Isotopenverhältnisse von nichtflüchtigen und thermolabilen Stoffen zu bestimmen.

Das Ziel der vorliegenden Arbeit war, flüssigchromatographische Methoden für Sulfonamid- und Trimethoprimantibiotika sowie für das Herbizid Glyphosat und seinen Hauptmetaboliten Aminomethylphosphonsäure zu entwickeln. Diese Methoden sollten eine komponentenspezifische Kohlenstoffisotopenanalyse ermöglichen, mit der ausgewählte umweltrelevante Abbauprozesse dieser Verbindungen untersucht wurden.

Die ersten zwei Kapitel befassen sich mit den Sulfonamidantibiotika Sulfadiazin, Sulfathiazol, Sulfametazine, Sulfamethoxazol und dem wirkungsverwandten Trimethoprim.

Zuerst wurde eine Hochtemperaturflüssigchromatographie dieser Stoffe entwickelt, mit der alle Analyten vollständig auf einer Oktadekyl-Säule mit Hilfe eines rein wässrigen Eluenten getrennt werden können. Die kleinste Menge, die zur präzisen Messung benötigt wird, betrug je nach Substanz 0,3 bis 0,5 µg absolut. Ein beobachteter Offset der Kohlenstoffisotopenverhältnisse war substanzabhängig und lag zwischen 1,6 bis 3,4 ‰ auf der δ-Skala. Es konnte gezeigt werden, dass dieser Offset von einer unvollständigen Oxidation der Stoffe herrührte. Zudem war eine Korrektur der beobachteten Offsets möglich, sodass biasfreie Isotopenverhältnisse erhalten werden konnten.

Die Anwendbarkeit der Methode wurde durch die Analyse von pharmazeutischen Kombinationspräparaten bestehend aus Sulfamethoxazol und Trimethoprim und der direkten Photolyse von Sulfamethoxazol unter UV-Einstrahlung in wässriger Lösung gezeigt. Der Isotopeneffekt dieser Reaktion war sekundär, invers und relativ klein.

Das folgende Kapitel beinhaltet die chromatographische Methodenentwicklung für das Herbizid Glyphosat und seinen Metaboliten Aminomethylphosphonsäure. Drei verschiedene Trenntechniken, Umkehrphasenchromatographie, Kationen- und Anionenaustausch-chromatographie, wurden auf ihre Anwendbarkeit in der Kohlenstoffisotopenanalyse verglichen. Dabei zeigte sich, dass die Umkehrphasenchromatographie auf einer stationären Phase aus porösen Graphitpartikeln eine bessere Trennung von Glyphosat und Aminomethylphosphonsäure erreicht als Ionenaustauschmethoden. Aus den chromatographischen Daten der Methodenentwicklung konnten Fraktionierungsfaktoren für Glyphosat und Aminomethylphosphonsäure berechnet werden. Es hat sich gezeigt, dass kein Kohlenstoffisotopeneffekt bei Anionenaustausch, jedoch ein sekundärer Kohlenstoffisotopeneffekt bei Kationenaustausch einer Aminogruppe messbar ist. Aus der Größe der Fraktionierungsfaktoren kann geschlossen werden, dass die Sorption dieser Stoffe

im Boden resultierend aus Ionenaustausch oder van-der-Waals-Wechselwirkungen die Kohlenstoffisotopenverhältnisse nicht signifikant ändert.

Mithilfe der entwickelten Trennmethode wurde im folgenden Kapitel der abiotische Abbau von Glyphosat durch Mangandioxid auf einen messbaren Isotopeneffekt hin untersucht. Diese Reaktion zeigte eine Fraktionierung, die auf eine Mischung der Kohlenstoffisotopeneffekte zweier Reaktionswege zurückgeführt wurde. Neben dem erwarteten Produkt Sarkosin, wurde auch Aminomethylphosphonsäure detektiert. Ein Vergleich mit berechneten Isotopeneffekten (Streitwieser Grenzen) zeigte, dass andere Faktoren als Nullpunktsenergiedifferenzen, wie Unterschiede in der Symmetrie oder Trägheitsmomenten die Größe des Isotopeneffektes bestimmen. Zudem zeigte die Untersuchung der Kohlenstoffisotopenverhältnisse der Reaktionsprodukte, dass dieser Abbauweg von Glyphosat keinen Einfluss auf die $\delta^{13}C$-Werte von Aminomethylphosphonsäure hat. Dadurch könnte in Zukunft das Auftreten von Aminomethylphosphonsäure in Umweltproben auf Glyphosat-Abbau zurückführbar sein, da dieser Stoff auch aus dem Abbau anderer Phosphonate entstehen kann. Eine Voraussetzung dafür ist jedoch, dass auch positionsspezifische $\delta^{13}C$-Werte von Glyphosate bestimmt werden können.

Daher war das Ziel des letzten Kapitels dieser Arbeit, eine Methode zur Bestimmung von Kohlenstoffisotopenverhältnisse von Glyphosat an der P-C Position zu erarbeiten. Dafür wurden die magnetische Kernresonanzspektroskopie der ^{13}C-Satellitenlinien und eine mangankatalysierte Enzymreaktion gefolgt von der Flüssigchromatographie-Isotopenverhältnismassenspektrometrie der erhaltenen Fragmente ausgesucht. Aufgrund fehlender Linearität des Detektors der magnetische Kernresonanzspektroskopie und ungünstigen Reaktionsbedingungen lieferten jedoch beide Methoden keine verwertbaren Ergebnisse.

Durch die chromatographischen Methoden, die während dieser Arbeit entwickelt wurden, konnten neue Erkenntnisse zu Abbauwegen von Sulfamethoxazol und Glyphosate gewonnen werden. Diese Methoden werden sicherlich auch in kommenden Arbeiten zum chemischen Verhalten dieser Stoffe zum Einsatz kommen.

Table of Content

List of Figures

List of tables

1 Introduction

1.1 Overview of Stable Isotope Ratio Analysis

Isotopes are nuclides of an element having the same proton number but different atomic weights. Hence, they only differ in their neutron number. With a few exceptions (e.g., F, P, Mn) all elements have isotopes, either stable or radioactive. All isotopes of an element undergo the same chemical reactions, but radioactive isotopes will decay with a certain half-life time. Stable isotopes are defined as isotopes with such long decay times that they cannot be measured.[1]

Molecules, which have the same quantity of isotopic atoms but at different position, are called isotopomers. Often, the term "isotopic substitution" is used as well. Isotopologues are molecules which have a different number of isotopic atoms.[2]

In nature, kinetic, thermodynamic and magnetic isotope effects govern the observable variations of isotope effects (see **Chapter 1.2**). Hence, the origin of a sample can sometimes be deduced from its isotope ratios. **Figure 1.1** shows the variation of carbon isotope ratios of some natural substances. The most prominent example of an isotopic fractionation is the mass discrimination during photosynthesis. Plants which fix carbon from CO_2 by the C_3-type photosynthesis show a different carbon isotope ratio than plants performing a C_4-type photosynthesis. Thus, stable isotope ratio analysis (SIRA) can detect adulteration of products which are genuinely produced by C_4 plants by the use of C_3 plant material or vice versa. This method is common practice to detect wine and honey adulteration[3-4] and authenticity of other food products[5].

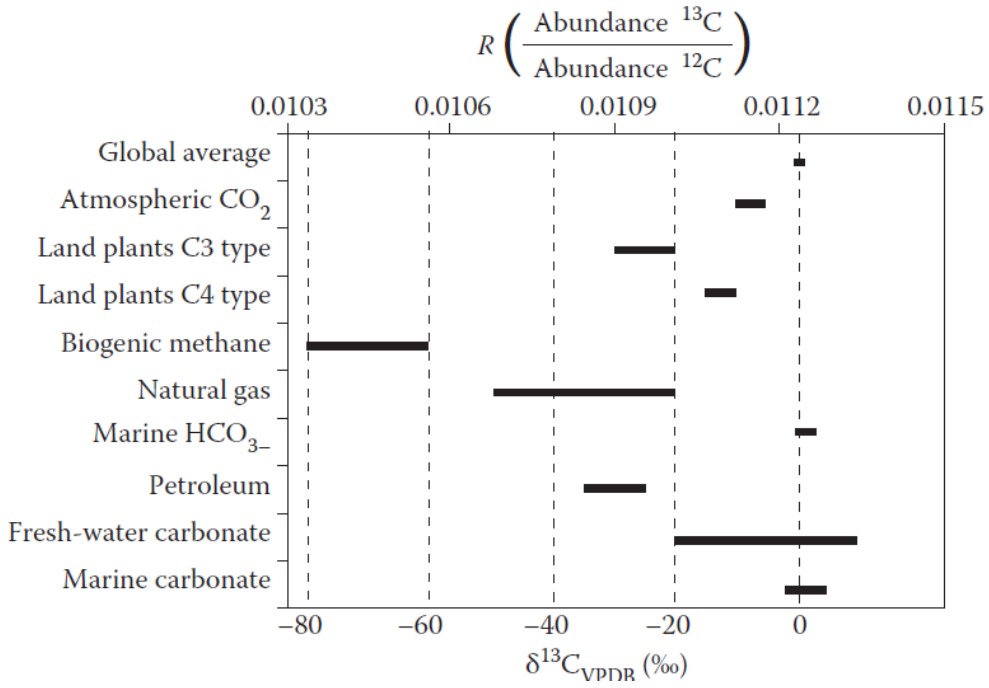

Figure 1.1 Carbon isotope ratio in various carbonaceous substances in nature. The top axis shows the $^{13}C/^{12}C$ ratio and the bottom axis carbon isotope ratios in the δ-scale (see **Chapter 1.2**) (source Aelion et al.[6])

The isotopic fingerprint of a substance can also be used to check the authenticity of a pharmaceutical product due to differences in synthesis or raw materials used. Especially in the pharmaceutical industry counterfeit products can be detected[7-8] and also illicit drugs can be traced[9].

Another example for SIRA application is the monitoring of pollutant remediation in groundwater.[10] Isotopologues will undergo the same chemical reactions, but they can differ in their reaction rate. Generally, the molecule with the light isotope will react faster than the molecule with the heavy isotope (normal isotope effect). When the decrease in concentration of the pollutant is accompanied by a change in isotope ratio, it can be concluded that it is being degraded[10-11]. In some cases it is even possible to assume degradation although a concentration decrease cannot be detected.[12] That makes SIRA a popular tool for attenuation studies at pollution sites with unclear hydrological conditions.

1.2 δ-Scale and Referencing

The determination of absolute amounts of isotopes in a sample is difficult and requires sophisticated instrumentation. Ratios of isotopes are easier to measure, but the obtained numbers are often so small that they are hard to handle. For this reason and in order to easily compare results between laboratories, the δ-notation has been introduced.[1]

All isotope ratios are reported as differences of the isotope ratio of the sample and isotope ratio of the international reference substance by the following equation:

$$\delta\ {}^{i}E = \frac{{}^{i}R_s - {}^{i}R_{ref}}{{}^{i}R_{ref}}$$

Here, ${}^{i}R_{ref}$ denotes the ratio of the heavy and light isotope in the reference material and ${}^{i}R_s$ is the same for the sample. Usually δ-values are given in per mill. **Table 1.1** gives an overview of the reference materials in use for different stable isotopes.

Table 1.1 Current international reference materials which define δ scales. Values adapted from Jochmann and Schmidt.[1]

Scale	Reference material	δ –value $\times 10^3$	Accepted isotope ratio	Type of material
$\delta\ {}^{13}C_{VPDB\text{-}LSVEC}$	NBS-19	+1.95	n.d.	Calcite
	LSVEC	-46.6	n.d.	Li_2CO_3
$\delta\ {}^{2}H_{VSMOW\text{-}SLAP}$	VSMOW	0	1.5575×10^{-4}	Water
	SLAP	-428	0.8912×10^{-4}	Water
$\delta\ {}^{15}N_{AIR\text{-}N2}$	AIR-N2	0	3.677×10^{-2}	Atmospheric N_2
$\delta\ {}^{18}O_{VSMOW\text{-}SLAP}$	VSMOW	0	2.0052×10^{-3}	Water
	SLAP	-55.5	n.d.	Water
$\delta\ {}^{34}S_{VCDT}$	VCDT	0	4.5005×10^{-2}	Ag_2S

All δ-scales have at least one anchor point. These anchor points are the primary reference materials, which define the scale. In case of carbon, this material originally was Pee Dee Belemnite (PDB), a belemnite guard from the Pee Dee formation in South Carolina, USA. After it got exhausted, NBS-19 was selected as a new anchor point at $+1.95 \times 10^{-3}$ determined by a number of laboratories. The absolute abundance ratio of PDB was calculated by Craig et al. a value of $^{13}C/^{12}C = 0.011237$[13], but about 30 years later Zhang and Li determined this value to be 0.0111802, which is the accepted value nowadays.[14] PDB is already exhausted and was replaced by the calcium carbonate NBS-19 and there up on, the scale was re-named to Vienna Pee Dee Belemnite (VPDB). Due to the growing interest in isotope ratios of biological samples, the need for a second anchor point arose. Different to most inorganic carbon compounds, these samples have $\delta^{13}C$ values far below 0. In order to increase the accuracy of very low $\delta^{13}C$ values, L-SVEC, a Li_2CO_3 prepared by Svec et al., was chosen as a second anchor point at a $\delta^{13}C$ value of -46.6×10^{-3}.[15]

Besides primary reference materials, certified reference materials can be purchased which are referenced against primary reference materials if available. They are distributed by the National Institute of Standards (NIST, USA), the International Atomic Energy Agency (IAEA, Austria) or the Institute for Reference Measurements and Materials (IRMM, Belgium).

1.3 Origin of isotopic fractionations

Isotopic substitution influences many properties of a molecule. Differences in mass moments of inertia (MMI), symmetry of the molecule and different populations of excited states contribute to the observable isotope effect. However, the most important factor influencing the magnitude of an isotope effect is a difference in zero point energy (ZPE) between the isotopic substituted and the non-substituted species.

The bond energy between two atoms can be described by the Morse potential (see **Figure 1.2**). The ZPE is lower for a heavy isotope substituted bond, which makes the bond stronger than the light isotope substituted. The energy potential in the range of the ZPE can be sufficiently described by a harmonic oscillator model. It gives the zero point energy E_0 and the corresponding vibrational frequency $\tilde{\nu}$ as:

$$\tilde{\nu} = \frac{1}{2\pi}\sqrt{\frac{k}{\mu}} \qquad \text{and} \qquad E_0 = \frac{1}{2} h\, \tilde{\nu}$$

As the force constant k is not affected by an isotopic substitution, the difference of the ZPE depends on the reduced mass μ. Thus, the higher the relative mass difference between the isotopes is, the bigger is the isotope effect. Therefore, hydrogen shows the largest isotope effects due to the biggest relative mass difference.[1]

Kinetic and thermodynamic or equilibrium isotope effects are mainly the result of ZPE differences. Kinetic isotope effects (KIE) can be approximated from spectroscopic data by the following equation:

$$KIE = \exp\left[\frac{h\,c\,\tilde{\nu}}{2\,k\,T}\left(1 - \sqrt{\frac{\mu_l}{\mu_h}}\right)\right]$$

After a calculation of force constant k from infrared absorption spectra it is possible to assess the KIE based on ZPE differences. This equation neglects other contributions such as tunneling effects and only accounts for the vibration energy of the stretching vibration. A precise calculation of KIE of a molecule of more than five atoms can only be performed by specialized software calculating force constants for reactants and transition state from the energy surface of the reaction coordinate. For heavier elements than hydrogen, other terms like the MMI can be bigger than ZPE and thus, lead to erroneous results.[16]

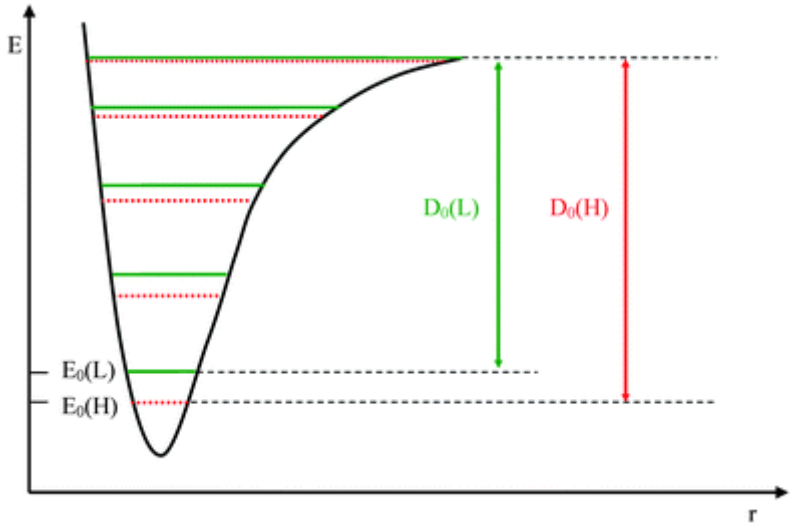

Figure 1.2 Energy as a function of interatomic distance between two atoms according to the Morse potential. The horizontal lines are the possible energy level of the light isotope substituted bond (green) and the heavy isotope substituted bond (red). D_0 correspond to the respective dissociation energies (source Vanhaecke et al.[17])

Mass dependent isotope effects are generally divided into kinetic and thermodynamic isotope effects. Thermodynamic isotope effects can be observed when ZPE differences influence equilibrium constants. The isotopic fractionation factor α is defined as the ratio of isotope ratios in product phase R_{Pr} and reactant phase R_{Reac}:

$$\alpha_{Pr\text{-}Reac} = \frac{R_{Pr}}{R_{Reac}} = \frac{1000 + \delta\ {}^{i}E_{Pr}}{1000 + \delta\ {}^{i}E_{Reac}}$$

If the observed reaction is not at equilibrium, a kinetic isotope effect can be measurable. KIE usually occur due to different reaction rates resulting from different bond strengths and different translational velocities according to the classical kinetic theory. The KIE is defined as:

$$KIE = \frac{{}^{l}k}{{}^{h}k}$$

With ^{h}k as the rate constant of the heavy substituted molecule and ^{l}k the rate constant of the light isotope molecule. Assuming the product does not react with the reactant and the reaction is irreversible a Rayleigh equation is used to quantify the change in isotope ratio in the course of the reaction:

$$\left(\frac{c_t}{c_0}\right)^{\varepsilon} = \frac{1 + \delta\ {}^{i}E_t}{1 + \delta\ {}^{i}E_o}$$

ε is the isotopic enrichment factor, c_0 and δ_0 are the concentration and the δ-value of the reactant at the beginning of the reaction. The concentration and the δ-value of the reactant at a certain time are denoted by the subscript t.

In order to determine ε the following linearized version of the Rayleigh equation is used:

$$\varepsilon \times \ln\frac{c_t}{c_0} = \ln\ \frac{1 + \delta\ {}^{i}E_t}{1 + \delta\ {}^{i}E_o}$$

In **Figure 1.3** the change in $\delta^{13}C$ with the remaining fraction of the reactant c_t/c_0 of a hypothetical reaction with an isotope enrichment factor ε of 10×10^{-3} and an initial $\delta^{13}C$ value of -30×10^{-3}. The instantaneously formed product always has a $\delta^{13}C$ value more negative than the reactant, which has reacted at this time. By the measurement of reactant and product one could alternatively determine ε, but it is practically impossible to measure the instantaneously formed product. Rather, a mixture of instantaneously formed products, i.e. accumulated product, can be measured. The $\delta^{13}C$ value of the accumulated product δ_{AP} can be calculated in the following way:

$$\delta\ {}^{i}E_{AP} = \delta\ {}^{i}E_o - \varepsilon \times \frac{f + \ln f}{1 - f}$$

with f as the remaining fraction c_t/c_0 of the reactant.

These equations can also be applied to reactions which are reversible, but only if the product is removed from the system.

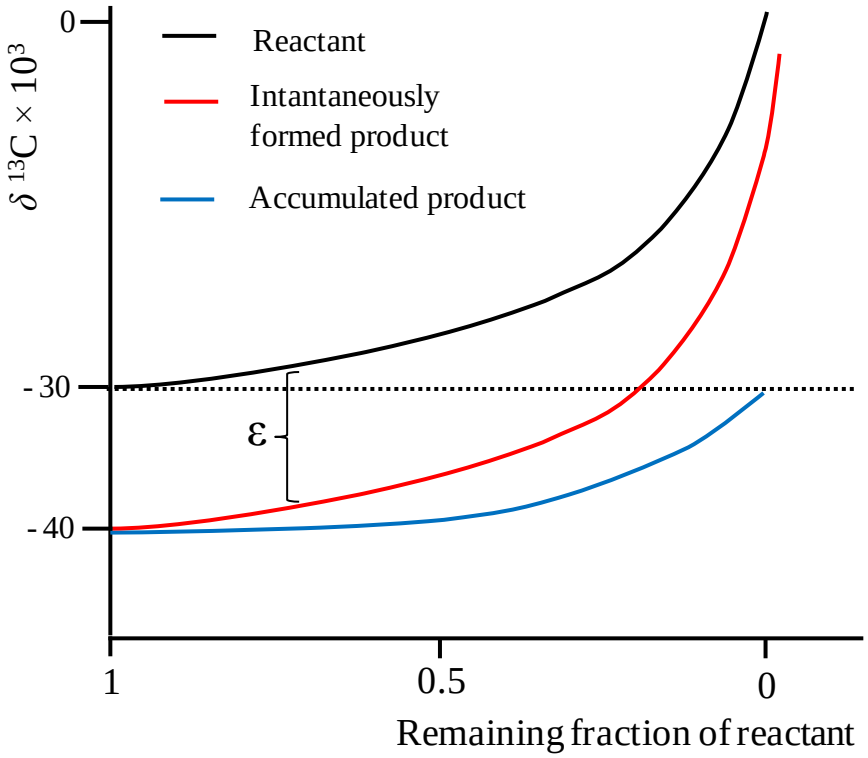

Figure 1.3 Change in δ^{13}C value with remaining fraction of the reactant of a hypothetical reaction associated with a normal isotope effect.

As example, the condensation or evaporation of water is described with these equations as well, although it basically is a reversible process. Thus, δ^{18}O and δ^{2}H values of precipitated water depend on latitude. The so-called "*global meteoric water line*", a dependency of δ^{18}O on $\delta\,^{2}$H values, can be established and thus the geographical origin of water identified.[18]

KIE can be calculated from enrichment factors ε from the following equation deriving from first order rate laws for the reactions of the two isotopologues:[11]

$$KIE = \frac{^{l}k}{^{h}k} = \frac{1}{\varepsilon + 1}$$

In most cases, it is not possible to directly measure the shift of a δ^{13}C value at the reactive position. Hence, ε is "diluted" by atoms which do not participate in the reaction and their isotope ratio does not change. Therefore, the measured ε is corrected by a factor n/x to yield the apparent kinetic isotope effect (AKIE)[11]:

$$\mathrm{AKIE} = \frac{1}{\frac{n}{x}\,\varepsilon + 1}$$

where n denotes the number of atoms of the monitored elements at the reactive positions and x the total number of these atoms.

If the fractionation factor α or KIE is higher than 1 or ε is negative, a normal isotope effect is observed, i.e. more molecules with the lighter isotope accumulate in the product phase. Inverse isotope effects are observed if more molecules with the heavier isotope are present in the product phase than in the reactant.

1.4 Instrumentation for isotope ratio analysis

In isotope ratio analysis one can distinguish bulk methods (bulk stable isotope analysis, BSIA) from compound-specific methods (compound-specific stable isotope analysis, CSIA). In CSIA, only compounds of interest are converted to the measured gas, which usually requires a hyphenated chromatographic system prior to isotopic analysis.

The determination of the isotope ratio of the whole sample, without separation of analytes, is called BSIA. It can be performed by an offline conversion of the sample to the measured gas or by online combustion in a hyphenated elemental analyzer (EA). The latter is a very popular method, since it yields a high precision and accuracy, is amendable for all light elements and has short analysis times along with high sample throughput.

Although the existence of isotopes was proven in the beginning of the 20th century, it was the invention of the sector field mass spectrometer equipped with a Faraday cup detector by Alfred Nier in 1947 which fostered the application of isotope ratios in various scientific fields.[1] Nier's sector field mass spectrometer was the first mass detection system which achieved the required precision to reveal small variations of stable isotope ratios in nature. The first works published in this area dealt with the carbon and oxygen isotope variation of CO_2 in the geochemical context. At that time, mostly gas samples or carbonates were analyzed.

In 1978, a hyphenation of gas chromatography (GC) with isotope ratio mass spectrometry (IRMS) has been published but it was the combustion interface described by Merrit and Hayes, which was commercialized in 1988, which served as a prototype for commercial GC-IRMS systems.[19]

During the 1980s elemental analyzers where coupled to isotope ratio mass spectrometers by a continuous flow inlet system. Up to then, dual inlet like inlet systems have been used and samples had to be laboriously prepared to obtain a sample gas. This new inlet system opened the way to couple GC with IRMS and to analyze compound-specific isotope ratios.

More recently, efforts were made to couple liquid chromatography (LC) to IRMS. A few types of interfaces of different working principles have been developed. The main difficulty was to obtain a gas from non-volatile analytes in an aqueous mixture. In 2003, Gille St-Jean published the coupling of a total organic carbon (TOC) analyzer with IRMS, which mixed the aqueous sample with a strong oxidizing reagent and purges out CO_2.[20] A similar concept was miniaturized and modified to a flow reactor by Thermo™ in 2004. The commercial system is available since 2006.[21]

Over the last decades the instrumentation of the isotope ratio mass spectrometer has only slightly been changed. But in the last few years a different measuring principle has been adopted for the determination of light stable isotope ratios. Cavity ring down spectroscopy (CRDS) has gained a lot of popularity, especially in atmospheric science. Dedicated systems can measure stable isotope ratios of carbon, nitrogen, hydrogen and oxygen from gaseous samples. They are much less expensive than IRMS equipment, can be taken into the field and do not require any sample pretreatment. Additionally, it is possible to determine position-specific nitrogen isotope ratios of N_2O which is impossible with a common IRMS. Nowadays it is already possible to use CRDS to determine isotope ratios after EA combustion or after a

TOC analyzer as offered by Picarro Inc. However, such systems lack flexibility since they are dedicated to only one gas and element at a time.

In the 1980s, nuclear magnetic resonance spectroscopy (NMR) was used to measure hydrogen stable isotope ratios for the first time. Soon after also carbon isotope ratio analysis was realized by NMR. Nowadays the isotope ratio analysis is called site-specific natural isotopic fractionation (SNIF-NMR). Although this technique is very powerful as it can determine position-specific isotope ratios as well, the instrumentation is difficult to handle, very expensive and hyphenations for compound-specific isotope analysis are not possible yet. Additionally, these systems require highly concentrated samples and only have been used for carbon and hydrogen isotope analysis. Only a few laboratories in the world use this technique, in particular for the detection of wine adulteration.

The following chapters will describe the instrumentation of the IRMS, EA-IRMS and GC-IRMS. LC-IRMS will be treated in **Chapter 1.5** and **1.7** as it is major part of this work.

1.4.1 Isotope Ratio Mass Spectrometer

Isotope ratio mass spectrometers are designed to measure light gases such as CO_2, H_2, CO, SO_2, N_2 or SF_6. As only carbon isotope ratios have been determined in this thesis, the description of instrumental setups is mainly focused on the measurement of this element.

Dedicated peripherals either introduce offline produced light gases into the IRMS or convert the analytes into light gases. There are two modes to measure isotope ratios. The first one is the dual inlet. This device consists mainly of two bellows, one filled with reference gas, the other with sample gas, and a change-over valve directly coupled to the ion source of the IRMS (see **Figure 1.4A**). Here, sequential measurement of reference gas and sample gas obtains a very high precision down to 0.01 ‰ for $\delta^{13}C$ values.[22] This method requires a sample gas free of any impurities of hydrocarbons and an offline sample preparation if organic samples are to be measured.

The other mode of measuring isotope ratios is the continuous flow method. In contrast to the dual inlet, it maintains a stable pressure in the ion source, but yields a somewhat lower precision of 0.5 ‰ for carbon, nitrogen and oxygen measurements and about 3 ‰ for $\delta^{2}H$. The interfaces are connected to the IRMS by open splits. The open split consists of a glass tube, in which three capillaries are positioned (see **Figure 1.4B**). The capillary coming from the interface is fixed at a special position, whereas the capillary to the IRMS is movable and can be moved close to the outlet of the interface capillary for measurement. The IRMS capillary transports a stable amount of gas into the IRMS, proportional to its dimensions and the pressure in the IRMS. The third capillary provides a stable helium flow to keep air out the open split volume and purge out residual flow from the interface capillary. The inlet for the reference gas used to calculate δ-values and calibrate the mass analyzer works in a similar way.

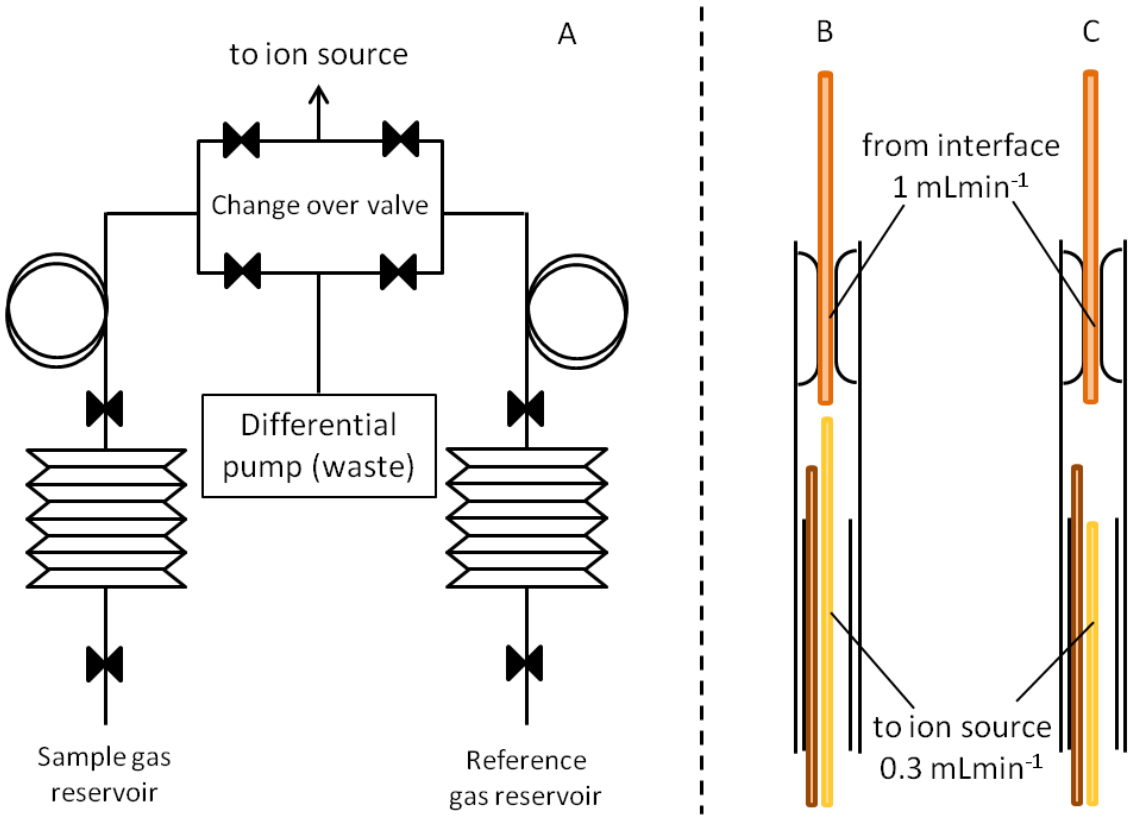

Figure 1.4 Gas introduction systems for IRMS. (A) The schematic setup of a dual inlet system which alternately introduces sample and reference gas into the ion source. (B; C) Principle of the open split to introduce a continuous flow of gas into the ion source. Sample and reference gas are fed into the IRMS by moving capillaries

The isotope ratio mass spectrometer consists of an ion source, a mass separator and a detection system. In the ion source the sample gas is ionized by electron impact ionization. A filament emits an electron beam towards a trap electrode. The electron trajectory is optimized to a spiral by a magnetic field. The electrons impact the sample gas and strike out electrons. The sample gas is converted to a radical cation as in the case of carbon isotope analysis:

$$CO_2 + e^- \rightarrow CO_2^{\cdot+} + 2\ e^-$$

The efficiency of this process is rather low, in most instruments, only 1 out of 1000 molecules gets ionized and measured. The remaining molecules either decay into CO^+ and $O^{\cdot}$, are sputtered against the ion optics or do not get ionized at all.[22] Some gases like CO_2 or SO_2 can adsorb to components of the ion source and are lost to detection or cause memory effects[22-23].

The ionized molecules are extracted from the ionization chamber by a repeller potential inside the ionization chamber and/or an extraction lens. The ion beam is accelerated and shaped by various electronic lenses. It exits the ion source and enters the magnetic sector, where a mass-to-charge ratio separation occurs. In IRMS, only singly charged molecules are of relevance, thus the mass-to-charge ratio directly reflects the molecular mass.

The ion beam is deflected by a magnetic field applied perpendicular to the flight trajectory according to the Lorentz rule:

$$r = \frac{1}{B} \times \sqrt{\frac{2 \times U \times m}{e \times z}}$$

Here, r is the radius of the flight path, B the magnetic field, *U* the accelerating voltage, e the elementary charge, m the mass and z the charge of the ion. The larger the mass of the ion the less it is deflected in the magnetic field.

The deflected ion beam is detected by a series of Faraday cups. Due to the applied potential each ion which enters a Faraday cup causes a potential drop which is recorded. This signal is amplified and digitalized.

The simultaneous recording of the ion beams of all isotopes of interest yields the high precision of δ-values. A conventional quadrupole mass spectrometer cannot achieve the required precision due to the sequential analysis of masses.[1]

The ionization process is not free of isotopic fractionation. The pressure in the ionization chamber can strongly influence the measured δ-value. Therefore, it is crucial to maintain a stable gas pressure in the ion source and use either a reference gas or a reliable standard material to account for this. Besides this, a large amount of water can cause the protonation of CO_2 and interfere with $^{13}CO_2$ (m/z 45).

Another isobaric interference for $^{13}CO_2$ is $^{12}C^{17}O^{16}O$. This interference can be corrected for by the introduction of a reference gas with known $\delta^{13}C$ value and application of a correction like Craig's[13] or Santrock's algorithm[24]. The m/z 45 ion beam is corrected with the m/z 46 ion beam of $^{12}C^{18}O^{16}O$. The amount of $^{12}C^{18}O^{16}O$ is proportional to the amount of $^{12}C^{17}O^{16}O$ with a coefficient λ if the fractionation effect is mass-dependent.

Due to these interferences and ionization effects during the ion formation, it is mandatory to measure isotope ratios as relative ratios. This is mostly done by injecting reference gas pulses at beginning or end of the measurement. But it is also possible to use an internal standard of known δ-value which is chemically similar to the sample.

1.4.2 Elemental analyzer coupled to IRMS

EA-IRMS can be used for solid and liquid samples. Liquid samples are injected directly into the oxidation column, while solid samples are weighted in small tin or silver cups. Before the packed cup enters the oxidation column, it is purged with an inert gas in order to exclude air from the analysis. The oxidation column is either a quartz tube or a glassy carbon tube, depending on the elements to be measured (see **Figure 1.5**). The tube is filled with specific catalysts in order to completely oxidize the whole sample. For this purpose, oxygen can be accessorily injected into the tube. The oxidation column is typically held at temperatures around 1100 °C. Hence, the sample is converted into light gases within a very short time. The formed gases pass an optional reduction oven usually filled with elemental Cu that scavenges O_2 and converts nitrous oxides to N_2. The gas mixture is dried and enters a chromatographic column that separates the gases. These enter the IRMS by an open split and are detected. Usually the isotope ratios of two elements in the sample can be determined from one run.

Due to fractionations during combustion and ionization, the results of a sample measurement have to be corrected by standards of known isotopic composition. Additionally, blank corrections sometimes have to be performed.[25]

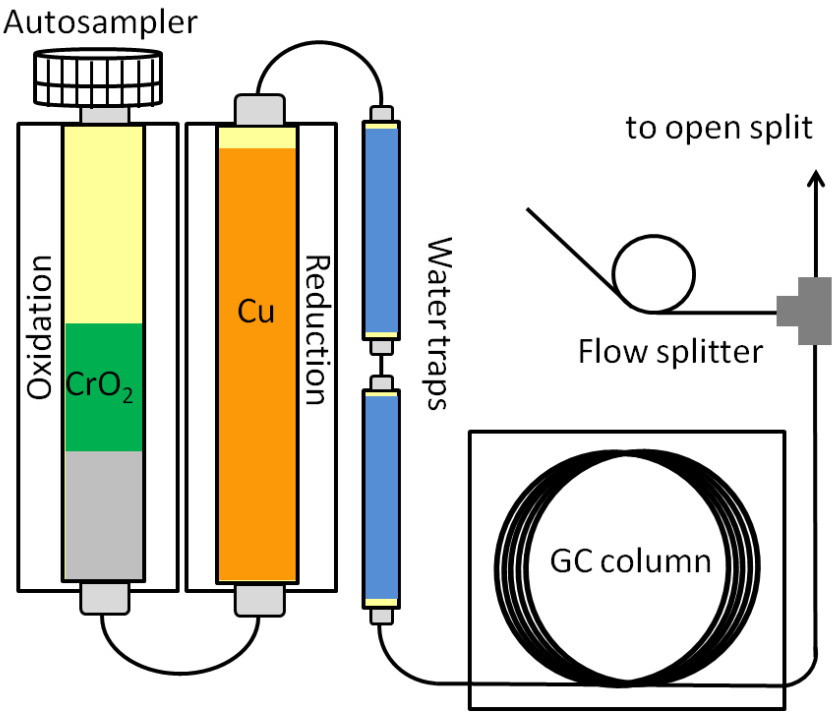

Figure 1.5 Schematic setup of an EA-IRMS system for carbon and nitrogen analysis.

1.4.3 Gas chromatography coupled to IRMS

The vast majority of CSIA is carried out on gas chromatographs coupled to IRMS (GC-IRMS). The interface for GC-IRMS consists of an oxidation reactor, an optional reduction reactor, a Nafion™ membrane water trap and the open split for sample and reference gas inlet (see **Figure 1.6**). The oxidation reactor is mounted in a furnace and consists of an alumina tube filled with catalysts for the conversion of analytes into the gases to be measured. The most common catalysts are wires of Pt, Ni and Cu for carbon measurements. For oxygen measurements platinum tubes filled with nickel are used. Bare alumina tubes which need to be coated with elemental carbon by the user are applied in hydrogen measurements.

Catalysts in the oxidation reactor need to be conditioned. In case of carbon, the wires inside the tube need to be oxidized on the outside to provide the necessary oxygen for CO_2 formation. This is done by backflushing the oxidation reactor with a mixture of oxygen and helium. In order to protect the chromatographic column from oxidation, a valve is installed between oxidation reactor and GC column and the backflush diverted to the atmosphere.

For carbon isotope analysis an optional reduction reactor can be operated. When analytes containing nitrogen are oxidized nitrous oxides are formed which would interfere with CO_2. Therefore, the reduction reactor reduces nitrous oxides to N_2 and also scavenges O_2 from the decomposition of the oxidation reactor. When nitrogen isotope ratios are measured, such a reduction reactor is mandatory.

During oxidation of organic compounds water is formed which needs to be removed in order not to cause interferences in the ion source by CO_2 protonation (see above). In most cases this

is done by a membrane of Nafion™, a sulfonated tetrafluoroethylene polymer. The carrier gas transports CO_2 and water through the Nafion™ capillary. Water can penetrate through the walls of the capillary and is removed into a counterstream of helium on the outside. Due to the concentration gradient this process is almost quantitative.

When nitrogen isotopes are measured, a liquid nitrogen trap after the open split freezes out CO_2 that otherwise would form CO^+ in the source and falsify the m/z 28 and 29 measurement.

The conversion of the analyte to hydrogen and CO is called thermal conversion and takes place at temperatures above 1000 °C:

$$C_nH_xO_y \xrightarrow{\text{elemental C as catalyst}} \frac{x}{2}H_2 + y\,CO + (n - y)\,C$$

In oxygen isotope analysis one has to ensure that no oxygen from instrumental parts can exchange with the oxygen in the measurement gas CO. Thus, the conversion reactor is made of pure platinum instead of alumina. Before the analytes enter the conversion reactor, some H_2 is mixed into the stream in order to support the conversion.

Table 1.2 Conversion conditions in case of Thermo Scientific instruments.

Element	Measured gas	Catalyst	Temperature
Carbon	CO_2	Oxidized Pt, Ni, Cu wires Optional reduction step by Cu	940 °C
Nitrogen	N_2	Oxidized Pt, Ni, Cu wires Additional reduction step by Cu	980 °C 650 °C
Oxygen	CO	Pt tube filled with Ni	1050 °C
Hydrogen	H_2	Elemental C coated either by CH_4 or injection of alkanes	1450 °C

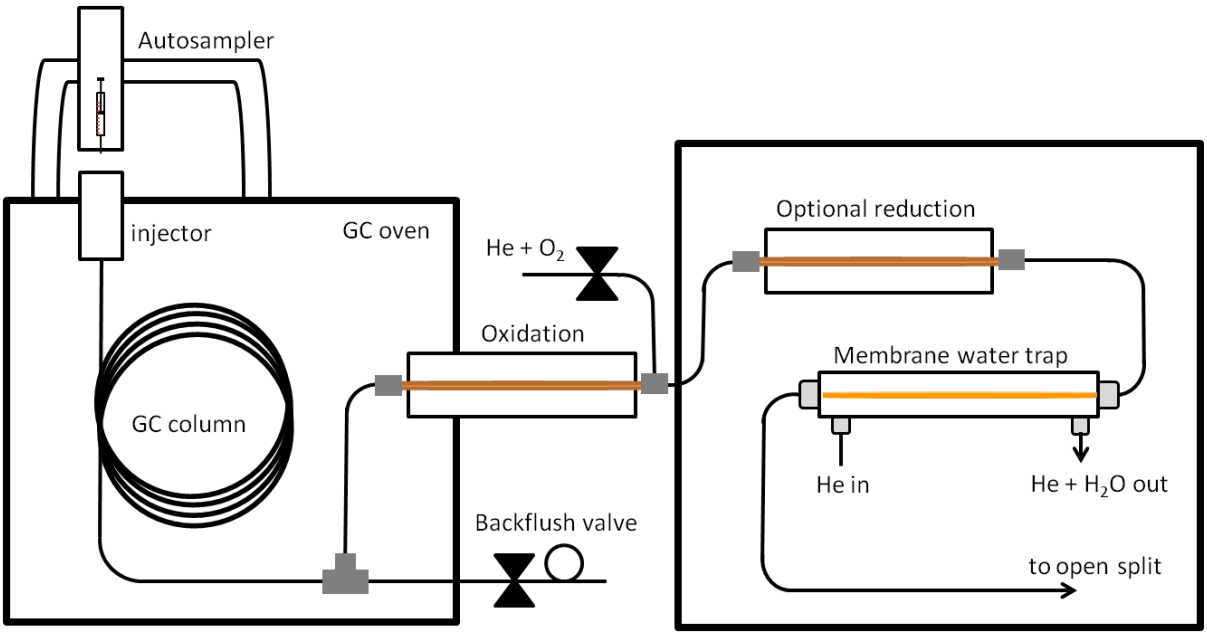

Figure 1.6 Schematic setup of a GC-IRMS system for carbon isotope measurement. The sample can be injected by an autosampler or an online sample extraction technique onto the column. The carrier gas transports the analytes into the oxidation reactor. Water is removed by a Nafion™ membrane before the formed CO_2 is transported to the open split.

1.5 Hyphenation of liquid chromatography and IRMS

Since the beginning of compound-specific isotope analysis, attempts were made to combine liquid chromatography with continuous flow IRMS. The first online system was demonstrated by Abramson and co-workers.[26-28] The chemical reaction interface (CRI) consisted of a solvent vaporizer and a microwave plasma to convert analytes to the light gases to be measured. At the same time the "moving belt interface" was demonstrated by Caimi and Brenna.[29] The LC effluent was sprayed and dried on a heated belt before a carrier gas stream introduced the obtained CO_2 into the IRMS. Although both methods have been applied in the academic field,[30] none was ever adopted in any commercially available interface system for LC-IRMS, due to their service-intensive components, low detection limits and fractionations during conversion.

The first commercial interface system has been introduced by Thermo Fisher Scientific, in 2004.[21] In opposite to the other systems, it performs the oxidation of the analytes in the aqueous phase and extracts the obtained CO_2 by a membrane into the carrier gas stream.[21] The functional principle was adopted from the work of Gille St-Jean who coupled a TOC analyzer to IRMS.[20]

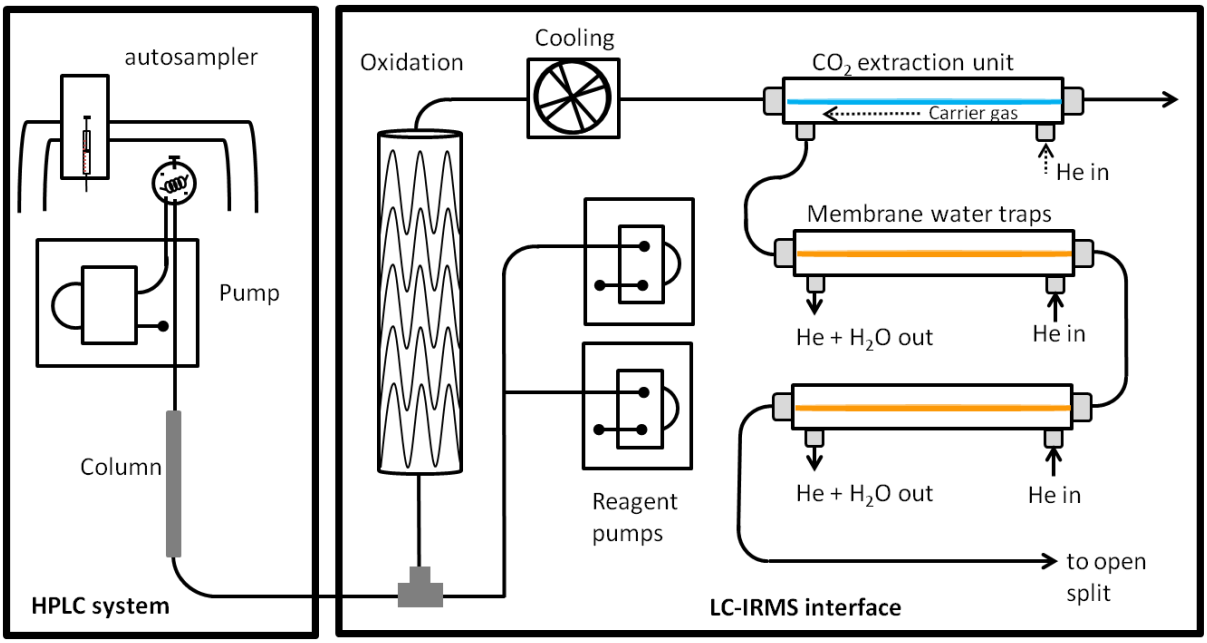

Figure 1.7 Scheme of a LC-IRMS wet oxidation interface offered by Thermo Scientific™.

The two commercially available interface systems, LC-IsoLink (Thermo Scientific) and Liquiface (Isoprime Ltd), use peroxodisulfate and ortho-phosphoric acid as reactants to convert any compound containing carbon to dissolved CO_2 (see **Figure 1.7**). The reagents are mixed with the HPLC effluent in a T-piece and are transported into the oxidation reactor. This reactor consists of a heated stainless steel capillary of about 5 m length. The temperature is usually set to 99.9°C in order to form sulfate radicals from peroxodisulfate. This "activation" can also be achieved by the addition of transition metals, whereas Ag^+ and Co^{2+} are the most effective catalysts, but are not used due to the risk of precipitate formation. Peroxodisulfate can also act as oxidant (E^0= 2.1 V), although at a much slower rate[31].

Sulfate radicals have a slightly higher standard redox potential of 2.6 V[31]. They preferably abstract electrons from organic molecules leaving an organic radical cation. Thus, electron donating groups like $–NH_2$, -OH or –OR (alkoxy) are easier to oxidize than molecules with electron withdrawing groups ($-NO_2$, -C=O) or halogenated molecules[31].

Sulfate radicals also generate hydroxyl radicals by electron abstraction from water. Hydroxyl radicals react with organic molecules by hydrogen abstraction or addition. They can combine to hydrogen peroxide, which can decompose organic molecules as well. Besides these reactions, a significant amount of oxygen is formed.

Since chloride readily reacts with sulfate radicals, it needs to be removed from samples e.g. with silver nitrate before injection if present. Otherwise oxidation of target substances may be incomplete resulting in wrong $\delta^{13}C$ values.

The flow path inside the oxidation reactor is specially designed to minimize peak broadening. The capillary is formed to serpentines (see **Figure 1.8**) which introduce a radial mixing in the tubing. Hence, longitudinal diffusion is minimized.[32]

Figure 1.8 Serpentine-shaped capillary inside the oxidation reactor in an LC-IsoLink interface sold by Thermo Scientific (Bremen, Germany)

The low pH resulting from the addition of ortho-phosphoric acid shifts the carbonate balance in favour of CO_2.[21] After passing a cooling fan, the stream arrives at the gas extraction unit. Here, the liquid flows through three membrane capillaries at which exterior a helium counter stream is applied. Because of the partial pressure gradient, CO_2 and other gases like H_2O or O_2 pervaporate from the liquid stream into the carrier gas. This gas extraction is almost quantitative due to the low pH and the increased surface from flow splitting into three capillaries. Subsequently, the carrier gas stream is dried by two gas driers equipped with Nafion™ membranes and is introduced into the IRMS by an open split.

Hettmann et al.[33] equipped such an interface with a reduction reactor in front of the open split in order to remove oxygen from the gas stream. The amount of oxygen which enters the ion source can be minimized and thus, the filament lifetime increased.[33]

This type of interface can be used for bulk stable isotope analysis by flow injection analysis (FIA) without prior chromatography.

1.6 Chromatography

A chromatographic separation is realized by interactions of the analyte between mobile and stationary phase. Here, the mobile phase can act as a pure carrier, as in GC, or actively control separation, e.g., as eluent in ion exchange chromatography.

When a mixture is injected onto a stationary phase, or chromatographic column, the analytes are transported by the flowing mobile phase. According to the physicochemical properties of the analytes, the interactions between stationary phase and analytes vary. Thus, given an appropriate time or number of interaction steps, the mixture of analytes will be separated.

In chromatography two main principles can be distinguished. In adsorption chromatography, the analytes adsorb on a solid stationary phase, whereas in partitioning chromatography the analytes partition into a liquid stationary phase. This classification does not explain the underlying physicochemical process.

In gas chromatography, analytes are generally separated according to their partitioning constant between mobile and stationary phase. In most cases van der Waals interactions or dipole-dipole interactions, as for alcohols on polar stationary phases, occur as well.

Both principles, adsorption and partitioning, can apply at once in high performance liquid chromatography (HPLC). Depending on the stationary phase, some analytes partition into the stationary phase while other analytes from this mixture can only adsorb to it. An example is the separation of alkanes on alkyl chain bonded silica column. The alkyl chain of the stationary phase can be regarded as liquid phase where small analytes can partition into. Analytes of alkyl chain longer than the alkyl chain of the stationary phase cannot be solved into this liquid phase[34-35]. Hence, they only adsorb to the surface.[34-35]

Physicochemical processes in HPLC which occur between analyte and mobile or stationary phase are the following: van der Waals forces, i.e. (i) dispersion interactions (London forces) and (ii) dipole-dipole interactions, (iii) hydrogen bonding, (iv) ionic interactions and (v) charge transfer.[35]

(i) Dispersion interactions occur from instantaneous dipoles which result from random positions of electrons. Asymmetric distribution of electrons in a molecule causes a slight displacement of electrons in an adjacent molecule. This induces instantaneous dipole moments for both molecules and results in a rather weak attraction.

(ii) A) Two molecules with large permanent dipoles of the opposite polarity are attracted towards each other. B) A permanent dipole induces a dipole at another molecular entity. Because the molecules need to be in close proximity to each other and properly aligned

in space the contribution of such interactions to van der Waals forces is very small in condensed phases.

(iii) Hydrogen bonding occurs between a covalently bound hydrogen atom and a proton acceptor, which is a free electron pair of the interacting species.

(iv) Ionic interactions are attractions between permanently charged groups or charged groups and dipols. Charged groups of the analytes interact with charged functional groups of the mobile or stationary phase of the opposite charge. Besides this, charged groups can induce dipoles on the interacting species.

(v) Charge transfer or π- π interactions which occur mostly between aromatic compounds.

The retention of an analyte on the column is an equilibrium process. The concentration of the analyte in the stationary phase is proportional to its concentration in the mobile phase. Thus a distribution coefficient K can be defined as the ratio of the analyte concentration in the stationary phase c_s and mobile phase c_m, respectively. The retention time t_R is the time the analyte needs to migrate through the column. It is determined as the time at which an analyte arrives at the detector subtracted by the dead time t_0, the detection time of an unretained compound (see **Figure 1.9**). The retention time is dependent on the retention factor k:

$$t_R = t_0 \, (1 + k) \qquad \text{with} \qquad k = \frac{C_s \, V_s}{C_m \, V_m}$$

The retention factor k is thus:

$$k = \frac{t_R - t_0}{t_0}$$

The resolution of two peaks R_s can be calculated from their retention times and peak width at the baseline w_b:

$$R_s = 2 \cdot \left(\frac{t_{r(2)} - t_{r(1)}}{w_{b(2)} + w_{b(1)}} \right)$$

Instead of w_b, the peak width at half height w_h can be used, since w_b is sometimes difficult to determine:

$$R_s = 2 \cdot \frac{t_{r(2)} - t_{r(1)}}{1.7 \left(w_{h(2)} + w_{h(1)} \right)}$$

A full separation between two peaks is obtained if R_s is 2. If two peaks overlap by 5% the resolution is 1.5, which is baseline separation.[36]

The term selectivity describes the separation power of a column. Alternatively, it is called relative retention factor because it is defined as:

$$\alpha_s = \frac{k_2}{k_1}$$

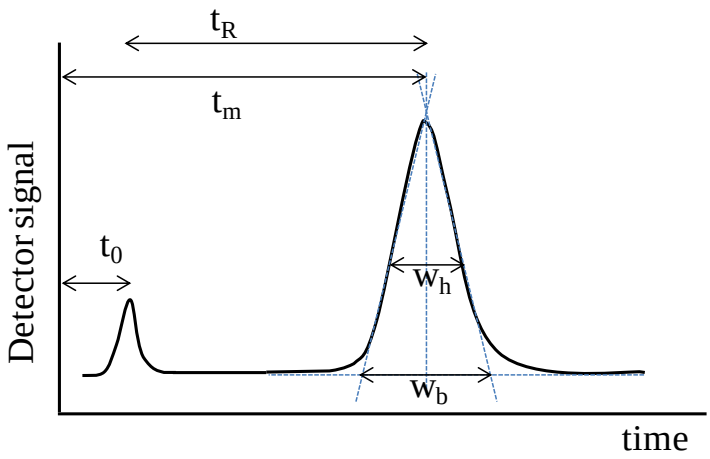

Figure 1.9 Measurement of peak width and retention time.

Basically, a chromatographic separation is the result of consecutive equilibrium processes of the analytes between stationary and mobile phase. Each equilibrium step is called theoretical plate. The sum of all plates, the theoretical plate number, can be determined from w_b and t_R:

$$N = 16 \left(\frac{t_R}{w_b}\right)^2$$

N is also called column efficiency, since it describes the ability of the column to produce narrow peaks and good resolution. R_s and N are related by the following equation:

$$R_s = \frac{1}{4} \left(\frac{k}{(1+k)}\right) (\alpha\text{-}1)\ N^{0.5}$$

The plate height H is also a measure of efficiency as it describes the efficiency per unit length of the column:

$$N = \frac{L}{H}$$

L is the length of the column. The smaller H, the narrower are the peaks and the better is the resolution:

$$H = \frac{L\ w_b^2}{16\ t_R^2}$$

The ideal shape of a chromatographic peak corresponds to a Gaussian distribution function due to diffusion processes. The observed peak shape is the result of several processes of diffusion and mass transfer. Besides extra column band broadening from injection, capillaries and the like, longitudinal diffusion, eddy diffusion, mobile phase transfer and stationary phase transfer control the width of the peak and thus influence H (see **Figure 1.10**).

Longitudinal diffusion along the column axis causes the increase of the band width of the analyte. This process is dependent on time and occurs whether there is eluent flow or not, but its contribution is lower at high mobile phase flow rates.

$$\frac{B}{\bar{u}} = \frac{2\ \gamma_P\ D_m}{\bar{u}}$$

D_m is the diffusion coefficient of the analyte in the mobile phase and γ_P is a factor related to the column packing.

Eddy diffusion causes the analytes to take different paths along the particles and thus results in different migration times. It is strongly dependent on d_P, the particle diameter and the consistency of the column packing λ_P:

$$A = 2\,\lambda_P\,d_P$$

Due to diffusion some analytes remain inside the pores of the particles longer than others, thus they need more time to leave the column (stationary phase mass transfer). Mobile phase mass transfer contributes to peak broadening due to higher mobile phase velocities at the center of the stream than at the walls. When the flow rate is increased, the relative difference of the flow velocities also increases. $C_s\bar{u}$ is the term relating to the mass transfer between stationary and mobile phase.

The van Deemter equation sums up the contribution of these three terms:

$$H = A + \frac{B}{\bar{u}} + C\,\bar{u}$$

From plots of H against ū, the optimum flow rate can be determined to obtain narrow peaks and the best resolution.

The maximum number of baseline separated peaks which can be obtained with a column on a certain separation length is the peak capacity n. It is defined as:

$$n = 1 + \frac{\sqrt{N}}{4}\,\ln\frac{V_R^n}{V_R^1}$$

V_R^1 is the retention volume of the first eluting peak and V_R^n the retention volume of the last peak.

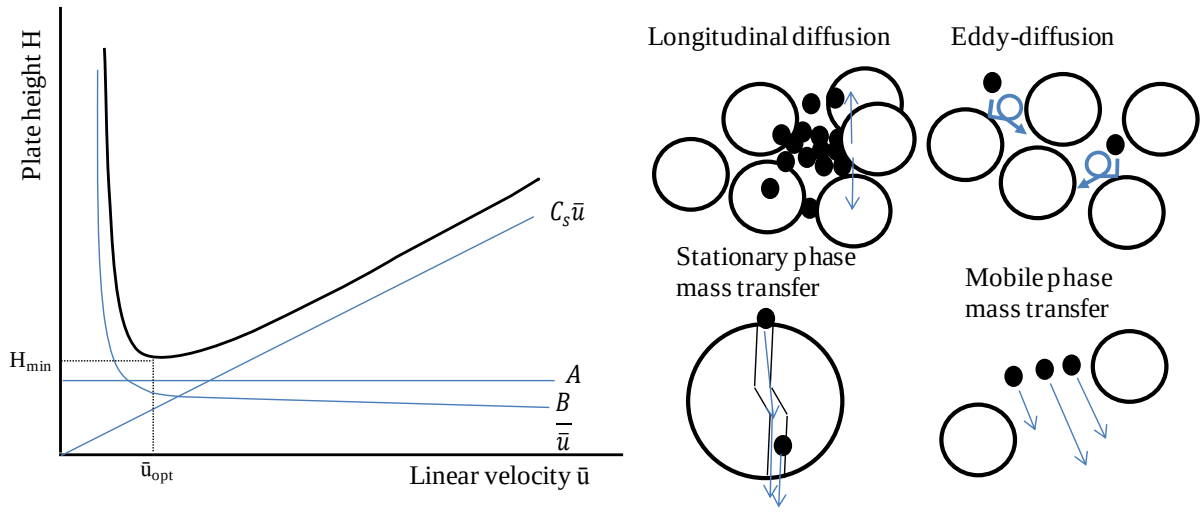

Figure 1.10 Relationship of plate height H and linear velocity ū, and different factors contributing to peak broadening. (modified from Snyder et al.[35])

1.6.1 Chromatographic isotope effect

In general, methods developed for IRMS require a baseline separation of analytes. Due to an isotope effect in chromatography overlapping peaks can cause erroneous results. Depending on the type of chromatography and the involved interactions between stationary phase and compounds, either a normal or inverse isotope effect can be observed. Typically, there is an inverse isotope effect in GC-IRMS[37-38]. The molecules with the heavier isotope are eluted slightly faster than molecules with the lighter isotope. If the ratio of m/z 44/45 is monitored, a characteristic swing can be observed (see **Figure 1.11**). This inverse isotope effect can usually be observed when van der Waals interactions dominate the separation mode, like in GC or reversed phase LC[39-40]. In these cases, the molar volume of isotopically substituted compounds is lower than that of unsubstituted isotopologues because of the shorter atomic bond lengths. Thus the van der Waals interaction surface is lower and such compounds are eluted earlier.

In cation exchange a normal isotope effect was observed[40-41]. That means the lighter isotopologue is eluted faster than the heavier. The resulting m/z 44/45 ratio drops at the front of the peak and increases at its tail which can be seen in **Figure 1.11**. The isotopic substitution with a heavier atom decreases the acidity of the molecule, thus, it can bind stronger to the anchor group and elute later[41].

Due to the fact that retention in HPLC is not associated to solely one interaction type, it is not easy to predict the observed isotope effect. Besides, for some separation modes like anion exchange or size exclusion, isotope effects have not been investigated yet.

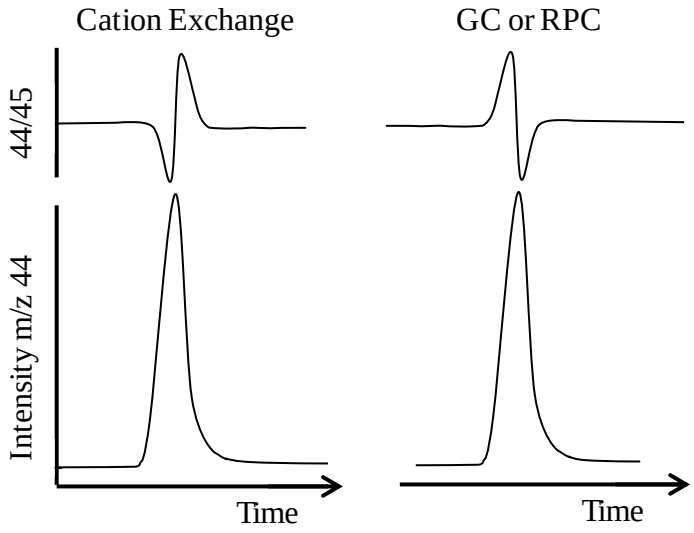

Figure 1.11 Chromatographic isotope effect in cation exchange chromatography and GC or RP-LC. Note that in case of LC various processes make up the separation, which complicates the prediction of the observed isotope effect.

1.7 Liquid Chromatography compatible with LC-IRMS

The compatibility of the employed liquid chromatography depends strongly on the type of interface used for LC-IRMS. Despite their drawbacks in detection limits, accuracy and challenging instrumentation, the CRI and the moving belt interface were superior to the nowadays available interface in terms of element specificity and chromatographic flexibility. Both systems have a solvent evaporation step which allows the use of conventional reversed phase and normal phase separations. They are not limited to one element: besides carbon isotope ratios, nitrogen isotope ratio measurements may be possible as well.[42] Nevertheless, both systems fail in hyphenation with IRMS due to large fractionations during conversion and problematic instrumental setups.

The two commercially available interfaces, LC-IsoLink™ and Liquiface™, are restricted to completely carbon free eluents because of the continuous non-selective oxidation of the column effluent. Along with the analyte, organic or inorganic additives containing carbon would also be converted to CO_2 and saturate the IRMS carbon signal. Thus, for these interface systems only ion exchange chromatography, mixed-mode or fully aqueous RP-LC are suitable. The following discussion will be focused on the use of chromatographic separations combined with commercial LC-IRMS systems.

1.7.1 Ion exchange chromatography

Ion exchange chromatography is the most popular method in LC-IRMS because it does not require organic solvents in the eluent. Cation and anion exchange and ion exclusion have been used in literature for LC-IRMS.

In ion exchange chromatography, the charged analyte is attracted to anchor groups of the opposite charge on the stationary phase. The counter ions of the mobile phase compete for the anchor groups and thus elute the analytes. Dedicated stationary phases consist of styrene-divinylbenzene polymers or silica. These supports are modified with functional groups which carry a charge; so-called anchor groups. Strong cation exchangers have sulfonated groups, whereas weak cation exchangers are carboxylic groups. Anion exchange resins are mostly quaternary amines grafted on polymeric support materials like latex. But also silica can be used as supporting material.

LC-IRMS with anion exchange separation has been used for the analysis of aminosugars from soil[43], pyrogenic organic matter[44], amino acids[45], nucleotide triphosphates[46], glycerol[47] and carbohydrates[47-50]. For many methods basic eluents have to be used. The handling of basic eluents may not be that easy, since CO_2 from air is readily regassing into the solutions causing a higher background. Thus, Boschker et al.[49] used a low concentrated NaOH solution in combination with $NaNO_3$ in order to enhance the separation. Hence, a similar separation of carbohydrates was achieved compared to a highly concentrated NaOH eluent in gradient mode[47].

In contrast to ion exchange chromatography, ion exclusion chromatography is based on the repulsion between analytes and stationary phase. The analyte cannot enter the stationary phase if the charge density is too high. Such a compound would be eluted without retention. If the

analyte has a low charge density, it can enter the stationary phase and interact with the polymeric support. Thus, compounds with phenyl groups usually have a strong retention in ion exclusion chromatography. This mechanism has been used for the analysis of small organic acids[51], ethanol and glycerol[52-53].

The analysis of ethanol and glycerol with LC-IRMS was also conducted with ligand exchange chromatography. A coordination center, typically Ca^{2+}, Pb^{2+} or H^{+}, attached to an anionic anchor group interacts with the analyte. These cations can also be used to exclude ions in ligand exclusion chromatography. This has been shown in LC-IRMS for the analysis of sugars from honey[4].

Cation exchange chromatography has been used rarely compared to anion exchange chromatography although the acidic eluents are very suitable for LC-IRMS due to the acidic condition during oxidation. The LC-IRMS works published up to date deal with amino acids[54-55], sugars[21] and ethanol and glycerol[56].

The analysis of the compound classes described above can be easily conducted with aqueous eluents, but molecules which have a higher hydrophobicity can be strongly retained on the support material which usually is polystyrene-divinylbenzene. A certain amount of organic solvents would be necessary but cannot be used in LC-IRMS.

1.7.2 Reversed phase chromatography

In reversed phase liquid chromatography (RP-LC) a nonpolar stationary phase and a polar mobile phase are used. Analytes are retained mostly by van der Waals but also by dipole interactions on the column. In conventional RP-LC the proportion of organic solvent in the buffer is increased to stepwise elute the compound from the column. In LC-IRMS it is not possible to use organic solvents, only aqueous buffers are used. Thus, the elution strength of water mostly is too low to elute analytes from the column. Aqueous RP-LC without modification of the eluent can only be used with very polar compounds. On the other hand it is difficult to retain very polar compounds on alkyl chained stationary phases, like octadecyl, since dispersion interactions are weak. For example, it is not possible to retain most amino acids on an octadecyl stationary phase. Only hydrophobic amino acids like phenylalanine can be retained and eluted.

Another constrain using RP-LC with purely aqueous eluents is column de-wetting. Due to the hydrophobic nature of the stationary phase, water will be repelled out of the particle pores by time. Only if the column is maintained at a certain pressure water can be kept inside the pores and the whole stationary phase can be used for interactions with the analyte. The other possibility is to use stationary phases with embedded polar groups. Such columns have been used for various studies using RP-LC with LC-IRMS. Formic acid, acetic acid, methanol, ethanol, short-chain organic acids[57], acetaminophen and acetylsalicylic acid[21] have been measured on such modified octadecyl silica columns. The herbicide bentazon has been separated for LC-IRMS measurement on a silica based amide-embedded C_{16} column.[58]

1.7.3 High temperature liquid chromatography

The elution strength of an aqueous eluent can be modified by the application of elevated temperatures. An increase of temperature causes the static permittivity of water to decrease[59]. The static permittivity is a measure for polarity and may be taken to assess the elution strength. Thus, solvent gradients can be replaced or supported by temperature gradients[60]. In conventional HPLC, using organic solvents, an increased temperature can save solvent consumption. The temperature is applied to column and mobile phase to prevent peak broadening from thermal gradients. High temperature liquid chromatography (HTLC) can be performed in ovens, similar to GC ovens, or by contact heaters. Due to a better heat conduction and much shorter eluent preheating capillary, contact heating usually yields better separations than air-bath ovens[60].

Common silica based columns are only stable up to 80°C. Above this temperature increased column bleed is a sign of bonded phase lost and irreparable column damage[61]. Since the LC-IRMS is sensitive to inorganic and organic carbon, such column bleed has to be taken into account when using HTLC in combination with LC-IRMS. The first application of HTLC-IRMS was reported by Godin et al.[51] They used a porous graphitic carbon (PGC) column to separate hydrosoluble fatty acids and phenolic acids. This column has a strong retention for many compounds, including very polar ones. It is also stable at high temperature operation but nevertheless it was shown that temperature gradients can result in a significant column bleed.[51] Zhang et al.[62] evaluated other stationary phases for HT use in LC-IRMS. Similar to Godin et al. they investigated the effect of column bleed at high temperatures on the measured $\delta^{13}C$ values of reference gas pulses and ethanol. From these data maximum operating temperatures have been derived for a zirconium based column coated with polybutadiene (ZirChromPDB) and two hybrid particle stationary phases (XBridge C18 and YMC Triart). Temperatures up to 200°C were used without a compromise in $\delta^{13}C$ values[62]. In this work, caffeine and its derivatives as well as phenols were successfully analyzed under HT condition with LC-IRMS[62].

1.7.4 Mixed Mode Chromatography

Ion exchange sometimes suffers from low selectivity and broad peaks. In order to overcome this, mixed-mode columns have been introduced. The stationary phase consists of alkyl chains with charged ionic groups which are bonded to silica. They provide hydrophobic interactions along with ion exchange. Thus, small molecules can be retained better and retention can also be controlled by the pH of the eluent.

The application of mixed-mode chromatography (MMC) in combination with LC-IRMS is mainly focused on amino acids[63-68], although works on the isotopic signature of gluthatione and its dimer[69-70] have been published in this context as well.

The first work on amino acids isotope analysis featuring a separation method consisting of ion exchange and hydrophobic interaction was presented by Godin et al although it was not a MMC separation.[55] They used a kind of two-dimensional approach to separate amino acids on a cation exchange column connected to a C_{30} silica column. This method could baseline separate 11 of 15 amino acids.

Using a MMC column of silica-based C_{12} with embedded anionic group it is possible to resolve almost all physiological amino acids[66]. Thus, various methods employing MMC for amino acid analysis for LC-IRMS were published. Most methods use columns of 25 or 50 cm in order to increase resolution[63-68]. But on the other hand, analysis times are very long, up to 3h for one chromatographic run[66] (see **Figure 1.12**).

Nevertheless, a comparison of LC-IRMS with GC-IRMS for the analysis of amino acids has shown that a slightly better precision and accuracy of $\delta^{13}C$ values can be achieved using LC-IRMS since it does not require derivatization[67]. Although more sample is required for LC-IRMS, GC-IRMS cannot measure arginine, since it is not easily derivatized[67]. Despite these disadvantages, GC-IRMS of amino acids is still useful, in particular for $\delta^{15}N$ determinations.

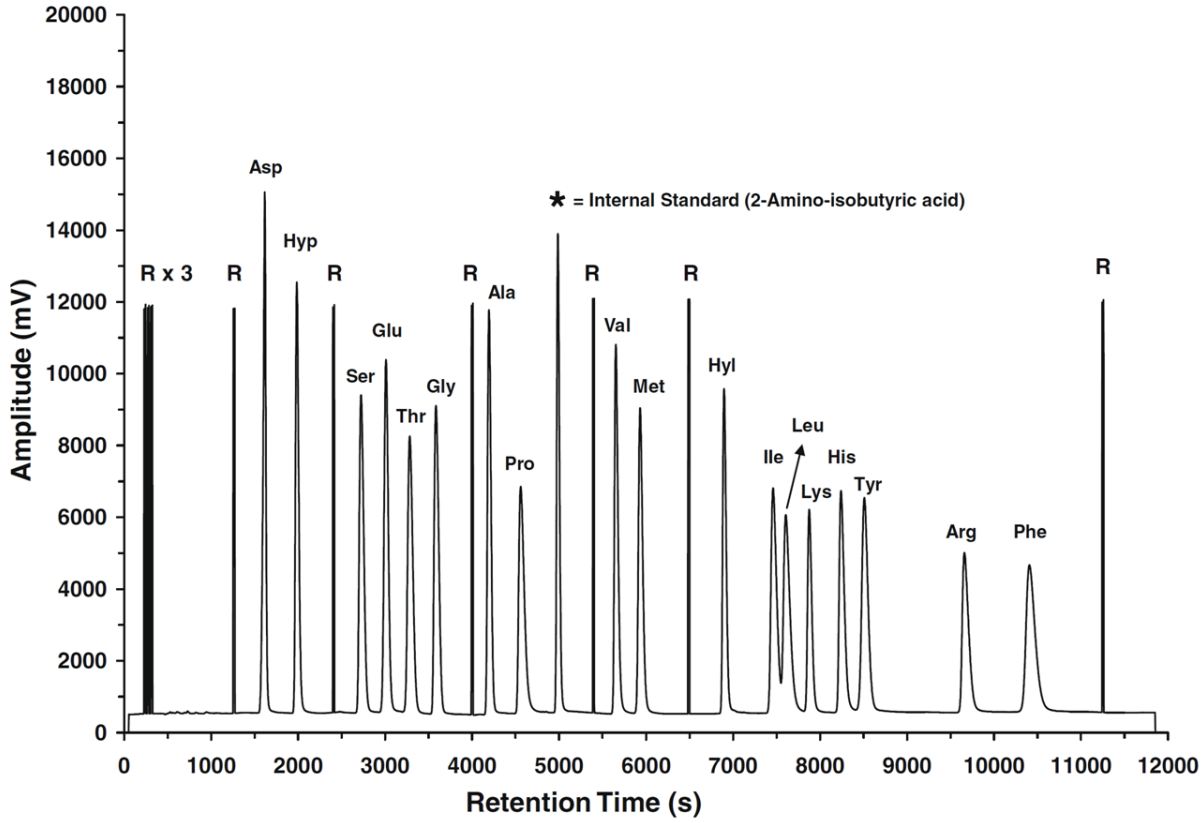

Figure 1.12 LC–IRMS chromatogram (m/z 44) of standard amino acid mixture containing approximately 1320 ng of carbon for each amino acid. R, reference gas pulse. Source Smith et al.[66]

1.8 Applications of LC-IRMS

Due to the rather low sensitivity, research conducted by LC-IRMS focused mainly on amino acids and carbohydrates. But due to the broad abundance of these compounds in nature, many scientific fields like food science, archeology and ecology have benefited from LC-IRMS. But also the measurement of anthropogenic pollutants and biological metabolites is emerging. From all these, a few applications in food science, geochemistry and biochemistry will be introduced.

1.8.1 Food Science and Archeology

LC-IRMS has found broad application in food science so far. Caffeine[71], carbohydrates[56, 72], ethanol[53, 56] and amino acids[65, 68] have been research interests in many publications.

The monitoring of the authenticity of honey by LC-IRMS is already routine analysis. In 2008, Elflein and Raetzke[4] published a method to detect C_4 and C_3 plant sugar syrup addition to honey. The detection of adulteration of honey has been performed up to that time by EA-IRMS. Since bees produce honey from C_3 plants, only an addition of C_4 sugar syrup could be detected. This method was improved by measuring the honey protein in addition to the carbohydrate $\delta^{13}C$ value. But some honeys like acacia or lavender honey have a very low protein content and the protein $\delta^{13}C$ value can be falsified by yeast residues or feeding supplements. The new method consists of measuring $\delta^{13}C$ values of the total honey and the protein by EA-IRMS and LC-IRMS measurement of glucose, fructose, trisaccharides and disaccharides. Differences among the $\delta^{13}C$ values of each parameter should not exceed ±2.1 ‰. A second criterion is the difference of $\delta^{13}C$ value of glucose and fructose being smaller than ±1 ‰. The last indicator for an authentic honey is a difference between the $\delta^{13}C$ value of protein and total honey being bigger than -1 ‰. By this procedure, the detection limit of adulteration was lowered from 27% to 8% syrup addition. Besides, also the addition of C_3 sugar syrup can be detected.

In 2012, Zhang et al.[71] published a method to distinguish natural from synthetic caffeine in beverages by HTLC-IRMS. All caffeine producing plants which are consumed by humans are C_3 plants. Their plant material has a $\delta^{13}C$ value in the range of about -20 to -30 ‰, as well as its caffeine. Synthetic caffeine often is produced by the Traube synthesis. This yields a $\delta^{13}C$ value lower than -32 ‰. Hence, it can be traced by the $\delta^{13}C$ value of caffeine if beverages are produced with synthetic caffeine. Thus, misleading declarations stating that all ingredients were natural could be identified in a few cases. Sample preparation for this method is minimal, only dilution and filtration, which shows it potential for routine analysis.

But also without HPLC separation, LC-IRMS can be useful in detection of adulterated or mislabeled food. Jochmann et al. used the LC-IRMS in FIA mode to measure carbon bulk isotope ratios of various spirits as a fast screening method prior to further investigation. Since ethanol is present at high concentrations of about 40% in spirits, this bulk $\delta^{13}C$ value mainly represents the $\delta^{13}C$ value of ethanol. It was shown that spirits like cachaça and rum which are produced from sugar cane, a C_4 plant, can be clearly distinguished from C_3 plant spirits like brandy, which is distilled from wine. The range of $\delta^{13}C$ values of vodka was very broad compared to the other products (about 8 ‰). The authors concluded that the addition of molasses from sugar cane especially in cheaper products could have increased the $\delta^{13}C$ value, since European vodka is produced from C_3 plants like potatoes or wheat.

The analysis of amino acids is a broad field of interest in LC-IRMS. The isotopic analysis of single amino acids can reflect the diet of the individual[65, 73]. Differences of $\delta^{13}C$ values between glutamic acid and phenylalanine as well as glutamic acid and glycine together with the bulk $\delta^{15}N$ values can show if the diet was based on marine protein and distinguish C_3 from C_4 plant consumers. Single amino acid isotope analysis by LC-IRMS of archeological samples from human bone collagen from ancient human groups from Japan and Korea

revealed a high marine protein based diet.[64, 73] Bone collagen analysis of archeological human remains from Mesoamerica reflected their C_4 plant based diet.

1.8.2 Geochemistry and Environmental Chemistry

In flow injection mode, LC-IRMS can be easily used to measure dissolved inorganic carbon. The possibility to study the hydrology in estuarine basins has been shown by J. Brandes[74] for the Savannah River, GA, USA. Very small sample volumes of a few µL were required and a precision of 0.06 ‰ was achieved.

Heuer et al.[57] used LC-IRMS to study acetate and other volatile fatty acids in marine sediments. It was revealed that in the sediment pore water from the Gulf of Mexico $\delta^{13}C$ values of acetate, propionate and butyrate are strongly depleted in ^{13}C. They found $\delta^{13}C$ values between about -40 and -80 ‰ for these compounds. Acetate from pore water from the deep sea had even more negative $\delta^{13}C$ values between -60 and -90 ‰ which can be a sign of methane turnover.

1.8.3 Biochemistry

LC-IRMS has been used to determine ^{18}O isotope effects during enzyme catalyzed hydrolysis of nucleotide triphosphates[75], although it is impossible to measure oxygen isotopes by the available LC-IRMS hyphenations. The authors used a mixture of isotopically labeled substrate in that work. The mixture contained guanosine triphosphate (GTP) which was depleted in ^{13}C and a portion of GTP which was enriched with ^{13}C in all positions and labeled with ^{18}O at the reactive positions[75]. Therefore, from measured $\delta^{13}C$ values of the product, guanosine diphosphate, and the substrate the change in ^{18}O could be concluded[75].

2 Scope of this work

The main aim of this work was to develop liquid chromatographic methods for the stable isotope analysis of anthropogenic compounds present in the environment. As target substances sulfonamide drugs, trimethoprim, glyphosate and aminomethyl phosphonic acid were chosen.

Due to their wide agricultural and domestic use, these compounds are common pollutants of soil and surface waters. Although kinetics and basic attenuation processes have already been identified, it often is difficult to distinguish between them in real environmental compartments. Moreover, degradation products may not always be specific for the target compounds as it is the case for glyphosate and its metabolite aminomethylphosphonic acid. Compound-specific isotope analysis can overcome these difficulties and is nowadays a common tool in degradation studies. It can identify degradation and sometimes even distinguish reaction pathways. For that purpose, it is necessary to study possible isotope effects of various degradation reactions of the analyte under controlled laboratory conditions.

Due to the analytical challenge of LC-IRMS, CSIA measurements of polar herbicides and pharmaceuticals published in literature are scarce. The main restriction is the incompatibility of the LC-IRMS to use organic solvents in chromatography. Additionally, the IRMS measures all compounds as CO_2, which requires a good separation of the target substance from other sample constituents. Hence, a careful selection of the analytical columns and separation conditions is mandatory in order to obtain reliable isotope ratios.

The first chapter of this work deals with method development for the analysis of the sulfonamide drugs and trimethoprim. It will be shown that high temperature liquid chromatography can be excellently used in combination with LC-IRMS to determine carbon isotope ratios of these compounds. Subsequently, the direct photolysis of a selected sulfonamide will be studied in the second chapter as this process is a prominent attenuation process in the environment.

The next three chapters cover the analysis of the important herbicide glyphosate. In Chapter 5, three possible liquid chromatographic methods to determine glyphosate and its metabolite aminomethylphosphonic acid will be developed and compared for their practicability in LC-IRMS. Consequently, the developed method will be used to investigate the isotope effect during abiotic oxidation of glyphosate by manganese dioxide in the following chapter. In the last chapter two approaches to measure the carbon isotope ratio of glyphosate at the reactive position, originating aminomethylphosphonic acid, will be examined in order to better understand carbon isotope fractionation during manganese dioxide oxidation. Therefore, nuclear magnetic resonance spectrometry and a cleavage reaction of glyphosate with following LC-IRMS measurement will be used.

References

1. Jochmann, M. A.; Schmidt, T. C., *Compound-specific stable isotope analysis*. Cambridge : Royal Society of Chemistry: Cambridge H1 - E33 UTI1892+9, 2012.

2. IUPAC, Compendium of Chemical Terminology (the "Gold Book"). **2006**.

3. Cabanero, A. I.; Recio, J. L.; Ruperez, M., Liquid chromatography coupled to isotope ratio mass spectrometry: A new perspective on honey adulteration detection. *Journal of Agricultural and Food Chemistry* **2006,** *54* (26), 9719-9727.

4. Elflein, L.; Raezke, K. P., Improved detection of honey adulteration by measuring differences between C-13/C-12 stable carbon isotope ratios of protein and sugar compounds with a combination of elemental analyzer - isotope ratio mass spectrometry and liquid chromatography - isotope ratio mass spectrometry (delta C-13-EA/LC-IRMS). *Apidologie* **2008,** *39* (5), 574-587.

5. Forstel, H., The natural fingerprint of stable isotopes--use of IRMS to test food authenticity. *Anal Bioanal Chem* **2007,** *388* (3), 541-4.

6. Aelion, C. M.; Höhener, P.; Hunkeler, D.; Aravena, R., *Environmental isotopes in biodegradation and bioremediation*. CRC Press: Boca Raton, FL, USA, 2010.

7. Jasper, J. P.; Fourel, F.; Eaton, A.; Morrison, J.; Phillips, A., Stable isotopic characterization of analgesic drugs. *Pharmaceutical Technology* **2004,** *28* (8), 60-67.

8. Silvestre, V.; Mboula, V. M.; Jouitteau, C.; Akoka, S.; Robins, R. J.; Remaud, G. S., Isotopic C-13 NMR spectrometry to assess counterfeiting of active pharmaceutical ingredients: Site-specific C-13 content of aspirin and paracetamol. *Journal of Pharmaceutical and Biomedical Analysis* **2009,** *50* (3), 336-341.

9. Kurashima, N.; Makino, Y.; Urano, Y.; Sanuki, K.; Ikehara, Y.; Nagano, T., Use of stable isotope ratios for profiling of industrial ephedrine samples: application of hydrogen isotope ratios in combination with carbon and nitrogen. *Forensic Sci Int* **2009,** *189* (1-3), 14-8.

10. Schmidt, T. C.; Zwank, L.; Elsner, M.; Berg, M.; Meckenstock, R. U.; Haderlein, S. B., Compound-specific stable isotope analysis of organic contaminants in natural environments: a critical review of the state of the art, prospects, and future challenges. *Analytical and Bioanalytical Chemistry* **2004,** *378* (2), 283-300.

11. Elsner, M., Stable isotope fractionation to investigate natural transformation mechanisms of organic contaminants: principles, prospects and limitations. *Journal of Environmental Monitoring* **2010,** *12* (11), 2005-2031.

12. Kujawinski, D. M.; Stephan, M.; Jochmann, M. A.; Krajenke, K.; Haas, J.; Schmidt, T. C., Stable carbon and hydrogen isotope analysis of methyl tert-butyl ether and tert-amyl

methyl ether by purge and trap-gas chromatography-isotope ratio mass spectrometry: Method evaluation and application. *Journal of Environmental Monitoring* **2010,** *12* (1), 347-354.

13. Craig, H., Isotopic standards for carbon and oxygen and correction factors for mass-spectrometric analysis of carbon dioxide. *Geochimica et Cosmochimica Acta* **1957,** *12*, 133-149.

14. Zhang, Q.-L.; Li, W.-J., A calibrated measurement of the atomic-weight of carbon. *Chinese Science Bulletin* **1990,** *35*, 290.

15. Coplen, T. B.; Brand, W. A.; Gehre, M.; Groning, M.; Meijer, H. A.; Toman, B.; Verkouteren, R. M.; International Atomic Energy, A., After two decades a second anchor for the VPDB delta13C scale. *Rapid Commun Mass Spectrom* **2006,** *20* (21), 3165-6.

16. Cook, P. F., *Enzyme mechanism from isotope effects*. Boca Raton [u.a.] : CRC Press: Boca Raton, 1991.

17. Vanhaecke, F.; Balcaen, L.; Malinovsky, D., Use of single-collector and multi-collector ICP-mass spectrometry for isotopic analysis. *Journal of Analytical Atomic Spectrometry* **2009,** *24* (7), 863-886.

18. Sharp, Z., *Principles of Stable Isotope Geochemistry*. Pearson Prentice Hall: Upper Saddle River, USA, 2007.

19. Sessions, A. L., Isotope-ratio detection for gas chromatography. *Journal of Separation Science* **2006,** *29* (12), 1946-1961.

20. St-Jean, G., Automated quantitative and isotopic (C-13) analysis of dissolved inorganic carbon and dissolved organic carbon in continuous-flow using a total organic carbon analyser. *Rapid Communications in Mass Spectrometry* **2003,** *17* (5), 419-428.

21. Krummen, M.; Hilkert, A. W.; Juchelka, D.; Duhr, A.; Schluter, H. J.; Pesch, R., A new concept for isotope ratio monitoring liquid chromatography/mass spectrometry. *Rapid Communications in Mass Spectrometry* **2004,** *18* (19), 2260-2266.

22. Brand, W. A., Mass Spectrometer Hardware for Analyzing Stable Isotope Ratios. In *Handbook of Stable Isotope Analytical Techniques*, de Groot, P. A., Ed. 2004; Vol. 1.

23. Elsig, J.; Leuenberger, M. C., C-13 and O-18 fractionation effects on open splits and on the ion source in continuous flow isotope ratio mass spectrometry. *Rapid Communications in Mass Spectrometry* **2010,** *24* (10), 1419-1430.

24. Santrock, J.; Studley, S. A.; Hayes, J. M., Isotopic analyses based on the mass spectrum of carbon dioxide. *Anal Chem* **1985,** *57* (7), 1444-8.

25. Werner, R. A.; Brand, W. A., Referencing strategies and techniques in stable isotope ratio analysis. *Rapid Communications in Mass Spectrometry* **2001,** *15* (7), 501-519.

26. Abramson, F. P.; Black, G. E.; Lecchi, P., Application of high-performance liquid chromatography with isotope-ratio mass spectrometry for measuring low levels of enrichment of underivatized materials. *Journal of Chromatography A* **2001,** *913* (1-2), 269-273.

27. Chen, P.; Teffera, Y.; Black, G. E.; Abramson, F. P., Flow injection with chemical reaction interface-isotope ratio mass spectrometry: An alternative to off-line combustion for detecting low levels of enriched C-13 in mass balance studies. *Journal of the American Society for Mass Spectrometry* **1999,** *10* (2), 153-158.

28. Teffera, Y.; Kusmierz, J. J.; Abramson, F. P., Continuous-flow isotope ratio mass spectrometry using the chemical reaction interface with either gas or liquid chromatographic introduction. *Analytical Chemistry* **1996,** *68* (11), 1888-1894.

29. Caimi, R. J.; Brenna, J. T., High-precision liquid chromatography-combustion isotope ratio mass-spectrometry. *Analytical Chemistry* **1993,** *65* (23), 3497-3500.

30. Brand, W. A.; Dobberstein, P., Isotope-Ratio-Monitoring Liquid Chromatography Mass Spectrometry (IRM-LCMS): First Results from a Moving Wire Interface System. *Isotopes in environmental and health studies* **1996,** *32* (2-3), 275-83.

31. Tsitonaki, A.; Petri, B.; Crimi, M.; Mosbæk, H.; Siegrist, R. L.; Bjerg, P. L., In Situ Chemical Oxidation of Contaminated Soil and Groundwater Using Persulfate: A Review. *Critical Reviews in Environmental Science and Technology* **2010,** *40* (1), 55-91.

32. Kolev, S.; McKelvie, I., *Advances in Flow Injection Analysis and Related Techniques*. Elsevier: 2008; p 808.

33. Hettmann, E.; Brand, W. A.; Gleixner, G., Improved isotope ratio measurement performance in liquid chromatography/isotope ratio mass spectrometry by removing excess oxygen. *Rapid Communications in Mass Spectrometry* **2007,** *21* (24), 4135-4141.

34. Tchapla, A.; Colin, H.; Guiochon, G., Linearity of homologous series retention plots in reversed-phase liquid chromatography. *Analytical Chemistry* **1984,** *56* (4), 621-625.

35. Snyder, L. R.; Kirkland, J. J.; Dolan, J. W., *Introduction to Modern Liquid Chromatography*. 3. ed.; Wiley: Hoboken, New Jersey; USA, 2010.

36. Hinshaw, J. V., When Peaks Collide. *Lc Gc Europe 23* (7), 362-+.

37. Ricci, M. P.; Merritt, D. A.; Freeman, K. H.; Hayes, J. M., Acquisition and Processing of Data for Isotope-Ratio-Monitoring Mass-Spectrometry. *Organic Geochemistry* **1994,** *21* (6-7), 561-571.

38. Filer, C. N., Isotopic fractionation of organic compounds in chromatography. *J. Label. Compd. Radiopharm.* **1999,** *42* (2), 169-197.

39. Caimi, R. J.; Brenna, J. T., Quantitative evaluation of carbon isotopic fractionation during reversed-phase high-performance liquid chromatography. *Journal of Chromatography A* **1997,** *757* (1-2), 307-310.

40. Perrin, C. L., Secondary equilibrium isotope effects on acidity. In *Advances in Physical Organic Chemistry, Vol 44*, 2010; Vol. 44, pp 123-171.

41. Piez, K. A.; Eagle, H., C-14 Isotope Effect On The Ion-Exchange Chromatography Of Amino Acids. *Journal of the American Chemical Society* **1956,** *78* (20), 5284-5287.

42. McLean, M.; Vestal, M. L.; Teffera, Y.; Abramson, F. P., Element- and isotope-specific detection for high-performance liquid chromatography using chemical reaction interface mass spectrometry. *Journal of Chromatography A* **1996,** *732* (2), 189-199.

43. Bode, S.; Denef, K.; Boeckx, P., Development and evaluation of a high-performance liquid chromatography/isotope ratio mass spectrometry methodology for delta C-13 analyses of amino sugars in soil. *Rapid Communications in Mass Spectrometry* **2009,** *23* (16), 2519-2526.

44. Yarnes, C.; Santos, F.; Singh, N.; Abiven, S.; Schmidt, M. W. I.; Bird, J. A., Stable isotopic analysis of pyrogenic organic matter in soils by liquid chromatography-isotope-ratio mass spectrometry of benzene polycarboxylic acids. *Rapid Communications in Mass Spectrometry* **2011,** *25* (24), 3723-3731.

45. Abaye, D. A.; Morrison, D. J.; Preston, T., Strong anion exchange liquid chromatographic separation of protein amino acids for natural 13C-abundance determination by isotope ratio mass spectrometry. *Rapid Communications in Mass Spectrometry* **2011,** *25* (3), 429-435.

46. Du, X. L.; Black, G. E.; Lecchi, P.; Abramson, F. P.; Sprang, S. R., Kinetic isotope effects in Ras-catalyzed GTP hydrolysis: Evidence for a loose transition state. *Proceedings of the National Academy of Sciences of the United States of America* **2004,** *101* (24), 8858-8863.

47. Morrison, D. J.; Taylor, K.; Preston, T., Strong anion-exchange liquid chromatography coupled with isotope ratio mass spectrometry using a Liquiface interface. *Rapid Communications in Mass Spectrometry* **2010,** *24* (12), 1755-1762.

48. Schierbeek, H.; Moerdijk-Poortvliet, T. C. W.; van den Akker, C. H. P.; te Braake, F. W. J.; Boschker, H. T. S.; van Goudoever, J. B., Analysis of [U-C-13(6)]glucose in human plasma using liquid chromatography/isotope ratio mass spectrometry compared with two other mass spectrometry techniques. *Rapid Communications in Mass Spectrometry* **2009,** *23* (23), 3824-3830.

49. Boschker, H. T. S.; Moerdijk-Poortvliet, T. C. W.; van Breugel, P.; Houtekamer, M.; Middelburg, J. J., A versatile method for stable carbon isotope analysis of carbohydrates by high-performance liquid chromatography/isotope ratio mass spectrometry. *Rapid Communications in Mass Spectrometry* **2008,** *22* (23), 3902-3908.

50. Rinne, K. T.; Saurer, M.; Streit, K.; Siegwolf, R. T. W., Evaluation of a liquid chromatography method for compound-specific delta(13) C analysis of plant carbohydrates in alkaline media. *Rapid communications in mass spectrometry : RCM* **2012,** *26* (18), 2173-85.

51. Godin, J. P.; Hopfgartner, G.; Fay, L., Temperature-programmed high-performance liquid chromatography coupled to isotope ratio mass spectrometry. *Analytical Chemistry* **2008,** *80* (18), 7144-7152.

52. Cabanero, A. I.; Recio, J. L.; Ruperez, M., Isotope ratio mass spectrometry coupled to liquid and gas chromatography for wine ethanol characterization. *Rapid Communications in Mass Spectrometry* **2008,** *22* (20), 3111-3118.

53. Cabanero, A. I.; Recio, J. L.; Ruperez, M., Simultaneous Stable Carbon Isotopic Analysis of Wine Glycerol and Ethanol by Liquid Chromatography Coupled to Isotope Ratio Mass Spectrometry. *Journal of Agricultural and Food Chemistry* **2010,** *58* (2), 722-728.

54. Godin, J. P.; Breuille, D.; Obled, C.; Papet, I.; Schierbeek, H.; Hopfgartner, G.; Fay, L. B., Liquid and gas chromatography coupled to isotope ratio mass spectrometry for the determination of C-13-valine isotopic ratios in complex biological samples. *Journal of Mass Spectrometry* **2008,** *43* (10), 1334-1343.

55. Godin, J. P.; Hau, J.; Fay, L. B.; Hopfgartner, G., Isotope ratio monitoring of small molecules and macromolecules by liquid chromatography coupled to isotope ratio mass spectrometry. *Rapid Communications in Mass Spectrometry* **2005,** *19* (18), 2689-2698.

56. Guyon, F.; Gaillard, L.; Salagoity, M.-H.; Medina, B., Intrinsic ratios of glucose, fructose, glycerol and ethanol C-13/C-12 isotopic ratio determined by HPLC-co-IRMS: toward determining constants for wine authentication. *Analytical and Bioanalytical Chemistry 401* (5), 1551-1558.

57. Heuer, V.; Elvert, M.; Tille, S.; Krummen, M.; Mollar, X. P.; Hmelo, L. R.; Hinrichs, K. U., Online delta C-13 analysis of volatile fatty acids in sediment/porewater systems by liquid chromatography-isotope ratio mass spectrometry. *Limnology and Oceanography-Methods* **2006,** *4*, 346-357.

58. Reinnicke, S.; Bernstein, A.; Elsner, M., Small and Reproducible Isotope Effects during Methylation with Trimethylsulfonium Hydroxide (TMSH): A Convenient

Derivatization Method for Isotope Analysis of Negatively Charged Molecules. *Analytical Chemistry* **2010,** *82* (5), 2013-2019.

59. Yang, Y.; Belghazi, M.; Lagadec, A.; Miller, D. J.; Hawthorne, S. B., Elution of organic solutes from different polarity sorbents using subcritical water. *Journal of Chromatography A* **1998,** *810* (1-2), 149-159.

60. Teutenberg, T., *High-Temperature Liquid Chromatography - A User's Guide for Method Development*. RSCPublishing: 2010; Vol. 1.

61. Teutenberg, T.; Tuerk, J.; Holzhauser, M.; Kiffmeyer, T. K., Evaluation of column bleed by using an ultraviolet and a charged aerosol detector coupled to a high-temperature liquid chromatographic system. *Journal of Chromatography A* **2006,** *1119* (1-2), 197-201.

62. Zhang, L.; Kujawinski, D. M.; Jochmann, M. A.; Schmidt, T. C., High-temperature reversed-phase liquid chromatography coupled to isotope ratio mass spectrometry. *Rapid Communications in Mass Spectrometry* **2011,** *25* (20), 2971–2981.

63. McCullagh, J. S. O., Mixed-mode chromatography/isotope ratio mass spectrometry. *Rapid Communications in Mass Spectrometry* **2010,** *24* (5), 483-494.

64. McCullagh, J. S. O.; Juchelka, D.; Hedges, R. E. M., Analysis of amino acid C-13 abundance from human and faunal bone collagen using liquid chromatography/isotope ratio mass spectrometry. *Rapid Communications in Mass Spectrometry* **2006,** *20* (18), 2761-2768.

65. Raghavan, M.; McCullagh, J. S. O.; Lynnerup, N.; Hedges, R. E. M., Amino acid delta C-13 analysis of hair proteins and bone collagen using liquid chromatography/isotope ratio mass spectrometry: paleodietary implications from intra-individual comparisons. *Rapid Communications in Mass Spectrometry* **2010,** *24* (5), 541-548.

66. Smith, C. I.; Fuller, B. T.; Choy, K.; Richards, M. P., A three-phase liquid chromatographic method for delta C-13 analysis of amino acids from biological protein hydrolysates using liquid chromatography-isotope ratio mass spectrometry. *Analytical Biochemistry* **2009,** *390* (2), 165-172.

67. Dunn, P. J. H.; Honch, N. V.; Evershed, R. P., Comparison of liquid chromatography-isotope ratio mass spectrometry (LC/IRMS) and gas chromatography-combustion-isotope ratio mass spectrometry (GC/C/IRMS) for the determination of collagen amino acid delta(13) C values for palaeodietary and palaeoecological reconstruction. *Rapid Communications in Mass Spectrometry* **2011,** *25* (20), 2995-3011.

68. Lynch, A. H.; McCullagh, J. S. O.; Hedges, R. E. M., Liquid chromatography/isotope ratio mass spectrometry measurement of delta(13) C of amino acids in plant proteins. *Rapid communications in mass spectrometry : RCM* **2011,** *25* (20), 2981-8.

69. Schierbeek, H.; Braakel, F. T.; Godin, J. P.; Fay, L. B.; van Goudoever, J. B., Novel method for measurement of glutathione kinetics in neonates using liquid chromatography coupled to isotope ratio mass spectrometry. *Rapid Communications in Mass Spectrometry* **2007,** *21* (17), 2805-2812.

70. Schierbeek, H.; Rook, D.; Braake, F.; Dorst, K. Y.; Voortman, G.; Godin, J. P.; Fay, L. B.; van Goudoever, J. B., Simultaneous analysis of C-13-glutathione as its dimeric form GSSG and its precursor [1-C-13]glycine using liquid chromatography/isotope ratio mass spectrometry. *Rapid Communications in Mass Spectrometry* **2009,** *23* (18), 2897-2902.

71. Zhang, L.; Kujawinski, D. M.; Federherr, E.; Schmidt, T. C.; Jochmann, M. A., Caffeine in Your Drink: Natural or Synthetic? *Analytical Chemistry* **2012,** *84* (6), 2805-2810.

72. Cabanero, A. I.; Recio, J. L.; Ruperez, M., Liquid Chromatography Coupled to Isotope Ratio Mass Spectrometry: A New Perspective on Honey Adulteration Detection. *J. Agric. Food Chem.* **2006,** *54* (26), 9719-9727.

73. Choy, K.; Smith, C. I.; Fuller, B. T.; Richards, M. P., Investigation of amino acid delta C-13 signatures in bone collagen to reconstruct human palaeodiets using liquid chromatography-isotope ratio mass spectrometry. *Geochimica Et Cosmochimica Acta* **2010,** *74* (21), 6093-6111.

74. Brandes, J. A., Rapid and precise delta C-13 measurement of dissolved inorganic carbon in natural waters using liquid chromatography coupled to an isotope-ratio mass spectrometer. *Limnology and Oceanography-Methods* **2009,** *7*, 730-739.

75. Du, X. L.; Ferguson, K.; Gregory, R.; Sprang, S. R., A method to determine O-18 kinetic isotope effects in the hydrolysis of nucleotide triphosphates. *Analytical Biochemistry* **2008,** *372* (2), 213-221.

3 HT-HPLC for the isotopic analysis of sulfonamide drugs and trimethoprim

Published in: Kujawinski, D. M.; Zhang, L.; Schmidt, T. C.; Jochmann, M. A., **When Other Separation Techniques Fail: Compound-Specific Carbon Isotope Ratio Analysis of Sulfonamide Containing Pharmaceuticals by High-Temperature-Liquid Chromatography-Isotope Ratio Mass Spectrometry**. *Analytical Chemistry* **2012,** *84* (18), 7656-7663.

Abstract

Compound-specific isotope analysis (CISA) of non-volatile analytes has been enabled by the introduction of the first commercial interface to hyphenate liquid chromatography with an isotope ratio mass spectrometer (LC-IRMS) in 2004, yet carbon isotope analysis of unpolar and moderately polar compounds is still a challenging task since only water as eluent and no organic modifiers can be used to drive the separation in LC. The only way to increase the elution strength of aqueous eluents in reversed phase LC is the application of high temperatures to mobile and stationary phase (HTLC-IRMS). In this context we present the first method to determine carbon isotope ratios of pharmaceuticals that cannot be separated by already existing separation techniques for LC-IRMS, such as reversed phase chromatography at normal temperatures, ion-chromatography and mixed mode chromatography. The pharmaceutical group of sulfonamides, which is generally mixed with trimethoprim in pharmaceutical products, has been chosen as probe compounds. Substance amounts as low as 0.3 µg are sufficient to perform a precise analysis. Successful applicability and reproducibility of this method is shown by the analysis of real pharmaceutical samples. The method provides the first tool to study the pharmaceutical authenticity as well as degradation and mobility of such substances in the environment by using the stable isotopic signature of these compounds.

3.1 Introduction

Compound-specific isotope analysis of non-volatile organic compounds is often performed by gas chromatography-isotope ratio mass spectrometry (GC-IRMS) with prior derivatization. [1] Although these methods give accurate and reproducible results, they are not applicable for many non-volatiles. The hyphenation of liquid chromatography (LC) to isotope ratio mass spectrometry enables the determination of carbon isotope ratios of very polar, thermolabile and high molecular weight compounds without the need for derivatization. [2] Due to the design of the interface organic modifiers cannot be used in LC eluents. [3] In order to precisely measure carbon isotope ratios, the analytes need to be detected as CO_2. In the interface, the whole column effluent is non-selectively converted to CO_2 by peroxodisulfate in a heated capillary, extracted from the aqueous phase into a carrier gas stream via a membrane, and transported to the IRMS inlet. Consequently, any additional carbon compound (either as

buffer or solvent) in the eluent besides analyte carbon would result in a severe decrease of sensitivity, wrong carbon isotope ratios or a saturation of the isotope ratio mass spectrometer signal.. This restricts the type of applicable separation techniques for LC-IRMS. Several methods have been reported for the determination of carbon isotope ratios of carbohydrates, amino sugars and amino acids based on ion exchange chromatography.[4-6]

However, with ion exchange as sole separation mechanism, it is difficult to obtain a full separation of proteinogenic amino acids.[2] The resolution of many amino acids can be substantially improved by adding the possibility for hydrophobic interactions by a further RP-column.[2] Almost all amino acids can be resolved by mixed-mode chromatography, i.e., the deliberate combination of RP and ion exchange interaction sites in one stationary phase, which is nowadays the most published method for LC-IRMS analysis of underivatized amino acids.[7] The stationary phase contains ion exchange groups bound to alkyl chains or phenyl rings, which also allow an operation with 100 % aqueous eluents without the risk of a loss of retention due to particle pore de-wetting.

There are no studies, which use ion chromatography or mixed mode chromatography for compound-specific isotope analysis of pharmaceuticals. Solely, carbon isotope ratios of paracetamol and aspirin have been measured to show the applicability of the LC-IRMS interface system. In this study a reversed phase (RP) silica based column at ambient temperature was used to separate those two compounds.[3] However, it is obvious, that also ion chromatography as well as mixed mode chromatography can be used for those pharmaceuticals. In the following, we will discuss, why reversed phase separation at ambient temperatures, HTLC separation with porous graphitic carbon materials, ion chromatography and mixed-mode phases cannot are not feasible for the here investigated pharmaceutical compound classes of sulfonamides and trimethoprim.

Sulfonamides are amphoteric target compounds which are negatively charged at pH values greater than 8 and positively at very low pH. In theory, both anion as well as cation exchange chromatography may work under these circumstances. However, a change of the pH to 8 would result in negatively charged sulfonamides but there is no anionic group at any pH for trimethoprim. To this end, a separation of the chosen target compounds would not be possible. Since trimethoprim is usually combined in pharmaceutical products containing sulfonamides, valuable information on its carbon isotope ratio would be lost. Another problem at pH 8 is an increased background caused by a much higher solubility of CO_2 from air in the employed eluents, which requires a sophisticated eluent preparation and conservation in order to maintain a low baseline in the chromatogram. Apart from the above mentioned criteria against anion exchange, cation exchange is not a good option, since the pH of the mobile phase should be two pH units below pK_a for good peak shape and so a high concentration of acid would be necessary in the eluent. Despite these rather practical reasons the retention of the target sulfonamides and trimethoprim on such columns will remain a mixture of ion exchange and reversed phase chromatography due to hydrophobic interactions with the polymeric support of the ion exchange resin.

Such an intentional combination of retention mechanisms is utilized in the mixed-mode columns mentioned above. In case of amino acids it was shown that these stationary phases work well because the elution strength of water is high enough to elute hydrophobic amino

acids form the mixed-mode phase without assistance of organic modifiers.[7] In contrast to this, using comparable mixed-mode phases for sulfonamides and trimethoprim a much higher retention than for a reversed phase separation is expected due electrostatic and strong hydrophobic interactions. Thus, this method would require an organic proportion in the mobile phase to aid elution, which is not compatible with LC-IRMS, or operate the chromatography at higher temperatures. But the temperature stability of mixed-mode columns remains to be examined.

An alternative approach that overcomes these described restrictions is high temperature liquid chromatography (HTLC). HTLC coupled to IRMS has already been used to determine carbon isotope ratios of small organic acids[8] and caffeine derivatives.[9] The elution strength of aqueous mobile phases without organic modifiers is often too low to elute compounds from unpolar stationary phases at ambient temperatures. Especially, for the here investigated compounds elution times increase dramatically, which results in inadequate retention times, a loss in resolution and signal sensitivity. The application of temperatures notably higher than ambient to mobile phase and column has been proposed to substitute organic solvents.[10] With increasing temperatures the static permittivity and viscosity of water decreases. At 150 °C (at a pressure of 50 bar) the static permittivity of water is nearly the same as that of about 70 % methanol or acetonitrile/water mixtures.[10] Thus, elution strength of pure aqueous mobile phases in RP chromatography at high temperatures is similar to solvent/water mixtures encountered in RP-LC. Temperature gradients instead of solvent gradients can be used to separate compounds on nonpolar stationary phases such as octadecyl silica or porous graphitized carbon (PGC). Temperature-programmed elution can even be predicted from two measurements with different temperature gradients.[11]

As the LC-IRMS detector is very sensitive to any carbon containing compound, a major concern using high temperature liquid chromatography (HTLC) is the carbon feed from the column into the interface. At high temperature column bleed is much higher due to faster hydrolysis of the support material and bonded phase. Column bleed invisible for most common LC detection techniques may overlay the analyte peak or produce elevated background levels. Thus, Zhang et al.[9] evaluated four stationary phases which have proven their temperature stability in previous studies. [12] Hybrid particles from ethylene bridged silica and zirconium dioxide based materials can be used with excellent results for LC-IRMS at HTLC conditions. Up to column-specific maximum temperatures column bleed did not affect $\delta^{13}C$ values of various probe compounds. [9] It also has to be considered that carry over or late elution of hydrophobic compounds retained on very unpolar phases like PGC can alter $\delta^{13}C$ values of the analytes due to ghost peaks or occasional change in background $^{13}C/^{12}C$-ratio. Additionally, $\delta^{13}C$-values of thermolabile analytes may be influenced by isotopic fractionations resulting from thermal degradation on the column.[13] Porous graphitic carbon columns such as the Hypercarb possess very high retention at ambient temperatures.[13] Although the retention times are decreased at higher temperatures, an unacceptable column bleed can be observed during temperature gradient elution.[8]

The aim of this work was to show that a HTLC can be used for the determination of carbon isotope ratios of sulfamerazine, sulfadiazine, sulfamethoxazole, sulfathiazole and trimethoprim. These antibiotic substances have been widely used in veterinary and human

medicine for some decades. Although they have been subject of many research campaigns in environmental[14] and pharmaceutical science[15] so far, but no determination of isotope ratios at natural abundance has been published. Several HTLC methods for trimethoprim and sulfonamide measurements have been published in literature [11, 16-17] for quantitative analysis, but to our best knowledge no carbon-free eluents have been used and no stable isotope signatures of these compounds have been determined. Until now, isotope ratios of polar active pharmaceutical ingredients can only be determined either by ^{13}C-NMR or labor-intensive offline techniques like preparative LC followed by elemental analyzer (EA-IRMS). Here, we demonstrate a pure aqueous separation of these compounds for its use in CSIA and proved its potential for verifying the authenticity of antibiotics containing sulfamethoxazole and trimethoprim via δ^{13}C values.

3.2 Experimental

3.2.1 Chemicals and Reagents

Analytical standards of sulfadiazine, sulfathiazole, sulfamerazine, sulfamethoxazole and trimethoprim were purchased from Sigma-Aldrich GmbH (Steinheim, Germany) in a purity of at least 98 %. Sulfamethoxazole and trimethoprim were purchased from Sigma-Aldrich GmbH (Steinheim, Germany) as well but in >99 % purity (VETRANAL™). Structures and pK_a-values of these compounds are listed in Table 3.1. Sodium peroxodisulfate ($Na_2S_2O_8$), phosphoric acid (H_3PO_4) and sodium hydrogenphosphate (NaH_2PO_4) for eluent and reagent solutions were supplied by Fluka (Steinheim, Germany). Reagent solutions and eluents were degassed in an ultrasonic bath (Bandein Eletronic, Berlin, Germany) under vacuum (Vacuubrand, Wertheim, Germany). In order to avoid regassing these solutions were continuously purged with helium of 99.999 % purity (Air Liquide, Oberhausen, Germany) at a flow rate of approximately 30 mL min^{-1}.

3.2.2 Analytical standard solutions

Standard solutions of sulfonamides were freshly prepared prior to each set of analyses by dissolving a required amount of substance in 15 mL HTLC buffer solution at approximately 60 °C.

Table 3.1 Physico-chemical properties and structures of the investigated substances

Compound	pK_{a1}[18]	pK_{a2}[18]	Molecular formula (MW/ g mol^{-1})	CAS-No.
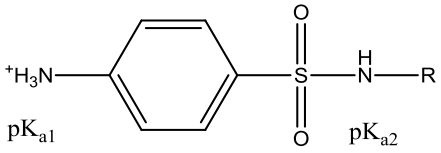				
Sulfadiazine 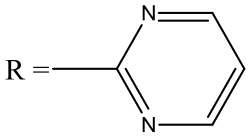	1.6	6.8	$C_{10}H_{10}N_4O_2S$ (250.28)	68-35-9
Sulfathiazole 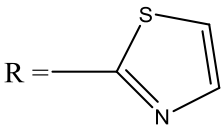	2.01	7.11	$C_9H_9N_3O_2S_2$ (255.32)	144-74-1
Sulfamerazine 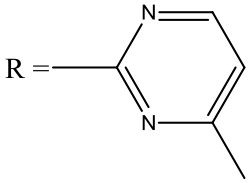	2.07	6.9	$C_{11}H_{12}N_4O_2S$ (264.31)	127-58-2
Sulfamethoxazole 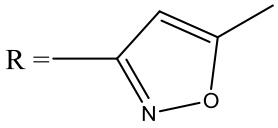	1.85	5.60	$C_{10}H_{11}N_3O_3S$ (253.28)	723-46-6
Trimethoprim 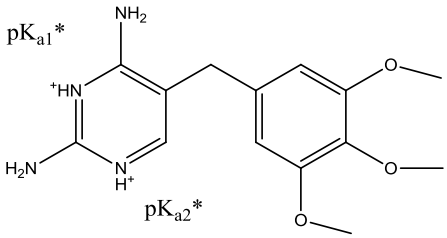	3.23	6.76	$C_{14}H_{18}N_4O_3$ (290.32)	738-70-5
*single mesomeric structure showing the inital protonation sites				

3.2.3 LC conditions

HTLC system consisted of a Rheos Allegro binary pump (Flux Instruments, Buchs, Switzerland) and a HT-HPLC 200 column oven (SIM Scientific Instruments Manufacturer GmbH, Oberhausen, Germany). The compounds were separated on an XBridge C_{18} column 100 x 2.1 mm, 3.5 µm particle size equipped with a 10 x 2.1 mm pre-column packed with the same material (Waters, Eschborn, Germany). A sodium phosphate buffer of 5 mM and pH 3 was used as the eluent at a flow rate of 500 µL min^{-1}. The temperature gradient was 60 °C for 3 min, then to 80 °C at 3 °C min^{-1}, held for 15 min, then to 100 °C at 3 °C min^{-1} and held for 5 min.

Flushing of the organic solvent from shipping or storage of the column prior to measurements was done while the column was installed in the HT-LC-IRMS system. In order to prevent precipitation the column was first flushed for 2 hours with pure water and afterwards equilibrated with the phosphate buffer for 1 hour at a flow rate of 500 µL min^{-1}.

3.2.4 LC-IRMS interface conditions

As interface between HPLC and IRMS an LC-IsoLink (Thermo Scientific, Bremen, Germany) was used. The wet chemical oxidation of the compounds was realized by online mixing of HPLC column effluent with phosphoric acid (1.5 M) and sodium peroxodisulfate (200 g L^{-1}) at a reactor temperature of 99.9 °C. For all experiments flow rates of both reagents were set to 50 µL min^{-1}. The formed CO_2 was separated from the aqueous phase by a gas exchange membrane and transferred to the open split in a Helium stream (Air Liquide, Oberhausen, purity 99.999 %) at a flow rate of 1.2 mL min^{-1}.

Without HPLC column this interface can be used for bulk carbon isotope ratio determination by flow injection analysis (FIA). The carrier flow rate to transport the bulk sample from the sample loop to the interface was set to 200 µL min^{-1}, 350 µL min^{-1} and 500 µl min^{-1} whereas reagent flow rates remained at 50 µL min^{-1} each.

The mass spectrometric detection was performed on a Delta V Advantage (Thermo Electron, Bremen, Germany) tuned on maximum linearity. Linearity and precision of the instrument were checked regularly by reference gas pulses of different amplitudes.

3.2.5 EA-IRMS

Elemental Analyzer CE 1110 (CE Instruments, Milano, Italy) coupled with a ConFlo IV Interface to an MAT 253 isotope ratio mass spectrometer (both Thermo Scientific, Bremen, Germany) was used to determine $\delta^{13}C$ values of the analytical standards and bulk isotope ratios of the homogenized pharmaceutical pills. EA-IRMS values were obtained as described by Werner and Brand.[19] Reference materials for calibration of the working standard acetanilide to IAEA scale were NBS-22 (oil; $\delta^{13}C = -30.031$ ‰), IAEA-CH-6 (sucrose; $\delta^{13}C = -10.449$ ‰) and IAEA 600 (caffeine; $\delta^{13}C = -27.771$ ‰).

3.2.6 Sample Preparation

Samples of pharmaceutical tablets (trade-names *cotrim* and *cotrimoxazole*) of six different manufacturers each containing 800 mg sulfamethoxazole and 160 mg trimethoprim were homogenized and dissolved with the HPLC eluent to 100 mg L^{-1} of the specific analyte according to the concentration declaration in the package inserts. Besides the active ingredients the pills contained excipients like starch and stearate salts.

3.2.7 Data acquisition and handling

Acquisition and processing of data was performed by Isodat 2.5. The background subtraction algorithm used for these measurements was "individual background". All reported $\delta^{13}C$ values are normalized to the VPDB scale. All standard deviations refer to triplicate measurements if not stated otherwise. $\delta^{13}C$ values of the pharmaceutical samples were corrected with the difference of $\delta^{13}C$ values between EA-IRMS measurements of the particular compound and HTLC-IRMS analyses. This corresponds to the principle of identical treatment as it was proposed by Werner and Brand.[19]

The reference gas pulses were used as an internal standard to calculate relative peak area per carbon. The pressure of the reference gas remained unchanged during the FIA measurements so that any variation of ionization between the runs is eliminated and peak areas can be compared.

Chromatographic resolution R_s was calculated according to equation:[20]

$$R_s = 2\left(\frac{t_{r(2)} - t_{r(1)}}{w_{h(2)} + w_{h(1)}}\right)$$

Here, t_r is the retention time of peak 1 or 2 and w_h is the peak width at half height for the two peaks.

3.3 Results and discussion

3.3.1 Chromatographic conditions

All selected compounds can be baseline separated by the use of a temperature gradient. Figure 3.1 shows a chromatogram and the temperature program applied. Resolution between sulfadiazine and sulfathiazole was three, which meets the requirement of a full separation (R = 2)[20] for compound-specific isotope analysis due to chromatographic isotope effects [21].

A temperature gradient with a low steepness of 3 °C min^{-1} was chosen to keep the rising of the baseline as low as possible. Godin et al. [8] reported low precision and accuracy when high rising backgrounds were observed due to steep temperature gradients on a PGC column. In contrast, Zhang et al. [9] did not observe significant loss in precision or accuracy using gradients between 6 and 9 °C min^{-1} for hybrid particles and zirconium based stationary phases. These findings demonstrate the importance of background subtraction algorithms. Godin et al.[8] and Zhang et al.[9] used the "dynamic background" function in ISODAT. In this work the slope of the background was between 0.17 and 0.5 mV s^{-1} so that individual background algorithm was used as suggested by Zhang et al. [9].

All sulfonamides have shown to be thermally stable during the chromatographic run. Peak shape as well as comparable $\delta^{13}C$ values to FIA of single compounds showed no indications of degradation inside the column. Only trimethoprim showed a large tailing which can either be a sign of thermal decomposition in the column or column overload. These triangular peak shapes at low pH have been associated to column overload of protonated basic substances on silica-based columns due to charge repulsion between retained protonated molecules [22-23](see Figure 3.1).

As pointed out by Godin et al.[8] thermal decomposition inside the column can influence $\delta^{13}C$ values. Since results obtained by FIA and HTLC are comparable (see Table 3.2), we suggest that even if thermal degradation of trimethoprim takes place, all metabolites elute as one peak and leave $\delta^{13}C$ values unaffected.

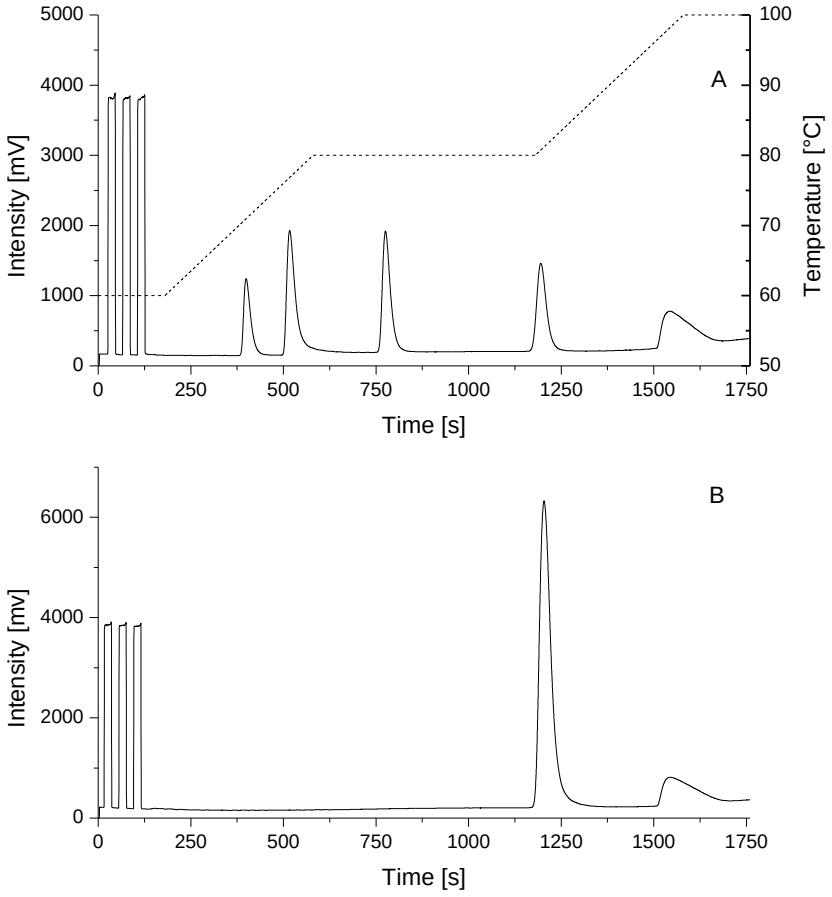

Figure 3.1 A) Chromatogram (*m*/*z* 44) of a standard mixture separated by a temperature gradient indicated by the dashed line. The elution order is sulfadiazine, sulfathiazole, sulfamerazine, sulfamethoxazole and trimethoprim. The concentration of each substance was 100 mg L^{-1}. **B) Chromatogram (*m*/*z* 44) of a pharmaceutical sample containing sulfamethoxazole and trimethoprim obtained by the same temperature gradient as above.**

3.3.2 Method detection limits and accuracy

Method detection limits (MDL) were calculated by the moving mean procedure[24] in order to account for any method-related offsets of $\delta^{13}C$ values. Here, the detection limit is defined as lowest concentration which is necessary to achieve the measurement of a $\delta^{13}C$ value with a defined precision (± 0.5 ‰) and accuracy with respect to signal height-independent isotope ratio[24].

MDLs of the selected sulfonamides and trimethoprim are given in Table 3.2. Sulfathiazole showed the lowest MDL of the selected compounds being 0.3 µg on column. If a poorer precision of isotope data is acceptable measurements of sulfadiazine, sulfamethoxazole and sulfathiazole can be performed even below those MDLs given in Table 3.2 (see Figure 3.2).

Comparing the results obtained by EA and both LC-IRMS measurement modes it can be seen that there is a discrepancy of $\delta^{13}C$ values for all selected compounds (see Table 3.2). This is in agreement with other studies where substance–specific differences of more than 1‰ have been reported for various substances[9, 25-26]. Although $\delta^{13}C$ values from EA measurements of the pure phase analytical standards might be biased by a contamination with other carbon

compounds, the authors believe that even with a compound with a high $\delta^{13}C$ value, such as a carbonate, the error is smaller than the analytical precision.

Table 3.2 HT-LC-IRMS performance evaluation

	MDL* [µg]	$\delta^{13}C_{HTLC}$ [‰]#	$\delta^{13}C_{FIA}$‡ [‰]#	$\delta^{13}C_{EA}$ [‰]#	$\delta^{13}C_{EA}-\delta^{13}C_{HTLC}$ [‰]
Sulfadiazine	0.4	−30.8 ± 0.1	−31.6 ±0.4	−29.2 ±0.2	1.6
Sulfathiazole	0.3	−28.5 ± 0.1	−29.6 ±0.4	−26.64 ±0.04	1.9
Sulfamerazine	0.5	−31.3 ± 0.3	−31.2 ±0.4	−28.90 ±0.03	2.4
Sulfamethoxazole	0.5	−30.7 ± 0.3	−30.3 ±0.2	−27.91 ±0.02	2.8
Trimethoprim	0.4	−37.6 ± 0.3	−37.6 ±0.2	−34.15 ±0.04	3.4

*as absolute amount on column

#Standard deviations refer to at least triplicate measurement

‡at a flow rate of 500 µL min^{-1}

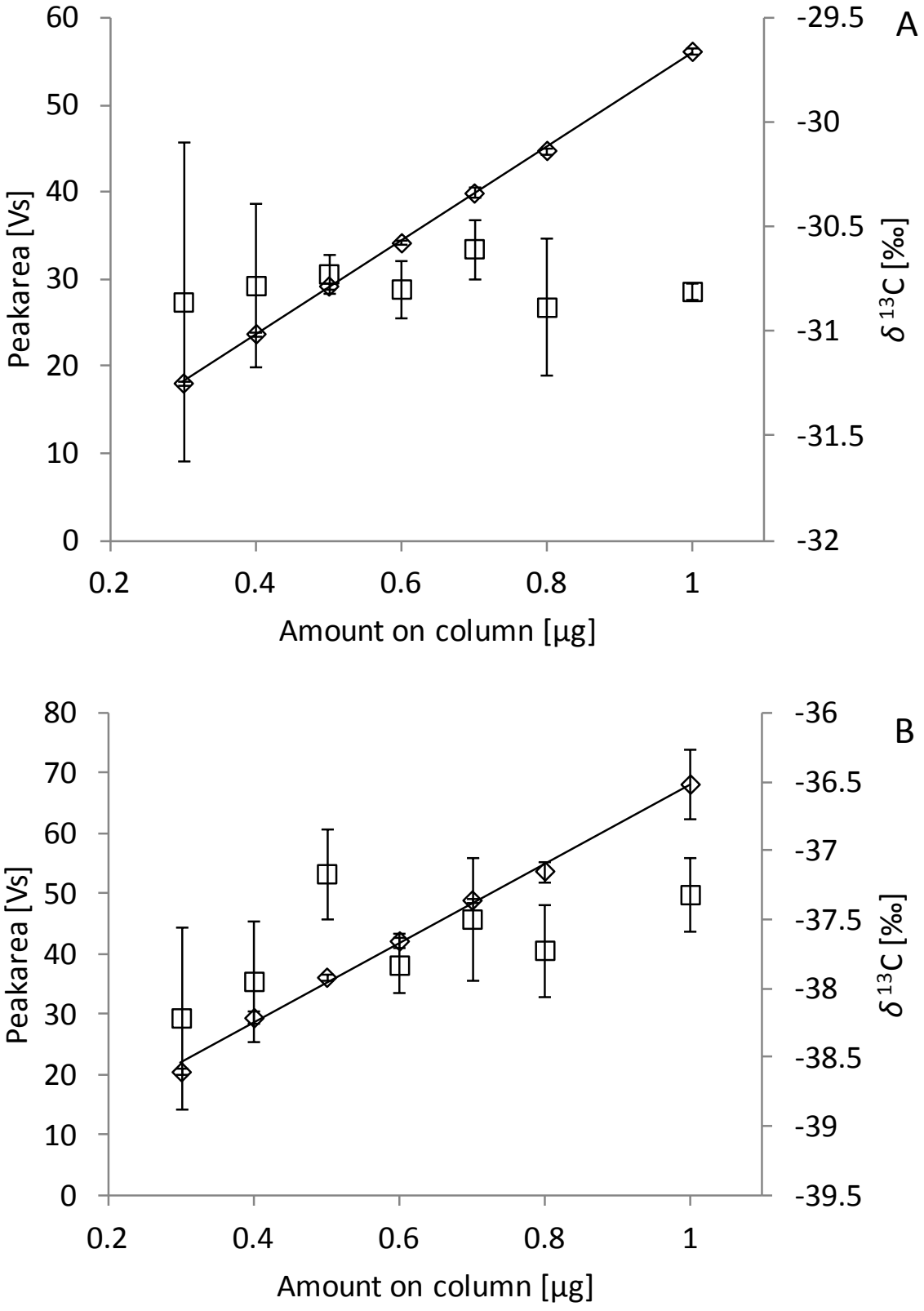

Figure 3.2 Representative calibration line of sulfadiazine (graph A) and trimethoprim (graph B). Diamonds correspond to the peak area of the m/z 44 trace whereas boxes relate to δ^{13}C values.

FIA-IRMS analyses have been conducted at different liquid carrier flow rates but with constant reagent flow rates to simulate the influence of HT-LC flow rate without compromising peak shape in order to investigate this offset. As can be seen from **Figure 3.3** the lower the carrier flow rate in the interface, the more do δ^{13}C-values of FIA approach δ^{13}C values of EA measurements. The peak area also shows a dependency on flow rate which confirms that oxidation is incomplete. Lower peak areas are observed in FIA when higher flow rates are applied because of reduced reaction time inside the oxidation reactor and lower reagent concentrations. The reagent is always delivered in far excess relative to the analyte so that concentration effects are irrelevant. In **Figure 3.4** the same data were used to compare the difference between EA measurements and FIA measurements with the relative carbon sensitivity (peak area per nmol C relative to the reference gas peak area) from flow rate variation. It shows that the sulfonamides have a similar mineralization mechanism assuming that ^{13}C and ^{12}C are equally distributed in the standard compounds.

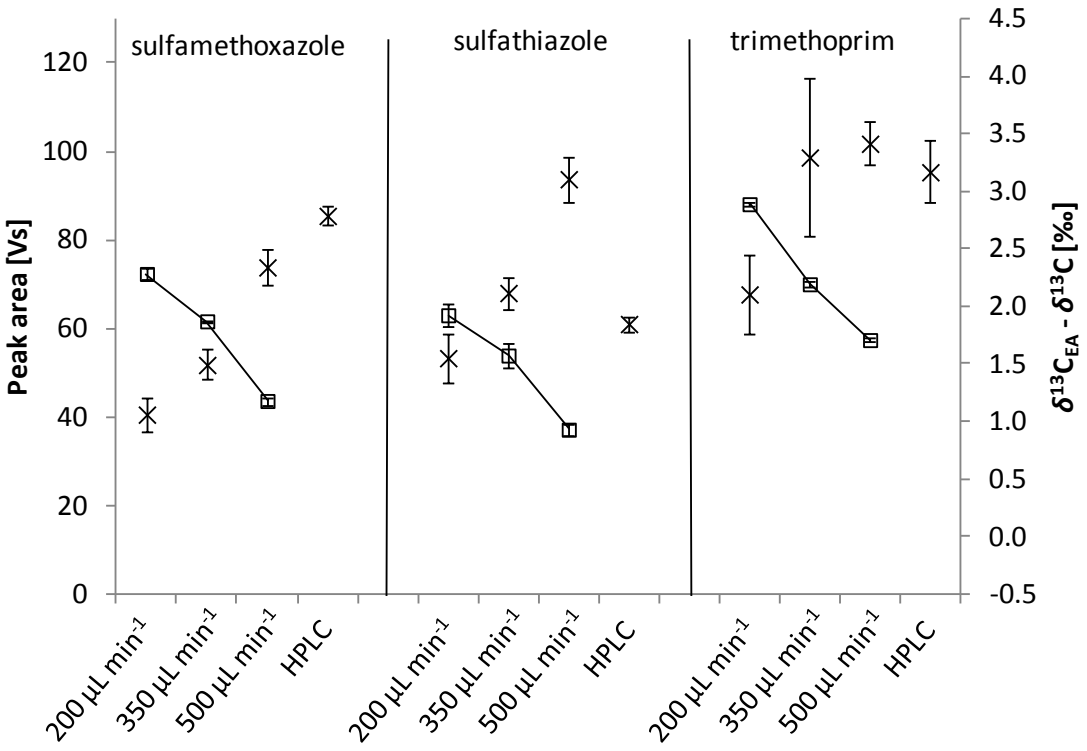

Figure 3.3 Peak areas (boxes) and δ^{13}C values (crosses) determined by FIA at various carrier flow rates and HTLC-IRMS at 500 µL min^{-1}. No peak areas are given for HTLC measurements due to incomparable ionization conditions with respect to FIA. Similar trends can be observed for sulfadiazine and sulfamerazine.

Incomplete extraction of formed CO_2 in the interface is not the reason for this bias since trimethoprim would follow the same trend as the sulfonamides and lead to a constant offset independent of substance. For all analytes δ^{13}C values were not dependent on concentration (see **Figure 3.2**). If incomplete gas extraction caused an isotopic fractionation, δ^{13}C values of

all analytes would be dependent on concentration to the same degree. Thus, this reproducible offset obviously derives from incomplete oxidation.

Smaller peak areas from incomplete conversion are unfavourable because of the loss in sensitivity resulting in the need to use lower flow rates in the HTLC. On the other hand, a reduction of the HTLC flow rate could lead to poor peak shape especially at the end of the chromatographic run where higher temperatures are employed and actually higher flow rates should be used in order not to affect efficiency[27]. Columns with a smaller inner diameter can be used due to their lower optimum flow rate but they might be overloaded by the injected sample amount required for LC-IRMS.[8]

For sulfamethoxazole, sulfamerazine and trimethoprim $\delta^{13}C_{HT\text{-}LC}$ values fit $\delta^{13}C_{FIA}$ values obtained at a flow rate of 500 µL min^{-1}. Sulfadiazine and sulfathiazole show a small difference of about 0.9 ‰.

Therefore, $\delta^{13}C$ values from samples have to be corrected by external standards if absolute values are needed.

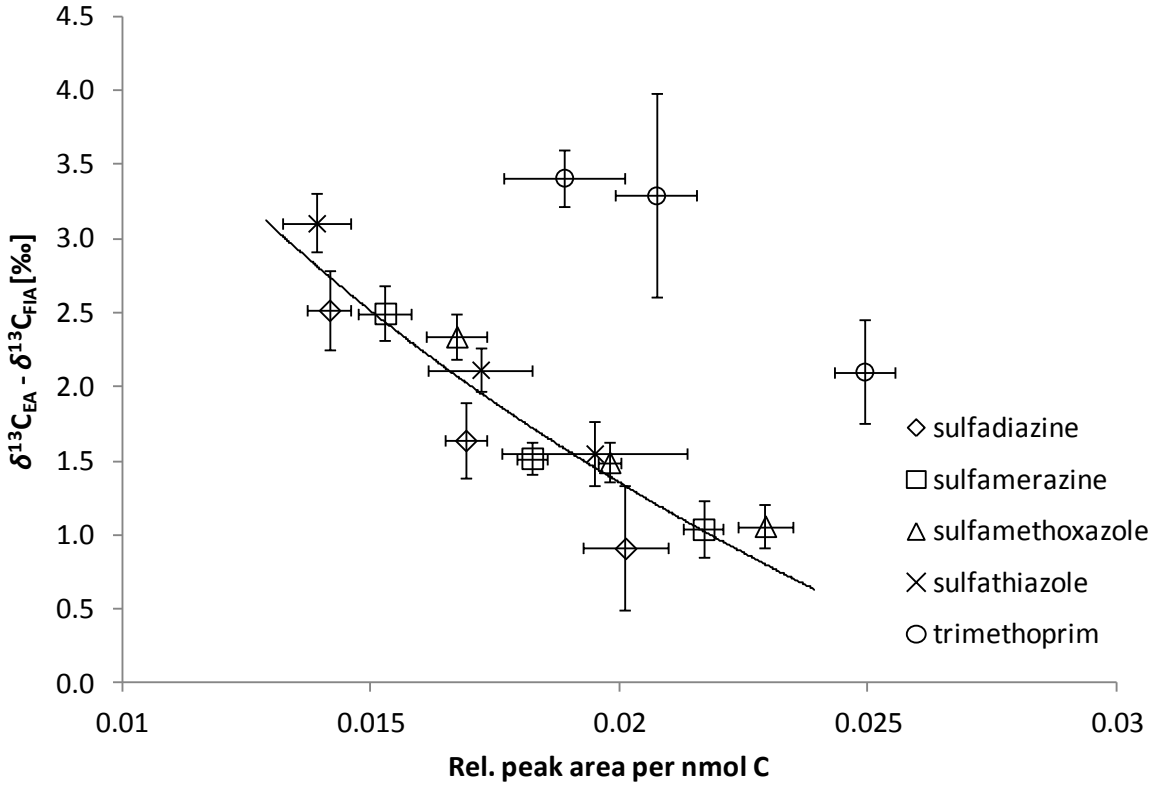

Figure 3.4 Dependency of the difference between EA-IRMS and FIA-IRMS derived $\delta^{13}C$ values on the relative peak area per nmol carbon obtained by different carrier flow rates. Peak areas per carbon amount were referenced to the reference gas peak in order to account for differences in ionization between the single measurements. The solid line represents a logarithmic fit of the sulfonamide results.

3.3.3 Sample analysis

Using common detection methods such as UV/vis or organic mass spectrometry many carbon-bearing substances are mostly not interfering with detection of the target analytes, in particular if analyte-specific wavelengths or mass-to-charge ratios are selected. Here, unexpected matrix compounds can cause errors in analyte peak area, e.g. if they co-elute or suppress ionization of the target analyte. However, a full baseline is not a prerequisite for an accurate concentration measurement; coelutions are accepted for the sake of analysis time. In contrast, in LC-IRMS, any carbon-containing compound is detected making baseline separation of matrix from the target compounds a crucial step in compound-specific LC-IRMS measurements. Overlapping peaks often cause inaccurate isotopic results as pointed out by McCullagh[7].

Pharmaceutical samples gave no noteworthy contribution of matrix peaks to the chromatogram (see **Figure 3.1B**). In the small set of samples analyzed in this work the variation of the corrected $\delta^{13}C$ values of sulfamethoxazole and trimethoprim from different manufacturers was small. However, there was a substantial difference between bulk sample $\delta^{13}C$ values and compound-specific $\delta^{13}C$ values (see **Table 3.3**).

It was observed that an aged column (column 1 in **Table 3.2**; >300 injections), showed an increased background signal due to column bleeding. To investigate the effect of an aged column on the measurement of the isotopic signature of the compounds, we compared the results with a second new column (see column 2 in **Table 3.3**). As shown in **Table 3.3**, repeated analysis of the pharmaceutical samples also proved a good repeatability of this method for most of the compounds. The same $\delta^{13}C$ values were obtained for five of the six measured samples. An exception was observed for sulfamethoxazole of brand B between the old (column 1) and the new column (column 2) and trimethoprim, which gave no reliable results. The difference of about 1 ‰ can be explained by a steep increase of the background caused by column bleeding.

A two dimensional plot of the $\delta^{13}C$ values of trimethoprim and sulfamethoxazole suggests that the combined analysis could identify falsified antibiotics containing these compounds (see **Figure 3.5**). Together with bulk $\delta^{13}C$ values the individual samples can be distinguished clearly from each other. But the analyzed set of samples is too small to draw statistically confirmed conclusions.

Table 3.3 Bulk and corrected compound-specific δ^{13}C-values of the measured pharmaceutical samples.

Brand	$\delta^{13}C_{bulk}$ [‰]	Sulfamethoxazole δ^{13}C [‰] column 1[a)]	Sulfamethoxazole δ^{13}C [‰] column 2[b)]	Trimethoprim δ^{13}C [‰] column 2
A	−29.6 ± 0.1	−27.6 ± 0.2	−27.7 ± 0.4	−31.1 ± 0.3
B	−29.7 ± 0.4	−27.6 ± 0.3	−28.6 ± 0.4	−30.9 ± 0.3
C	−28.46 ± 0.09	−28.4 ± 0.3	−28.4 ± 0.2	−31.9 ± 0.7
D	−28.5 ± 0.1	−28.0 ± 0.2	−28.1 ± 0.2	−32.1 ± 0.3
E	−30.0 ± 0.4	−27.4 ± 0.2	−27.2 ± 0.4	−30.8 ± 0.4
F	−29.67 ± 0.04	−28.2 ± 0.2	−28.4 ± 0.1	−31.7 ± 0.4

[a)]Old column >300 measurements.

[b)]New column

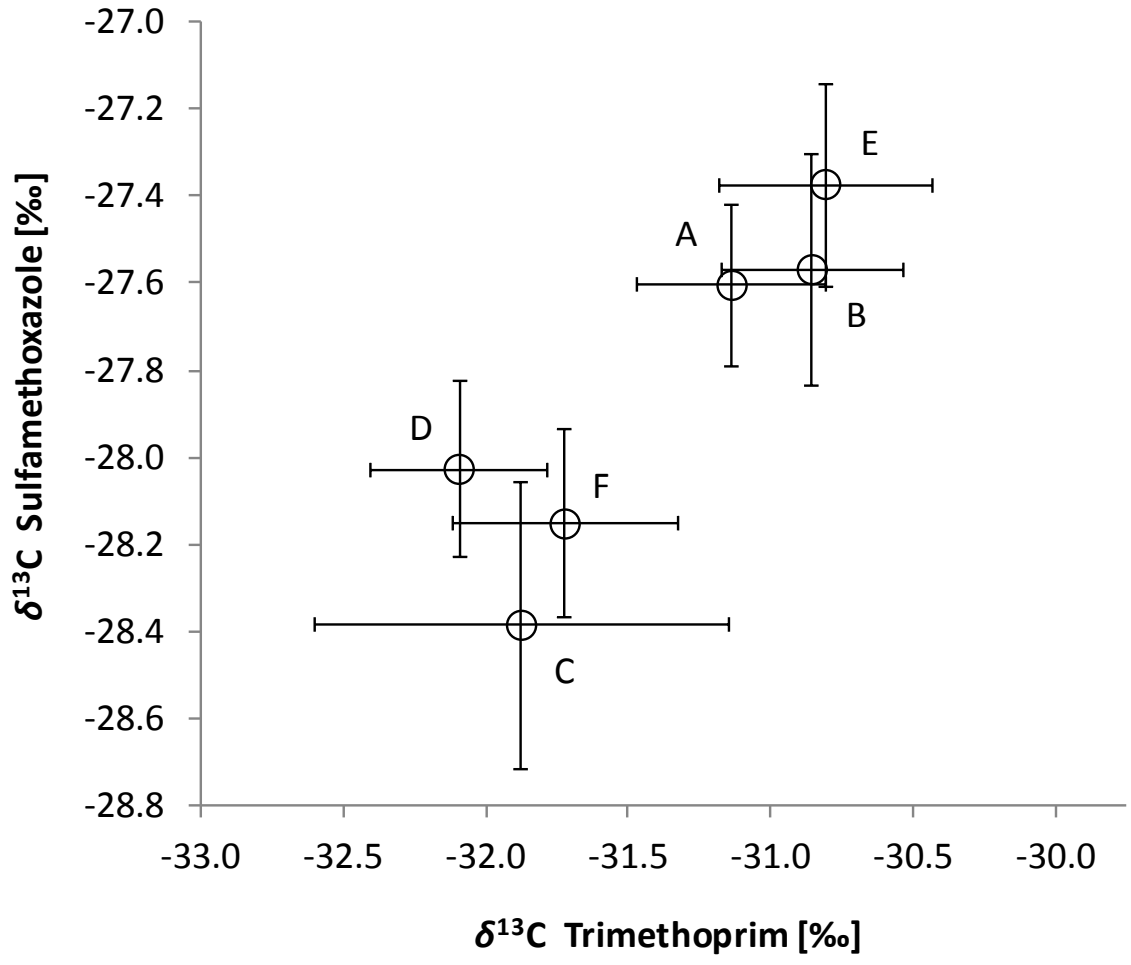

Figure 3.5 Corrected δ^{13}C values of trimethoprim and sulfamethoxazole from pharmaceutical products.

3.4 Conclusion

In this work we present the first method for compound-specific carbon isotope analysis of sulfonamide pharmaceuticals, which cannot be separated by conventionally used techniques for LC-IRMS. Substance amounts as low as 0.3 µg are sufficient to perform a precise analysis. The applicability of this method for pharmaceutical research and product authentication was demonstrated. It is also the first step towards a study of the degradation and mobility of these substances in the environment on an isotopic level. Following appropriate sample enrichment compound-specific $\delta^{13}C$ values of highly contaminated samples can be easily measured, but need to be corrected by external standards.

There are also some indications that the frequent offset of $\delta^{13}C$ values from LC-IRMS and EA-IRMS measurements derives from incomplete oxidation suggesting the need for improvements of the interface for higher sensitivity and accuracy.

References

1. Corr, L. T.; Berstan, R.; Evershed, R. P., Optimisation of derivatisation procedures for the determination of delta C-13 values of amino acids by gas chromatography/combustion/isotope ratio mass spectrometry. *Rapid Communications in Mass Spectrometry* **2007,** *21* (23), 3759-3771.

2. Godin, J. P.; Hau, J.; Fay, L. B.; Hopfgartner, G., Isotope ratio monitoring of small molecules and macromolecules by liquid chromatography coupled to isotope ratio mass spectrometry. *Rapid Communications in Mass Spectrometry* **2005,** *19* (18), 2689-2698.

3. Krummen, M.; Hilkert, A. W.; Juchelka, D.; Duhr, A.; Schluter, H. J.; Pesch, R., A new concept for isotope ratio monitoring liquid chromatography/mass spectrometry. *Rapid Communications in Mass Spectrometry* **2004,** *18* (19), 2260-2266.

4. Bode, S.; Denef, K.; Boeckx, P., Development and evaluation of a high-performance liquid chromatography/isotope ratio mass spectrometry methodology for delta C-13 analyses of amino sugars in soil. *Rapid Communications in Mass Spectrometry* **2009,** *23* (16), 2519-2526.

5. Morrison, D. J.; Taylor, K.; Preston, T., Strong anion-exchange liquid chromatography coupled with isotope ratio mass spectrometry using a Liquiface interface. *Rapid Communications in Mass Spectrometry* **2010,** *24* (12), 1755-1762.

6. Godin, J. P.; Breuille, D.; Obled, C.; Papet, I.; Schierbeek, H.; Hopfgartner, G.; Fay, L. B., Liquid and gas chromatography coupled to isotope ratio mass spectrometry for the determination of C-13-valine isotopic ratios in complex biological samples. *Journal of Mass Spectrometry* **2008,** *43* (10), 1334-1343.

7. McCullagh, J. S. O., Mixed-mode chromatography/isotope ratio mass spectrometry. *Rapid Communications in Mass Spectrometry* **2010,** *24* (5), 483-494.

8. Godin, J. P.; Hopfgartner, G.; Fay, L., Temperature-programmed high-performance liquid chromatography coupled to isotope ratio mass spectrometry. *Analytical Chemistry* **2008,** *80* (18), 7144-7152.

9. Zhang, L.; Kujawinski, D. M.; Jochmann, M. A.; Schmidt, T. C., High-temperature reversed-phase liquid chromatography coupled to isotope ratio mass spectrometry. *Rapid Communications in Mass Spectrometry* **2011,** *25* (20), 2971–2981.

10. Yang, Y.; Belghazi, M.; Lagadec, A.; Miller, D. J.; Hawthorne, S. B., Elution of organic solutes from different polarity sorbents using subcritical water. *Journal of Chromatography A* **1998,** *810* (1-2), 149-159.

11. Wiese, S.; Teutenberg, T.; Schmidt, T. C., A general strategy for performing temperature-programming in high performance liquid chromatography-Prediction of segmented temperature gradients. *Journal of Chromatography A* **2011,** *1218* (39), 6898-6906.

12. Teutenberg, T.; Hollebekkers, K.; Wiese, S.; Boergers, A., Temperature and pH-stability of commercial stationary phases. *Journal of Separation Science* **2009,** *32* (9), 1262-1274.

13. Thompson, J. D.; Carr, P. W., A study of the critical criteria for analyte stability in high-temperature liquid chromatography. *Analytical Chemistry* **2002,** *74* (5), 1017-1023.

14. Schauss, K.; Focks, A.; Heuer, H.; Kotzerke, A.; Schmitt, H.; Thiele-Bruhn, S.; Smalla, K.; Wilke, B.-M.; Matthies, M.; Amelung, W.; Klasmeier, J.; Schloter, M., Analysis, fate and effects of the antibiotic sulfadiazine in soil ecosystems. *Trac-Trends Anal. Chem.* **2009,** *28* (5), 612-618.

15. Huovinen, P., Resistance to trimethoprim-sulfamethoxazole. *Clinical Infectious Diseases* **2001,** *32* (11), 1608-1614.

16. Pereira, L.; Aspey, S.; Ritchie, H., High temperature to increase throughput in liquid chromatography and liquid chromatography-mass spectrometry with a porous graphitic carbon stationary phase. *Journal of Separation Science* **2007,** *30* (8), 1115-1124.

17. Giegold, S.; Teutenberg, T.; Tuerk, J.; Kiffmeyer, T.; Wenclawiak, B., Determination of sulfonamides and trimethoprim using high temperature HPLC with simultaneous temperature and solvent gradient. *Journal of Separation Science* **2008,** *31* (20), 3497-3502.

18. Qiang, Z. M.; Adams, C., Potentiometric determination of acid dissociation constants (pK(a)) for human and veterinary antibiotics. *Water Research* **2004,** *38* (12), 2874-2890.

19. Werner, R. A.; Brand, W. A., Referencing strategies and techniques in stable isotope ratio analysis. *Rapid Communications in Mass Spectrometry* **2001,** *15* (7), 501-519.

20. Hinshaw, J. V., When Peaks Collide. *Lc Gc Europe 23* (7), 362-+.

21. Blessing, M.; Jochmann, M. A.; Schmidt, T. C., Pitfalls in compound-specific isotope analysis of environmental samples. *Analytical and Bioanalytical Chemistry* **2008,** *390* (2), 591-603.

22. Snyder, L. R.; Kirkland, J. J.; Dolan, J. W., *Introduction to Modern Liquid Chromatography*. 3. ed.; Wiley: Hoboken, New Jersey; USA, 2010.

23. Buckenmaier, S. M. C.; McCalley, D. V.; Euerby, M. R., Overloading study of bases using polymeric RP-HPLC columns as an aid to rationalization of overloading on silica-ODS phases. *Analytical Chemistry* **2002,** *74* (18), 4672-4681.

24. Jochmann, M. A.; Blessing, M.; Haderlein, S. B.; Schmidt, T. C., A new approach to determine method detection limits for compound-specific isotope analysis of volatile organic compounds. *Rapid Communications in Mass Spectrometry* **2006,** *20* (24), 3639-3648.

25. Reinnicke, S.; Bernstein, A.; Elsner, M., Small and Reproducible Isotope Effects during Methylation with Trimethylsulfonium Hydroxide (TMSH): A Convenient Derivatization Method for Isotope Analysis of Negatively Charged Molecules. *Analytical Chemistry* **2010,** *82* (5), 2013-2019.

26. Smith, C. I.; Fuller, B. T.; Choy, K.; Richards, M. P., A three-phase liquid chromatographic method for delta C-13 analysis of amino acids from biological protein hydrolysates using liquid chromatography-isotope ratio mass spectrometry. *Analytical Biochemistry* **2009,** *390* (2), 165-172.

27. Teutenberg, T., *High-Temperature Liquid Chromatography - A User's Guide for Method Development*. RSCPublishing: 2010; Vol. 1.

4 Direct Photolysis of Sulfamethoxazole

Abstract

Although isotope ratio analysis is a common tool to investigate the behavior of organic substances in the environment, isotope effects related to photolytic processes of such compounds are scarcely explored. Magnetic isotope effects, resulting from the influence of a magnetic moment of an isotope on the spin of an electron, can be much bigger than mass-dependent isotope effects, so that they can even be utilized in chemical synthesis to produce isotopically labeled compounds by photochemical processes.

Hence, the work described in this chapter focuses on the measurement of carbon isotope ratios of sulfamethoxazole and its photolytic degradation products. These substances are prominent environmental pollutants and are generally removed from surface waters by photolysis. Biological degradation is negligible for this compound class due to its microbial properties.

In the previous chapter it was shown that high temperature liquid chromatography is the method of choice for the analysis of sulfonamides and trimethoprim by LC-IRMS. Based on this work, a suitable chromatographic column was selected to separate the target compound sulfamethoxazole from its photolysis products. In the second part, it was shown that direct photolysis of sulfamethoxazole leads to a small inverse isotope effect. The calculated enrichment factor ε was 0.7 ‰. The main detected transformation products, sulfanilic acid and 3-amino-5-methylisoxazole, point to a secondary carbon isotope effect, since no carbon bond is broken during this cleavage. Thus, ε cannot be assigned to a specific reactive position. The analysis of $\delta^{13}C$ values of the transformation products lead to the assumption that several processes with different isotope effects might take place.

4.1 Introduction

Due to the wide use of antimicrobial drugs in human or veterinary medication, sulfonamide pharmaceuticals are frequently detected in almost all compartments in nature.[1]

Because of their antimicrobial properties, a biological degradation is in most cases hampered. The main sink of sulfonamide pharmaceuticals are soil components, which act as sorbents. Depending on contact time, sulfonamides form bound residues with humic acids[2-3].

In surface waters the most prominent degradation mechanism is photolysis. Indirect photolysis occurs via activated species like humic acids or oxygen-containing radicals. Direct photolysis is enabled by the relatively strong absorption of UV light in the 250 to 270 nm range. Depending on the type of substituent different cleavage pathways are involved. Five ring-membered heterocyclic substituents cause a cleavage at the S-N or N-C bond of the sulfonamide group leading to sulfanilamide or sulfanilic acid and the substituent as products (see **Figure 4.2**).[4] If the sulfonamide contains a six ring-membered substituent, the reaction

involves rather SO_2 extrusion from the compound and various products from radical coupling.[5]

Although photolysis is an important transformation process of organic pollutants in the environment, only a few works have studied associated isotope effects in aqueous media. The measured carbon enrichment factors are inconsistent in terms of their algebraic sign. For the photolysis of diethyl phthalate in sea water a carbon isotope enrichment of -35 ‰ at the reactive position[6] was reported while only a very small carbon isotope effect during direct photolysis of oxalate in Fe(II) and Fe(III) solutions can be observed[7]. A very detailed work on various photolytic reactions can be found on the herbicide atrazine.[8] Indirect photolysis by OH radicals and excited 4-carboxybenzophenon showed a very low enrichment of ^{13}C and ^{15}N (-0.3‰ > ε_C, ε_N >-1.7‰) in contrast to moderately high deuterium enrichment (ε_H of -51.2 and -25.3‰) in the residual atrazine. During direct photolysis of atrazine no hydrogen isotope effect could be measured but carbon and nitrogen showed a moderate depletion of heavy isotopes (ε_C of 4.6 and ε_N 4.9‰).

The isotope effect encountered in photolysis reactions usually is a magnetic isotope effect although kinetic isotope effects can compete[9]. In many cases mass-dependent isotope effects are too small in order to contribute to the measured isotope fractionation[10]. After the homolytic cleavage of the bond the resulting radical pair can either dissociate or recombine to the reactant (see **Figure 4.1**). The recombination of the radical pair is only possible from the singlet state. Magnetic nuclei like ^{13}C promote a conversion from the triplet to singlet state by hyperfine coupling of the electron with the magnetic nucleus.[9] Non-magnetic nuclei cannot promote a triplet-singlet conversion, thus, the corresponding radical pair dissociates into photolysis products.[9] Here, factors controlling the recombination like diffusion, temperature, viscosity and lifetime of the radicals influence the magnitude of the magnetic isotope effect in contrast to the classical mass dependent isotope effect.[9]

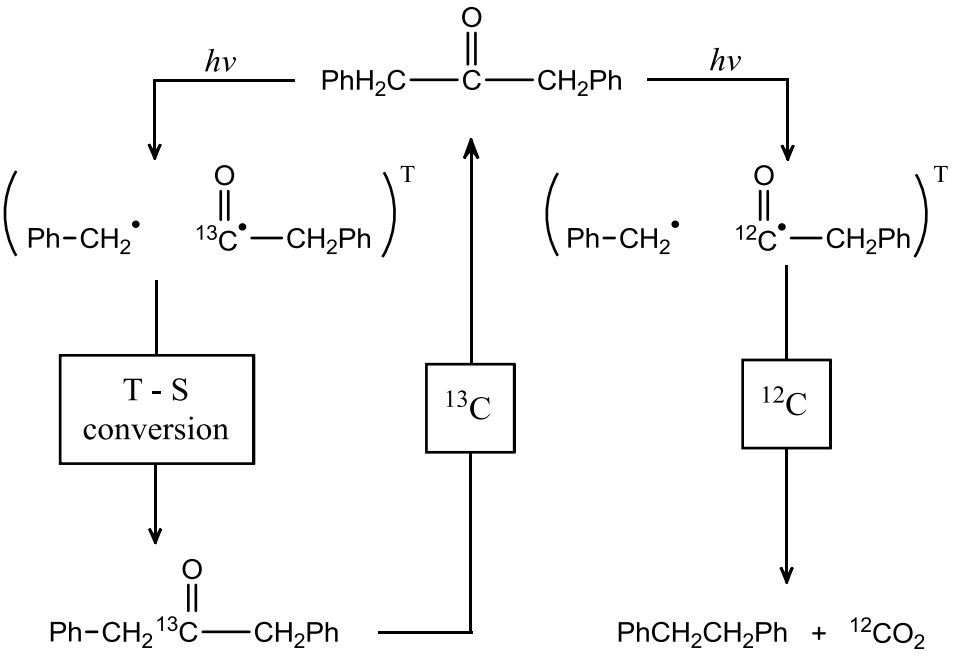

Figure 4.1 Isotopic sorting by radical coupling during photolysis of dibenzyl ketone. "T" and "S" mean triplet state or singlet state, respectively. Scheme redrawn from Buchachenko[10]

In contrast to dibenzyl ketone the direct photolysis of atrazine[8] is associated with an inverse isotope effect. Presumably, the photodissociation of atrazine leads radical pairs in the singlet state. Thus, a singlet to triplet conversion of the ^{13}C reactant may lead to the accumulation of ^{13}C in the photolysis products and accordingly results in an enrichment of ^{12}C in the reactant.

The aim of this work was to evaluate a possible carbon isotope effect during sulfamethoxazole degradation by UV photolysis. Up to now, it is only possible to investigate a direct photolysis due to the poor detection limits of the LC-IRMS. Indirect photolysis requires a low sulfamethoxazole concentration with respect to the sensitized species in order to suppress direct photolysis. Sulfamethoxazole was chosen as model substance since it can be easily chromatographically separated by RP chromatography and its degradation products are well known. It is also desirable to monitor $\delta^{13}C$ values of the degradation products. Therefore, a chromatographic method should be developed in first place. Although the compounds investigated in this study have a terminal amino group susceptible to cation ion exchange, this type of chromatography could not be considered due to their hydrophobic properties, which would require an organic solvent in the eluent to elute them from the stationary phase support. In **Chapter** 3 it has been shown that high temperature liquid chromatography (HTLC) can be excellently used in combination with IRMS for the analysis of sulfonamides. Hence, reversed phase columns were used to separate the analytes.

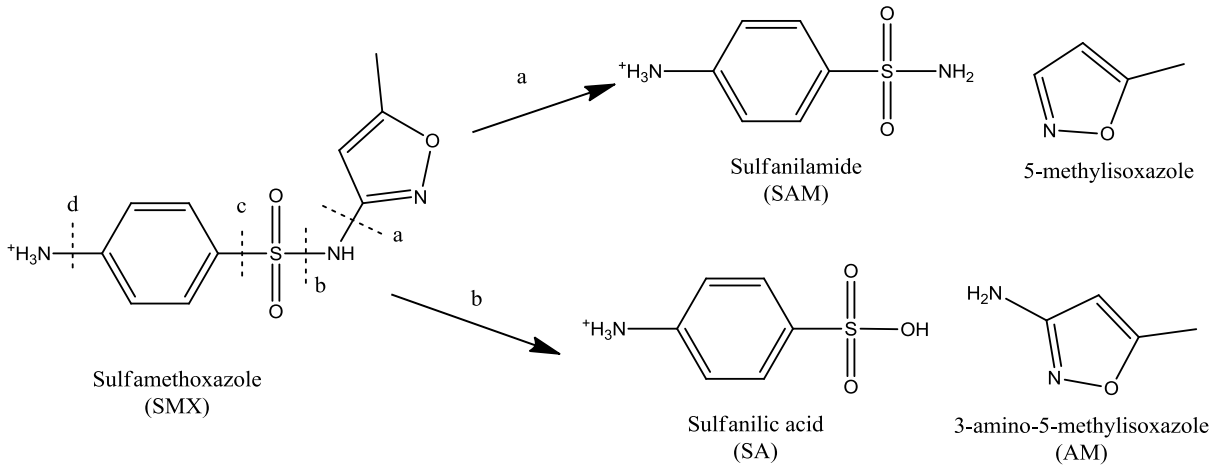

Figure 4.2 Possible bond cleavage by photolysis of sulfamethoxazole after Boreen et al.[4]. Cleavage at bonds c and d are also possible but have not been detected in this work.

4.2 Experimental:

4.2.1 Chemicals and Reagents

Sulfamethoxazole (99.9 %), sulfanilamide (99.9 %), 3-amino-5-methylisoxazole (>98 %) and sulfanilic acid (≥99 %) were purchased from Sigma-Aldrich (Steinheim, Germany). $Na_2S_2O_8$, H_3PO_4 and NaH_2PO_4 for eluent and reagent solutions were supplied by Fluka (Steinheim, Germany). Eluent and interface reagent solutions were continuously sparged with helium (purity 5.0, Air Liquide, Oberhausen, Germany) to avoid a regassing of CO_2.

4.2.2 LC-IRMS conditions

The HTLC system consisted of a Rheos Allegro binary piston pump (Flux/Thermo Scientific, Bremen, Germany), an HTC PAL autosampler (Axel Semrau, Sprockhövel, Germany), an HT-HPLC 200 oven (SIM, Oberhausen, Germany) with custom made alumina column holders and an LC-IsoLink as interface to the DeltaV Advantage isotope ratio mass spectrometer (Thermo Scientific, Bremen, Germany). A sodium phosphate buffer (5mM and pH 3) was used as an eluent for all analyses. The injection volume was 20 µL. The column effluent enters the interface where it is mixed with a stream of the phosphoric acid and peroxodisulfate reagent solution. The flow rate of each reagent was 50 $\mu Lmin^{-1}$. The concentrations of phosphoric acid and sodium peroxodisulfate were 1.5 M and 0.8 M, respectively. The stream is guided through a heated stainless steel capillary of 99.9 °C where all organic compounds are oxidized by heat-generated sulfate radicals. After a distance of about 5 m the capillary is cooled down and the stream enters a gas separation unit consisting from three membrane capillaries permeable to light gases. A counterstream of He of 1.2 $mLmin^{-1}$ transports the extracted CO_2 into two Nafion gas driers and subsequently into the open split connecting to the IRMS.

Hypercarb (Thermo Scientific, 3 µm particle size, 100 mm, 4.6 mm), TSKgel Amide (TOSOH Biosience, 3 µm particle size, 150 × 2.4 mm), Zorbax Extend C-18 (Agilent, 3 µm particle size, 150 × 3 mm), Kinetex C18 (Phenomenex, 2.6 µm particle size, 100 × 3 mm), ZirChrom-PBD (ZirChrom, 5 µm particle size, 150 × 3 mm) and X-Bridge C_{18} (Waters, 3.5 µm particle size, 100 × 2.1 mm) were investigated to yield the best separation of sulfamethoxazole and its photolysis products. The flow rate of the eluent was 500 $\mu Lmin^{-1}$, except for 200 $\mu Lmin^{-1}$ using the ZirChrom PBD column. The temperature programs are summarized in **Table 4.1**.

Table 4.1 Temperature programs and maximum operating temperatures of the investigated columns

Column	Temperature program				Max. T from manufacturer
	Start	Ramp	Final	Hold	
Hypercarb	30°C	5 °C/min	100°C	13 min	
TSKgel Amide	30°C	5 °C/min	70°C	13 min	80 °C
Kinetex C18	30°C	5 °C/min	60°C	13 min	
Zorbax Extend C18	30°C	5 °C/min	60°C	13 min	60 °C
ZirChrom-PBD	30°C	3 °C/min	50°C	13 min	150 °C
XBridge C_{18}	30°C	10 °C/min	80°C	13 min	80 °C

In order to determine the minimum amount of substances required for a reliable isotopic analysis, calibration solutions between 10 and 100 mgL^{-1} of each substance were measured. The minimum amount was determined by the moving mean procedure described by Jochmann et al.[11] Calibration data are given in the appendix.

4.2.3 Direct photolysis conditions

A merry go round UV reactor (Windaus Labortechnik, Clausthal-Zellerfeld) has been used for all experiments. The irradiation source was a low pressure UV lamp (Heraeus TQ 718, main wave length 254 nm). The irradiated solutions contained 100 mgL^{-1} and 200 mgL^{-1} sulfamethoxazole in ultra pure water without pH adjustment. Samples of about1.5 mL were taken with single use glass Pasteur-pipettes in intervals of 30 min, transferred into amber HPLC vials and directly injected into the LC-IRMS system. Standards of 100 mgL^{-1} and 200 mgL^{-1} were used as dark control during the experiments.

The fluency of the light source was determined by the uridine method described in von Sonntag and Schuchmann[12].

4.2.4 Data handling and calculations

Isotope ratios were recorded and calculated by Isodat 2.5 (Thermo Scientific, Bremen, Germany). The isotope enrichment factor was determined from a linear regression by the least squares method of the following equation:

$$\ln\left(\frac{\delta^{13}C_t + 1}{\delta^{13}C_0 + 1}\right) = \varepsilon \cdot \ln\frac{c_t}{c_0}$$

$\delta^{13}C_t$ and $\delta^{13}C_0$ are the carbon isotope ratios of sulfamethoxazole (SMX) at the different sampling times, ε is the carbon isotope enrichment factor and c_t and c_0 are the concentrations of SMX.

The pseudo first-order rate constant was calculated from a linear regression of a natural logarithmic plot of c_t/c_0 against the time.

4.3 Results and Discussion

4.3.1 Column selection

The aim of the method development was to obtain a baseline separation of all photolysis products and sulfamethoxazole. The investigated stationary phases were Zorbax Extend C-18, Kinetex C_{18}, TSKgel Amide, Hypercarb, XBridge C_{18} and ZirChrom-PBD. The last three columns mentioned have been used already for HTLC-IRMS[13] and can resist temperatures of more than 100 °C. The other columns are only suitable at temperatures up to 60 °C or 80 °C. At these temperatures column lifetime is much shorter and column bleed higher. The temperature programs used in this study started at 30 °C and achieved a final temperature of maximum 100 °C. The lowest possible starting temperature of the oven is 30 °C and it was chosen in order to achieve the strongest retention for the very polar analytes, sulfanilamide (SAM), 3-amino-5-methylisoxazole (AM) and sulfanilic acid (SA).

The best separation of the polar photolysis products was achieved on the TSKgel column since this column provides hydrophilic interactions due to its embedded carbamoyl group. SAM, SA and AM are fully separated but sulfamethoxazole cannot be eluted at 80 °C or is concealed by increased column bleed as can be seen in **Figure 4.3d**.

On the Kinetex column, SAM, SA and AM were baseline separated but the maximum temperature of this column was too low to elute SMX in a reasonable time. Hence, SMX peaks appeared in each subsequent analysis.

The Hypercarb column consisting of porous graphitic carbon particles was developed for its use in HPLC in order to retain very polar organic compounds. Although this column can be used under high temperature conditions, column bleed was too high for its use with LC-IRMS. From the standard mixture it was only possible to obtain one peak.

The ZirChrom PBD and the Zorbax Extend C18 columns were not suitable for the separation of the photolysis products and SMX due to a bad peak shape and coelutions.

Although the photolysis products were not fully separated, the XBridge C_{18} column was chosen for the analysis of the samples. In contrast to the other columns, its temperature stability and repeatability of chromatographic performance was already demonstrated (see **Chapter 3**).

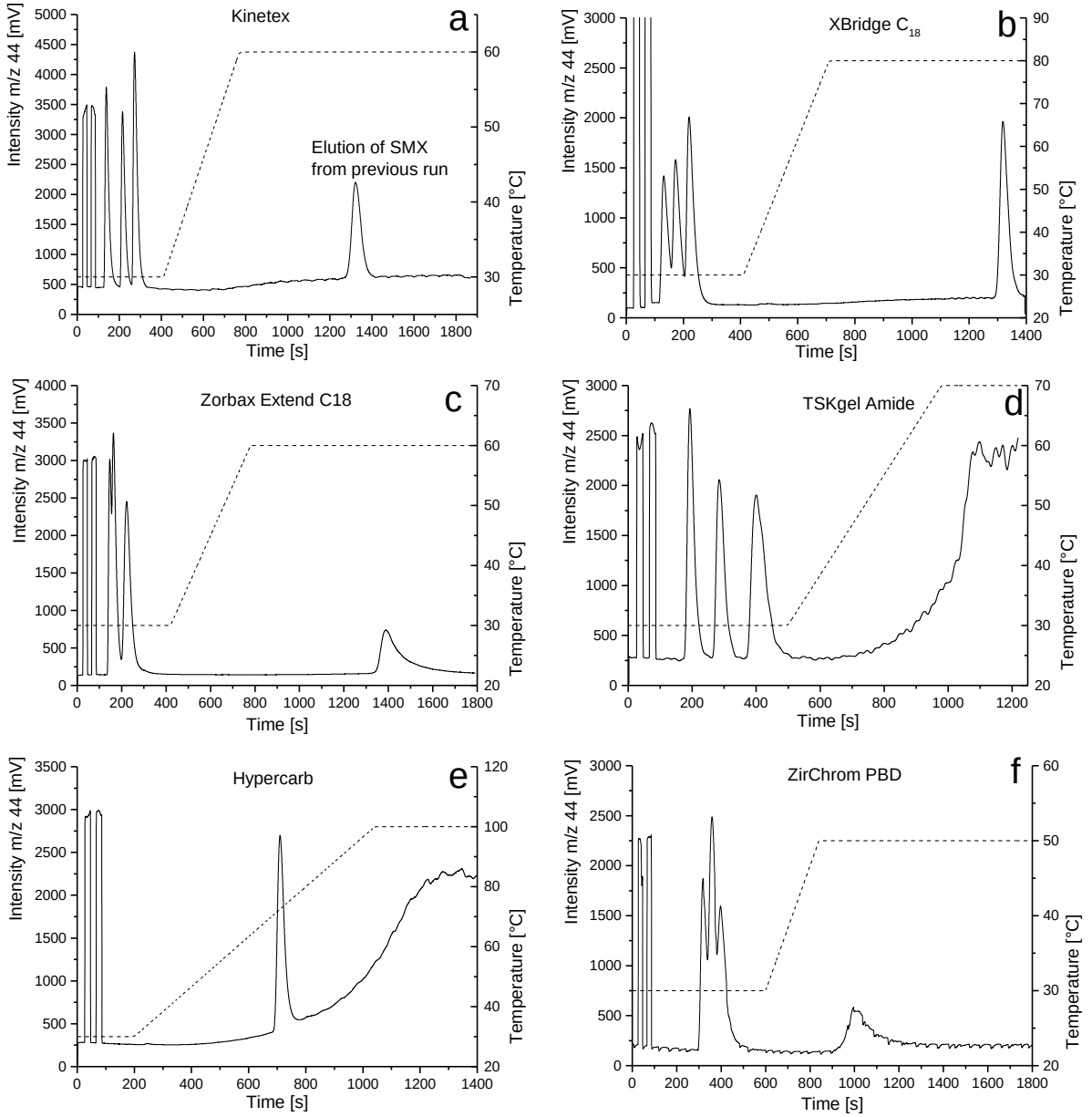

Figure 4.3 Chromatograms of standard mixtures containing SMX, SAM, SA and AM. The dashed lines are the temperature programs applied to eluent and column. The irregular baseline and peak in (f) results from temporary pulsations of a reagent pump.

4.3.2 Kinetics of direct photolysis and transformation products

Three degradation products were identified in the chromatograms of the irradiated solutions (see **Figure 4.4**). Two peaks could be assigned to SA and 3-amino-5-methylisoxazole by a match of retention times. These compounds were the main photolysis products in other studies as well[14-16]. One of the two unidentified minor peaks in the middle of the chromatographic run is probably 4-amino-5-methyl-2-oxazolylbenzene sulfonamide resulting from photoisomerization of the isoxazole ring (see Figure 4.5 Photoisomerization scheme of SMX yielding 4-amino-5-methyl-2-oxazolylbenzene sulfonamide after Zhou and Moore16.**Figure 4.5**). In some studies this compound has been identified as one of the major products.[14, 16]

The presence of a cleavage to sulfanilamide and 5-methylisoxazole cannot be excluded due to a small shoulder in the peak of SA and another unknown peak in the middle of the chromatographic run.

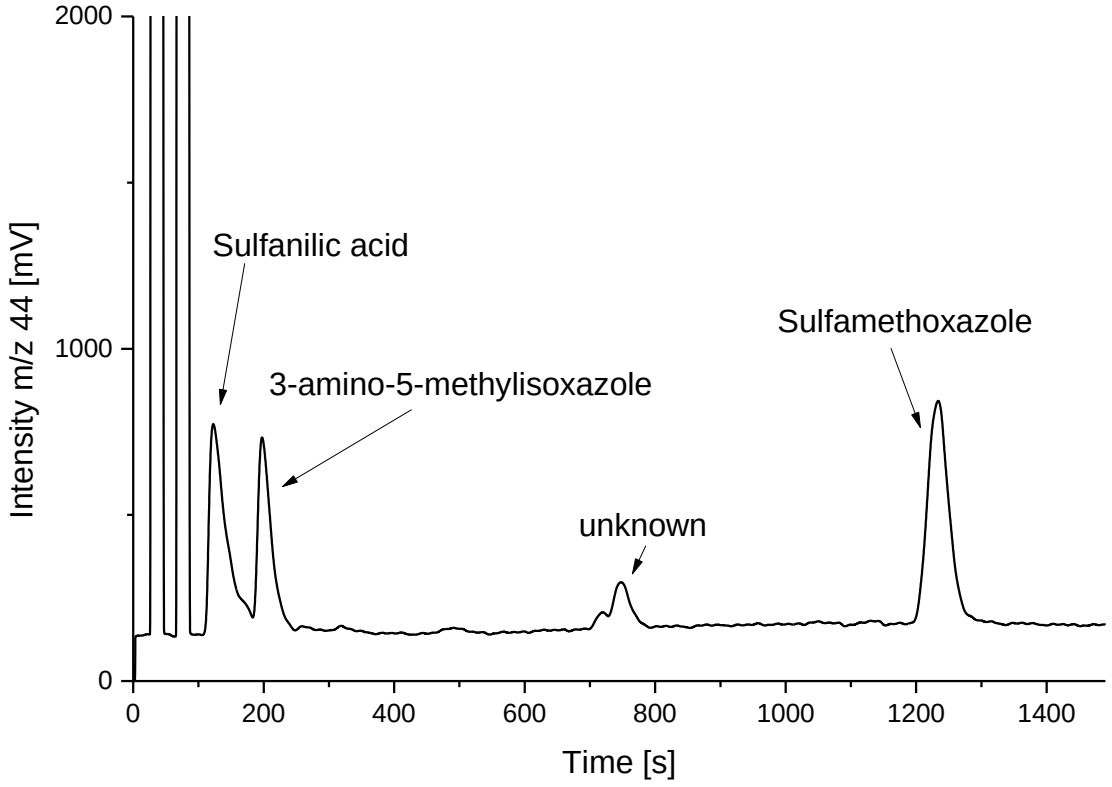

Figure 4.4 LC-IRMS chromatogram of a sample of SMX photolysis after 25 min irradiation time. The analysis was performed on an XBridge C_{18} column under the same condition as in **Figure 4.3b**.

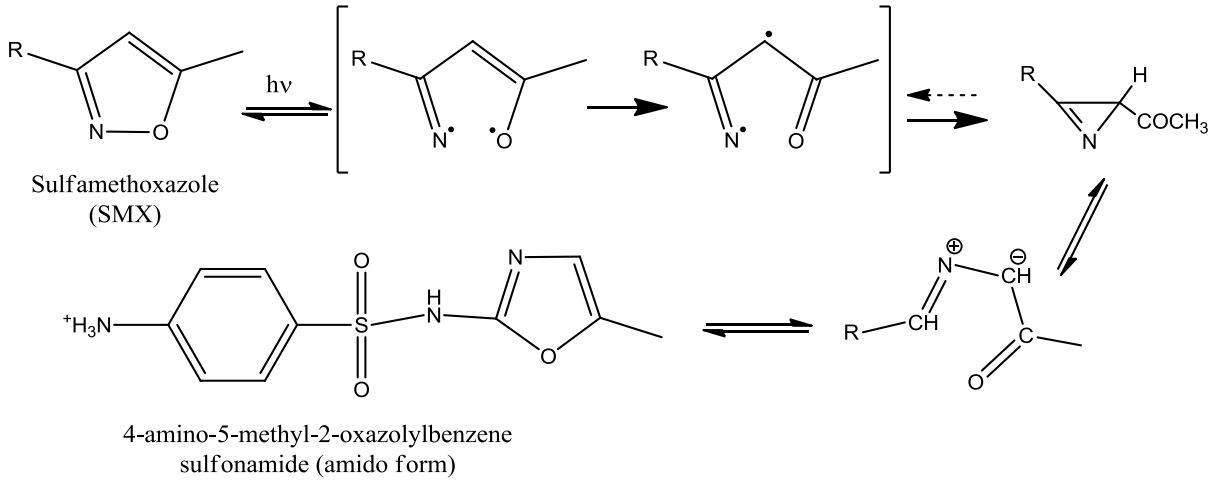

Figure 4.5 Photoisomerization scheme of SMX yielding 4-amino-5-methyl-2-oxazolylbenzene sulfonamide after Zhou and Moore[16].

The first order reaction rate constant was 7.9 $\times 10^{-4}$ s^{-1} (see **Figure 4.6**) and the quantum yield 0.0053 mol/Einstein. Due to the much higher starting concentration of SMX these values are lower than the reported ones. Liu et al.[17] reported a first order rate constant of 7.4 $\times 10^{-3}$ s^{-1} at 2.5 mgL^{-1} and Baeza and Knappe[18] a value of 2.4 $\times 10^{-3}$ s^{-1} at 1 mgL^{-1}. These differences might result from concentration gradients in the reaction vessel. Since most of the light is absorbed by the reagent at the outer part of the irradiated solution, the reagent in the inner part is less irradiated and hence is converted at a slower rate. For the same reason the quantum yield is also more than 10 times lower than determined in other studies[4, 18]. Stirring of the solution would have increased the overall reaction rate, but it was not possible using this reactor. However, in order to evaluate a possible isotope effect during direct photolysis the absolute reaction rate constant plays a minor role.

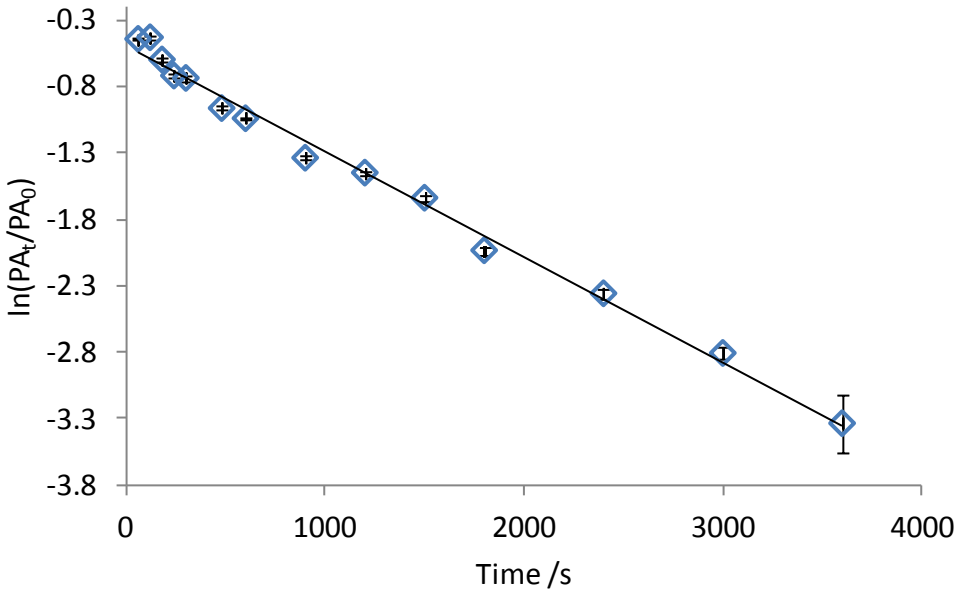

Figure 4.6 Logarithmic plot of the ratio of SMX peak areas at different irradiation times (PA_t) and before irradiation (PA_0) vs. time.

4.3.3 Carbon isotope fractionation

The carbon isotope fractionation during direct photolysis of SMX was very low. Instead of an enrichment of ^{13}C, SMX showed an enrichment of ^{12}C. A magnetic isotope effect from radical recombination and triplet-singlet conversion leads to a normal isotope effect, i.e., enrichment of ^{13}C. As in the case of atrazine[8] isotope effects due to a singlet to triplet conversion of the radical pair could be a reason for this inverse isotope effect.

A logarithmic plot of the change in isotope ratio against the remaining fraction had a slope of 0.7 ± 0.1 ‰ (see **Figure 4.7**). This enrichment factor is only slightly bigger than the total analytical uncertainty. During these experiments mainly SA and AM were formed pointing to a cleavage of the sulfonamide bond. Since no carbon bonds are broken only secondary isotope effects could cause a fractionation. Here, a nitrogen or a sulfur isotope effect is likely to occur, but up to now no method to measure these isotope ratios of sulfonamides has been published. Since there were some small peaks in the chromatograms which could not be assigned to a specific molecule it remains to be investigated if the small isotope effect originates from a parallel reaction involving a cleaved carbon bond.

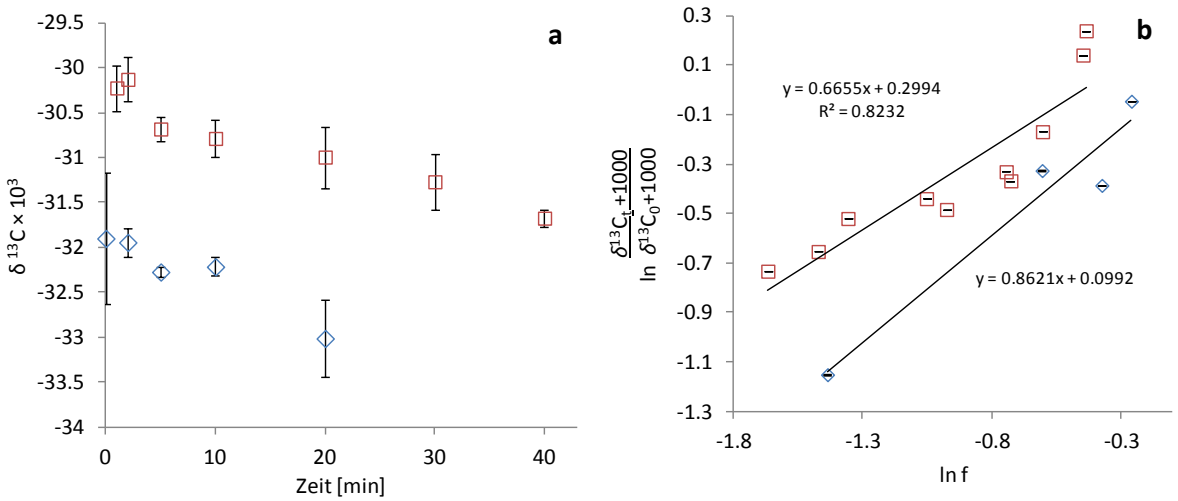

Figure 4.7 Carbon isotope ratios of SMX during direct photolysis. (a) $\delta^{13}C$ values after different irradiation times; starting $\delta^{13}C$ values differ due to different batches of the pure compound (b) Linear regression of the change in $\delta^{13}C$ value with remaining fraction f of SMX. The red squares show the experiment with a starting concentration of 200 mgL^{-1}, the blue diamonds indicate the experiment starting with 100 mgL^{-1}.

The shift in $\delta^{13}C$ values of the formed AM and SA during photolysis can be seen in **Figure 4.8**. Like SMX, the accumulated SA shows depletion of ^{13}C during the reaction. But it can be assumed that there is also a photolysis of the formed SA. Otherwise the shift of the $\delta^{13}C$ value of SA would be smaller since the measured SA is an accumulated product (see **Chapter 1.3**).

In contrast, AM shows an enrichment in ^{13}C. As a product of SMX photolysis this compound should show the same direction of $\delta^{13}C$ shift. The enrichment could be a result from a magnetic isotope effect from recombination of the biradical after photolytic N-O bond dissociation or reverse reaction of a photoisomerization[19-20]. Such rearrangements have been described for pyrolysis reactions and UV laser excitations but the radical reactions taking

place might also apply for isoxazole radicals in aqueous environments. The occurrence of transformation products of AM is possible but their concentration may be too low to be detected or oxidation of these compounds in the interface is not feasible.

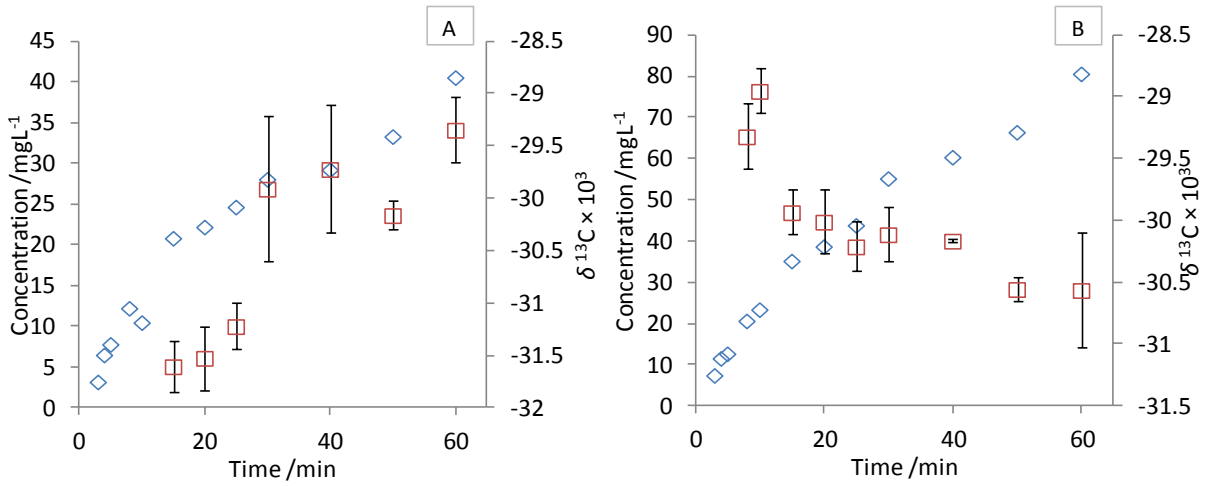

Figure 4.8 δ ^{13}C values of the SMX transformation products AM (A) and SA (B) at different irradiation times. Blue diamonds and red squares show concentration and δ ^{13}C values, respectively.

4.4 Conclusions

The detected photolysis products point to a secondary carbon isotope effect since no carbon bond was broken. But due to the rather poor detection limit of the LC-IRMS it cannot be ruled out that the molecule is cleaved at a carbon bond during a minor side reaction.

Due to the observed small inverse isotope effect during direct photolysis of SMX it can be concluded that a ^{13}C substitution in the molecule only has small influence on the singlet-triplet conversion of the generated radical pair and that the latter is not feasible. Thus, the probability of recombination is as high for ^{13}C containing molecules as for the ^{12}C containing ones. Nevertheless, it cannot be excluded that the observed isotope effect is not a sum of multiple isotope effects nor that there is no isotope effects in H, N or S.

Further research on the isotopic signature of photolysis products of SMX as well as position-specific isotope ratios of SMX can be useful. As the isotopic fractionation of photolysis can be wavelength specific, these experiments should be repeated at various wavelength as well as different pH values. The molar absorbance varies with pH, thus, it can have an influence on the extent of the isotope effect.

References

1. Sarmah, A. K.; Meyer, M. T.; Boxall, A. B., A global perspective on the use, sales, exposure pathways, occurrence, fate and effects of veterinary antibiotics (VAs) in the environment. *Chemosphere* **2006,** *65* (5), 725-59.

2. Schauss, K.; Focks, A.; Heuer, H.; Kotzerke, A.; Schmitt, H.; Thiele-Bruhn, S.; Smalla, K.; Wilke, B.-M.; Matthies, M.; Amelung, W.; Klasmeier, J.; Schloter, M., Analysis, fate and effects of the antibiotic sulfadiazine in soil ecosystems. *Trac-Trends Anal. Chem.* **2009,** *28* (5), 612-618.

3. Forster, M.; Laabs, V.; Lamshoft, M.; Putz, T.; Amelung, W., Analysis of aged sulfadiazine residues in soils using microwave extraction and liquid chromatography tandem mass spectrometry. *Anal Bioanal Chem* **2008,** *391* (3), 1029-38.

4. Boreen, A. L.; Arnold, W. A.; McNeill, K., Photochemical fate of sulfa drugs in the aquatic environment: Sulfa drugs containing five-membered heterocyclic groups. *Environmental Science & Technology* **2004,** *38* (14), 3933-3940.

5. Boreen, A. L.; Arnold, W. A.; McNeill, K., Triplet-sensitized photodegradation of sulfa drugs containing six-membered heterocyclic groups: Identification of an SO2 extrusion photoproduct. *Environmental Science & Technology* **2005,** *39* (10), 3630-3638.

6. Peng, X.; Feng, L.; Li, X., Pathway of diethyl phthalate photolysis in sea-water determined by gas chromatography-mass spectrometry and compound-specific isotope analysis. *Chemosphere* **2013,** *90* (2), 220-226.

7. Pavuluri, C. M.; Kawamura, K., Evidence for 13-carbon enrichment in oxalic acid via iron catalyzed photolysis in aqueous phase. *Geophysical Research Letters* **2012,** *39*.

8. Hartenbach, A. E.; Hofstetter, T. B.; Tentscher, P. R.; Canonica, S.; Berg, M.; Schwarzenbach, R. P., Carbon, Hydrogen, and Nitrogen Isotope Fractionation During Light-Induced Transformations of Atrazine. *Environmental Science & Technology* **2008,** *42* (21), 7751-7756.

9. Buchachenko, A. L., Mie Versus Cie - Comparative-Analysis of Magnetic and Classical Isotope Effects. *Chemical Reviews* **1995,** *95* (7), 2507-2528.

10. Buchachenko, A. L., Magnetic isotope effect. *Theoretical and Experimental Chemistry* **1995,** *31* (3), 118-126.

11. Jochmann, M. A.; Blessing, M.; Haderlein, S. B.; Schmidt, T. C., A new approach to determine method detection limits for compound-specific isotope analysis of volatile organic compounds. *Rapid Communications in Mass Spectrometry* **2006,** *20* (24), 3639-3648.

12. von Sonntag, C.; Schuchmann, H.-P., UV Disinfection of drinking water and by-product formation-some basic considerations. *Journal of Water Supply: Research and Technology - Aqua* **1992,** (41), 67-74.

13. Zhang, L.; Kujawinski, D. M.; Jochmann, M. A.; Schmidt, T. C., High-temperature reversed-phase liquid chromatography coupled to isotope ratio mass spectrometry. *Rapid Communications in Mass Spectrometry* **2011,** *25* (20), 2971–2981.

14. Trovo, A. G.; Nogueira, R. F. P.; Agueera, A.; Sirtori, C.; Fernandez-Alba, A. R., Photodegradation of sulfamethoxazole in various aqueous media: Persistence, toxicity and photoproducts assessment. *Chemosphere* **2009,** *77* (10), 1292-1298.

15. Bonvin, F.; Omlin, J.; Rutler, R.; Schweizer, W. B.; Alaimo, P. J.; Strathmann, T. J.; McNeill, K.; Kohn, T., Direct Photolysis of Human Metabolites of the Antibiotic Sulfamethoxazole: Evidence for Abiotic Back-Transformation. *Environmental Science & Technology* **2013,** *47* (13), 6746-6755.

16. Zhou, W.; Moore, D. E., Photochemical Decomposition of Sulfamethoxazole. *International Journal of Pharmaceutics* **1994,** *110* (1), 55-63.

17. Liu, X.; Garoma, T.; Chen, Z.; Wang, L.; Wu, Y., SMX degradation by ozonation and UV radiation: A kinetic study. *Chemosphere* **2012,** *87* (10), 1134-1140.

18. Baeza, C.; Knappe, D. R. U., Transformation kinetics of biochemically active compounds in low-pressure UV Photolysis and UV/H2O2 advanced oxidation processes. *Water Research* **2011,** *45* (15), 4531-4543.

19. Zhang, Y.; Xu, J.; Zhong, Z.; Guo, C.; Li, L.; He, Y.; Fan, W.; Chen, Y., Degradation of sulfonamides antibiotics in lake water and sediment. *Environmental Science and Pollution Research* **2013,** *20* (4), 2372-2380.

20. Niu, J.; Zhang, L.; Li, Y.; Zhao, J.; Lv, S.; Xiao, K., Effects of environmental factors on sulfamethoxazole photodegradation under simulated sunlight irradiation: Kinetics and mechanism. *Journal of Environmental Sciences-China* **2013,** *25* (6), 1098-1106.

5 Carbon isotope ratio measurements of glyphosate and AMPA by liquid chromatography coupled to isotope ratio mass spectrometry

Published in: Kujawinski, D. M.; Wolbert, J. B.; Zhang, L.; Jochmann, M. A.; Widory, D.; Baran, N.; Schmidt, T. C., **Carbon isotope ratio measurements of glyphosate and AMPA by liquid chromatography coupled to isotope ratio mass spectrometry**. *Analytical and Bioanalytical chemistry* **2013,** *405* (9), 2869-78.

Abstract

The interest in compound-specific isotope analysis for product authenticity control and source differentiation in environmental sciences has grown rapidly during the last decade. However, the isotopic analysis of very polar analytes is a challenging task due to the lack of chromatographic techniques which can be used coupled to isotope ratio mass spectrometry. In this work we present the first method to measure carbon isotope compositions of the widely applied herbicide glyphosate and its metabolite aminomethylphosphonic acid (AMPA) by liquid chromatography coupled to isotope ratio mass spectrometry (LC-IRMS). We demonstrate that this analysis can be carried out either in cation exchange or in reversed phase separation mode. The reversed phase separation yields a better performance in terms of resolution compared to the cation exchange method. The measurements of commercial herbicide samples show its principal applicability and revealed a wide range of $\delta^{13}C$ between –24 and –34 ‰. The absolute amounts, in the sub-microgram range, required to perform a precise and accurate determination of carbon isotope compositions of both glyphosate and AMPA were determined. The method proposed is sensitive enough to further perform the experiments that are necessary to better understand the carbon isotope fractionation associated to the natural degradation of glyphosate into AMPA. Furthermore, it can be used for contaminant source allocation and product authenticity as well.

5.1 Introduction

During the last decades the production and usage of glyphosate increased steadily, becoming one of the most used herbicides in Europe for agricultural and non agricultural uses[1]. Its charged functional groups (see **Figure 5.1**) facilitate sorption to soil[2] and some microorganisms are capable of degrading glyphosate degradation by using its phosphate.[3] However sorption, degradation and leaching can be very variable from a soil to another.[1, 4]

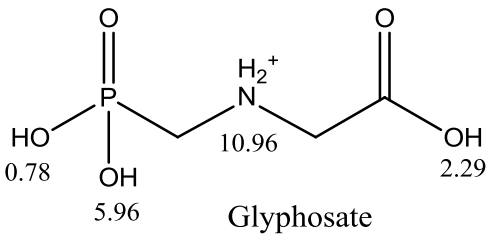

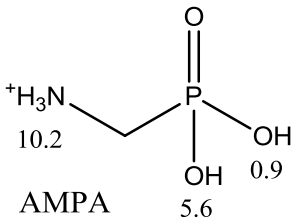

Figure 5.1 Chemical structures and pK_a values of glyphosate and aminomethylphosphonic acid (AMPA).

Aminomethylphosphonic acid (AMPA) is the major metabolite of glyphosate in the environment. It may also occur as a byproduct from the transformation of other phosphonate contaminants such as nitrilotris(methylenephosphonic acid) (NTMP)[5], which complicates the identification of glyphosate degradation pathway. The microbiological degradation of glyphosate follows two main pathways. In the first pathway, the P-C bond of glyphosate is broken to form sarcosine and phosphate[6]. The second pathway generates AMPA and glyoxylic acid. [6]

The investigation of carbon isotope compositions ($\delta^{13}C$) has widely demonstrated its added value as a tool in environmental contaminant research so far[7-8]. Many enzymatic and abiotic reactions can be associated with a measurable shift in carbon isotope compositions (i.e. carbon isotope fractionation; $\Delta^{13}C$). Abiotic and biotic, as well as the type of reaction can sometimes be differentiated by the use of isotope ratio enrichment factors (ε). [9] Thus, degradation of a contaminant can be identified even if no metabolites can be detected or dilution distorts concentration determination in a plume[10]. The investigation of possible isotope effects associated with the degradation of glyphosate and its sorption to soil can help to identify the sinks for this contaminant.

To our knowledge, such investigations have not been performed yet in the case of glyphosate, possibly due to the lack of suitable analytical methods. Although glyphosate can be separated by gas chromatography[11], the required derivatization can be a potential source of errors in $^{13}C/^{12}C$ ratio determination due to kinetic isotope effects and addition of extra carbon. In compound-specific carbon isotope ratio analysis (CSIA) the addition of extra-carbon to the targeted molecule is avoided, although it is desirable in conventional gas chromatography-mass spectrometry applications due to lower interferences at higher masses and higher sensitivity. Especially, the introduction of extra-carbon to compounds which already contain a low amount of carbon like glyphosate (only three carbon atoms) can lead to low isotopic precision. Furthermore, many of the reported derivatization procedures include the use of diazomethane[8, 11] which can produce an irreproducible isotope fractionation.[12] Silylation or esterification/acylation with fluorinated compounds have the advantage of a very good

chromatographic behavior of the derivatives but have the disadvantage of poisoning of the combustion reactor of the GC-IRMS by the formation of inert deposits or fluoride salts[13]. Hence, new chromatographic methods to measure isotope ratios of very polar analytes without mandatory derivatization have to be evaluated.

The commercial introduction of an interface coupling liquid chromatography (LC) to isotope ratio mass spectrometry (IRMS) in 2004 enabled the determination of carbon isotope compositions of highly polar and non-volatile analytes without the need for derivatization.[14] The liquid chromatography coupled to isotope ratio mass spectrometry (LC-IRMS) interface is based on a wet oxidation of the analytes followed by gas extraction of the formed CO_2 from the liquid phase (see Figure 5.2). The whole high-performance liquid chromatography (HPLC) column effluent is non-selectively oxidized by thermally activated peroxodisulfate. The formed CO_2 is extracted into a carrier gas by three gas-permeable membranes and transported to the IRMS inlet. For amino acid analysis, this system has proven to be superior to GC-IRMS analysis of derivatives in terms of accuracy, precision and resolution.[15]

LC-IRMS is restricted to LC eluents which are completely free of organic or inorganic carbon additives. Otherwise, a too high baseline or even a saturation of the IRMS signal can be observed. Thus, ion exchange is a separation mode frequently used in combination with online LC-IRMS.[16] Reversed phase separations have also been reported in combination with IRMS either by high temperature-LC[17] or at ambient temperatures for compounds which require rather low elution strength of the eluent.[14, 18]

In LC-IRMS, a full baseline separation of the analyte from matrix components is essential to ensure a reliable determination of $\delta^{13}C$ values because isotope effects during chromatography lead to a non-even distribution of the isotope ratio within a given chromatographic peak. The error introduced by overlapping peaks depends on the degree of co-elution, the magnitude of the isotope effect, and the difference of the isotope compositions of the overlapping compounds.[19] Furthermore, all carbon-containing substances are detected, meaning that even compounds not visible by many other detection techniques, such as small alcohols or acids in UV/vis, can mask the target compound. Hence, method development in LC-IRMS needs to be stronger focused on the sample to be measured than in quantitative analysis.[8, 20]

The aim of this work was to develop a chromatographic method to enable the determination of $\delta^{13}C$ of glyphosate and AMPA by LC-IRMS. As an amphoteric substance, glyphosate can be analyzed by either anion exchange or cation exchange chromatography. The latter is also used in the US Environmental Protection Agency EPA method 547 which includes post-column derivatization and fluorescence detection.[21] We exploited different chromatographic methods to obtain the best baseline resolution for matrix peaks and glyphosate. The applicability of the method is shown by measurements of commercial herbicides.

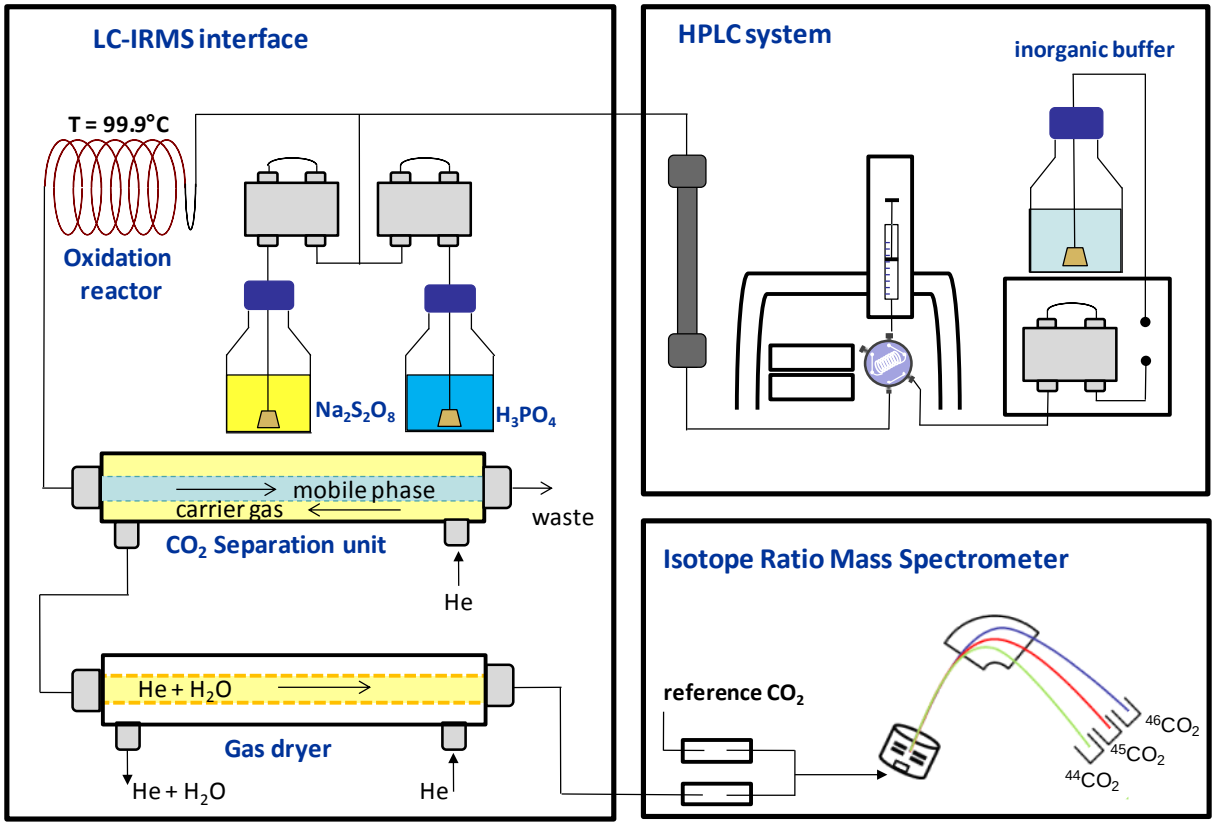

Figure 5.2 Schematic setup of the HPLC-IRMS system. The column effluent from the HPLC system is online mixed with an oxidation reagent and an inorganic acid. In a heated capillary dissolved CO_2 is formed and subsequently transfered into a carrier gas stream to reach the inlet of the IRMS.

5.2 Experimental

5.2.1 Chemicals and Reagents

Analytical standards of glyphosate and AMPA were purchased from Sigma-Aldrich GmbH (Steinheim, Germany) in a purity of at least 99 %. $Na_2S_2O_8$, KOH, H_3PO_4 and KH_2PO_4 used for eluent and reagent solutions were supplied by Fluka (Steinheim, Germany). Reagent solutions were degassed in an ultrasonic bath (Bandein Electronic, Berlin, Germany) under vacuum (Vacuubrand GmbH & Co., Wertheim, Germany) during 15 minutes. In order to avoid regassing of CO_2 all solutions were continuously purged with helium (purity 5.0, Air Liquide, Oberhausen, Germany).

5.2.2 HPLC conditions

The HPLC system consisted of a Rheos Allegro binary pump (Flux Instruments, Buchs, Switzerland) and a HTC PAL autosampler (Axel Semrau GmbH, Sprockhövel, Germany). A cation exchange column PRP-X400, 4.1 × 150 mm, 7 µm particle size (Hamilton AG, Bonaduz, Switzerland) was used to separate glyphosate and AMPA. The eluent was a 5 mM monobasic potassium phosphate (KH_2PO_4) adjusted to pH 1.9 with phosphoric acid at a flow rate of 500 µL min^{-1}. After 50 measurements the column was regenerated with 100 µL of a

0.1 M potassium ethylenediaminetetraacetate solution. The separation of glyphosate on the Hypercarb column 100 × 4.6 mm, 3 µm particle size (Thermo Fisher Scientific, Langerwehe, Germany) was performed with a 2.5 mM sodium phosphate buffer (NaH_2PO_4) pH 1.9 and a flow of 300 µL min^{-1}. The injected volume was 10 µL for PRP-X400 column and 20 µL when the Hypercarb column was used.

During the development of the method, anion exchange chromatography with an IonPac AS11, 4 × 250 mm, 13 µm particle size (Dionex/Thermo Fisher, Idstein, Germany) and 12 mM potassium hydroxide as eluent was also tested.

5.2.3 LC-IRMS conditions

An LC-IsoLink interface was used to couple the HPLC unit to a Delta V Advantage gas isotope ratio mass spectrometer (both Thermo Scientific, Bremen, Germany). The entire column effluent is mixed with peroxodisulfate (200 g L^{-1}) and phosphoric acid (1.5 M) via a T-piece. For all experiments the flow rate of both reagents was 50 µL min^{-1}. The stream passes through a heated capillary reactor where all carbon compounds are quantitatively converted to CO_2 at 99.9 °C[14]. Afterwards, the dissolved CO_2 is transported to a gas separation unit, where it is extracted from the aqueous phase into a carrier gas (He; Air Liquide, Oberhausen, purity 5.0) stream. The flow of the carrier gas flow to transfer the formed CO_2 to the open split was 1.2 or 2.3 mL min^{-1}.

The LC-IRMS interface was used for bulk $\delta^{13}C$ determination by flow injection analysis (FIA) by injecting aliquots from the analytical standards into a carrier flow of 200 µL min^{-1} water generated by the HPLC pump.

CO_2 reference gas peaks of different amplitudes were injected regularly to ensure good linearity and high precision of the mass spectrometric detection and $\delta^{13}C$ value determination.

5.2.4 Sample analysis

21 commercial herbicide samples of glyphosate (with agricultural and non agricultural uses) were diluted with the eluent to a concentration of 245 mg L^{-1} according to the concentration information indicated by the manufacturers. All samples were measured in triplicate. Standards of glyphosate at the same concentration were prepared in the eluent and run after every second sample measurement to ensure accurate and precise $\delta^{13}C$ values.

5.2.5 Elemental Analyzer-IRMS measurements

Aliquots of the analytical standard substances of glyphosate and AMPA were weighted in small tin cups (4 x 6 mm, IVA Analysentechnik, Meerbusch, Germany) at about 400 µg each and measured along with the working standard acetanilide (purity 99.9 %, Merck, Darmstadt, Germany) and blanks of empty tin cups. Combustion, chromatographic separation and detection of the obtained gases were performed with a CE 1110 elemental analyzer (EA) (CE Instruments, Milano, Italy) coupled to a MAT 253 IRMS via a ConFlow IV interface (both Thermo Scientific, Bremen, Germany). $\delta^{13}C$ values were corrected according to Werner and Brand[22]. The $\delta^{13}C$ value of the working standard acetanilide was determined accordingly by

correction with NBS-22 (oil; $\delta^{13}C = -30.031$ ‰), IAEA-CH-6 (sucrose; $\delta^{13}C = -10.449$ ‰) and IAEA 600 (caffeine; $\delta^{13}C = -27.771$ ‰).

5.2.6 Data acquisition and calculations

Acquisition and processing of data was performed by the Isodat 2.5 software. The background subtraction algorithm used for these measurements was "individual background". All reported carbon isotope compositions are expressed as $\delta^{13}C$ values based on VPDB scale. All standard deviations refer to at least triplicate measurements.

The isotopic fractionation associated with chromatographic separation was calculated by:

$$\alpha_{sep} = \frac{t_{12_C}}{t_{13_C}}$$

Here, α_{sep} is the fractionation factor and *t* the respective retention times of the ^{12}C and ^{13}C species as they appear in the traces of masses 44 and 45. The exact retention time was determined from the first derivative of the m/z 44 and 45 traces. Around zero of the derivatives, 20 points were chosen for a linear regression by the least-squares method. These calculations were made in triplicate for each α_{sep}.

5.3 Results and discussion

5.3.1 Chromatographic separation and its isotope effect

Some companies, e.g., Hamilton or Pickering Laboratories, distribute LC columns specially designed to separate glyphosate and its metabolite AMPA, either by cation or anion exchange chromatography. If anion exchange is employed, AMPA elutes earlier than glyphosate. In the case of cation exchange it is vice versa. In this work both alternatives were tested for their suitability for LC-IRMS analysis. Although a similar quality of separation between AMPA and glyphosate could be obtained with the IonPac AS11 column, the cation exchange was superior in background stability since the basic eluents employed in anion exchange chromatography have a strong affinity to concentrate CO_2 from air. Thus, the baseline increased over time and the eluent base had to be replaced more often. Although the water for eluent preparation had been degassed and continuously purged with nitrogen during potassium hydroxide dissolution and eluent usage, the baseline increased with time. For single runs, it even fluctuated during the measurement. This was accompanied by drifting retention times and a strong deviation in $\delta\ ^{13}C$-values. Although a higher amount of CO_2 in the carrier gas may improve linearity, due to the elimination of sorption effects[23], this is not the case if it originates from the eluents or the column since the feed of CO_2 is often not stable, resulting in a bad background correction or peak integration. This problem is avoided with cation exchange chromatography, because the eluent used for cation exchange had to be very acidic (pH 1.9) in order to obtain good peak shapes, since the second pK_a value of glyphosate is about 2. The CO_2 in the eluent can thus be very easily purged out.

AMPA and glyphosate are baseline-separated on the PRP-X400 cation exchange column with a resolution of 3 (see **Figure 5.3**). This column is recommended by the manufacturer to

analyze glyphosate. In commercial herbicide formulations glyphosate is added as an isopropyl amine salt in order to increase solubility. Other constituents are emulsifiers. None of these appeared in the chromatograms of most samples on the PRP-X400 column. Still, for two samples, we observed minor matrix components co-eluting with the front of the glyphosate peak when using the cation exchange column. The analysis of another glyphosate herbicide sample containing also the two herbicides diuron and 2-methyl-4-chlorophenoxyacetic acid (MCPA) resulted in a poor chromatographic separation from the glyphosate peak (**Figure 5.4**).

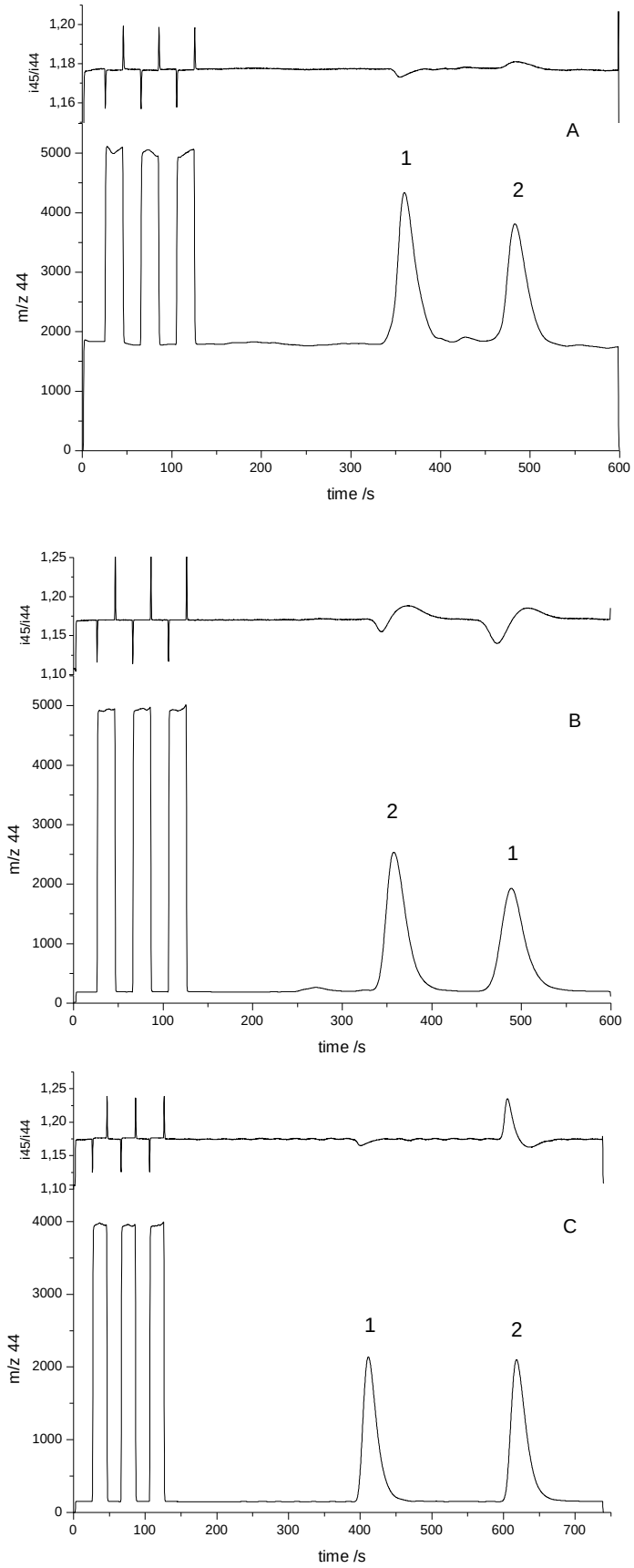

Figure 5.3 Chromatograms (m/z 44) of a standard containing 180 mg L^{-1} glyphosate (2) and 370 mg L^{-1} AMPA (1) on the AS11 (panel A), PRP-X400 (panel B) and on the Hypercarb column (panel C).

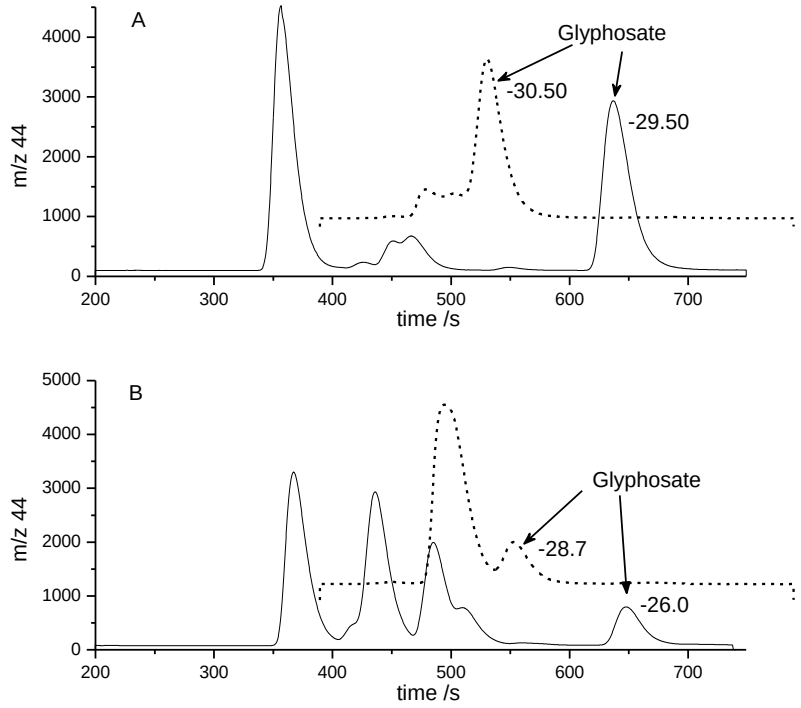

Figure 5.4 Chromatograms of two herbicide samples on Hypercarb (solid line) or PRP-X400 column (dashed line). All unmarked peaks are unknown matrix components of which two may be diuron and MCPA in sample B.

Changes in both the pH and counter ion of the eluent were not able to improve the peaks separation on the PRP-X400 column, arising from the need for another separation mode to be tested.

The use of reversed phase-LC (RP-LC) on a porous graphitic carbon column yielded an excellent chromatographic separation of glyphosate from the other two compounds and two unknowns (see lower chromatogram in **Figure 5.4**). This led to a reliable $\delta^{13}C$ measurement. In contrast, the measurements on the PRP-X400 column showed $\delta^{13}C$ values of glyphosate deviating of about 1 ‰, due to a poorer separation.

A resolution of 6 between glyphosate and AMPA can be achieved using the Hypercarb column. On the other hand, the analysis is quicker and cheaper using the PRP-X400, due to lower retention times and lower purchase cost of the column. The Hypercarb column has been designed to increase retention for small and very polar analytes. Due to charge-induced interactions with the polarizable graphitic surface small ionized samples like glyphosate can be retained. From the chromatographic isotope effect represented in the transient 45/44 mass trace ratio it can be recognized that here, the retention mechanism of glyphosate is different to ion exchange (note the mass 45/44 ratio trace in **Figure 5.3**). For cation exchange, the ^{13}C-substituted molecule will elute later than its counterpart. This may be due to an inductive effect decreasing the acidity and making the ^{13}C-substituted molecule bind stronger to the exchanger group[24]. The mass 45/44 ratio decreases and then increases again because the ^{12}C-containing molecule elutes first (normal isotope effect). In contrast, an inverse equilibrium isotope effect can be observed due to dominating van der Waals forces in GC-IRMS and RP-LC-IRMS.[25-26] The magnitude of the isotope effects solely from van der Waals forces or ion

exchange cannot be predicted or quantified, unless the intramolecular or position specific isotope distribution are known.[24] Nevertheless, an equilibrium fractionation factor for chromatographic separation α_{sep} can be calculated (see Experimental section for calculations), since a chromatographic process can be considered as a multiple equilibrium experiment. However, a change in chromatographic plate numbers does not influence α_{sep}. [27]

In the case of AMPA, the isotope effect which can be observed is directly resulting from the influence of ^{13}C substitution on the interactions with the stationary phase due to the fact that it has got only one carbon atom. The α_{sep} values for glyphosate are somewhat biased by ^{13}C substitution on positions which do not influence the isotopologue separation. However, from **Table 5.1** it can be seen that for glyphosate the isotope effects for both separations are of the same order of magnitude. For AMPA, the isotope effect of the separation on the Hypercarb column is smaller. In Figure 5.3 this can even be observed in the smaller change of the 45/44 mass ratio trace. A possible reason for this behavior is that glyphosate retention and its isotope effect on the Hypercarb column originates from the $–CH_2$-COOH group, which is missing in AMPA (see Figure 5.1). Thus, α_{sep} for AMPA on the Hypercarb column is smaller and even smaller than unity since other effects associated with a normal isotope effect predominate.

Table 5.1 Overview of the equilibrium fractionation factors for separation for glyphosate and AMPA on the Hypercarb and PRP-X400 column

Compound		α_{sep}	Retention time difference ($^{44}CO_2 - {}^{45}CO_2$) in s
AMPA	Hypercarb	$0.9998688 \pm 3 \times 10^{-7}$	-0.03 ± 0.0
	PRP-X400	$0.99919 \pm 3 \times 10^{-5}$	-0.25 ± 0.01
Glyphosate	Hypercarb	$1.00063 \pm 4 \times 10^{-5}$	0.29 ± 0.02
	PRP-X400	$0.999271 \pm 2 \times 10^{-6}$	-0.13 ± 0.0

Due to drifting retention times such calculations have not been performed for the anion exchange column, but from the 45/44 mass ratio trace in **Figure 5.3A**, it can be deduced that this effect is not significant for both analytes.

Although the α_{sep} given in **Table 5.1** appear to be partly smaller than the analytical precision (for example 0.9998688 means a change of only 0.2 ‰), it has to be considered that they are not determined from $\delta^{13}C$ values. The biggest errors of $\delta^{13}C$ values result from background subtraction and peak integration. These factors are not influencing the determination of retention times. During calculation of $\delta^{13}C$ values by the Isodat software a correction for this effect is performed by shifting the peak integration limits of the mass traces by a specific factor (“time shift”).[28]

5.3.2 Method detection limits and accuracy

Limits of precise isotope analysis (LPIA), based on a moving mean procedure described in Jochmann et al.[29], are 0.5 µg and 0.74 µg on column for glyphosate and AMPA, respectively (Figure 5.5). The precision of $\delta^{13}C$ measurements is better than 0.4 ‰. For the Hypercarb column, the MDL was 0.23 µg for glyphosate and 1.4 µg for AMPA. These limits are not column-specific, they rather represent the conditions of the interface and IRMS. The gas separation unit of the LC-IRMS also allows extraction of oxygen, which decreases filament life time. Furthermore, the ion source needs to be cleaned more often, since the CO_2 background in LC-IRMS is usually higher than in GC or EA-IRMS. By time, these factors can affect sensitivity and increase the detection limits. For this reason the carrier gas flow has been doubled for the analyses with the Hypercarb column in order to dilute the water, CO_2 and oxygen background in the IRMS. At the same time the injection volume has been increased to 20 µL. In our work, no significant differences in peak shape have been observed when the carrier gas flow was increased from 1.2 to 2.3 mL min^{-1}.

The analytical glyphosate standard showed no significant $\delta^{13}C$ offset (<0.5 ‰) from EA-IRMS measurements (**Figure 5.5**). We conclude that glyphosate and AMPA can be quantitatively converted into CO_2 in the interface, in contrast to other compounds measured by LC-IRMS.[17, 30]

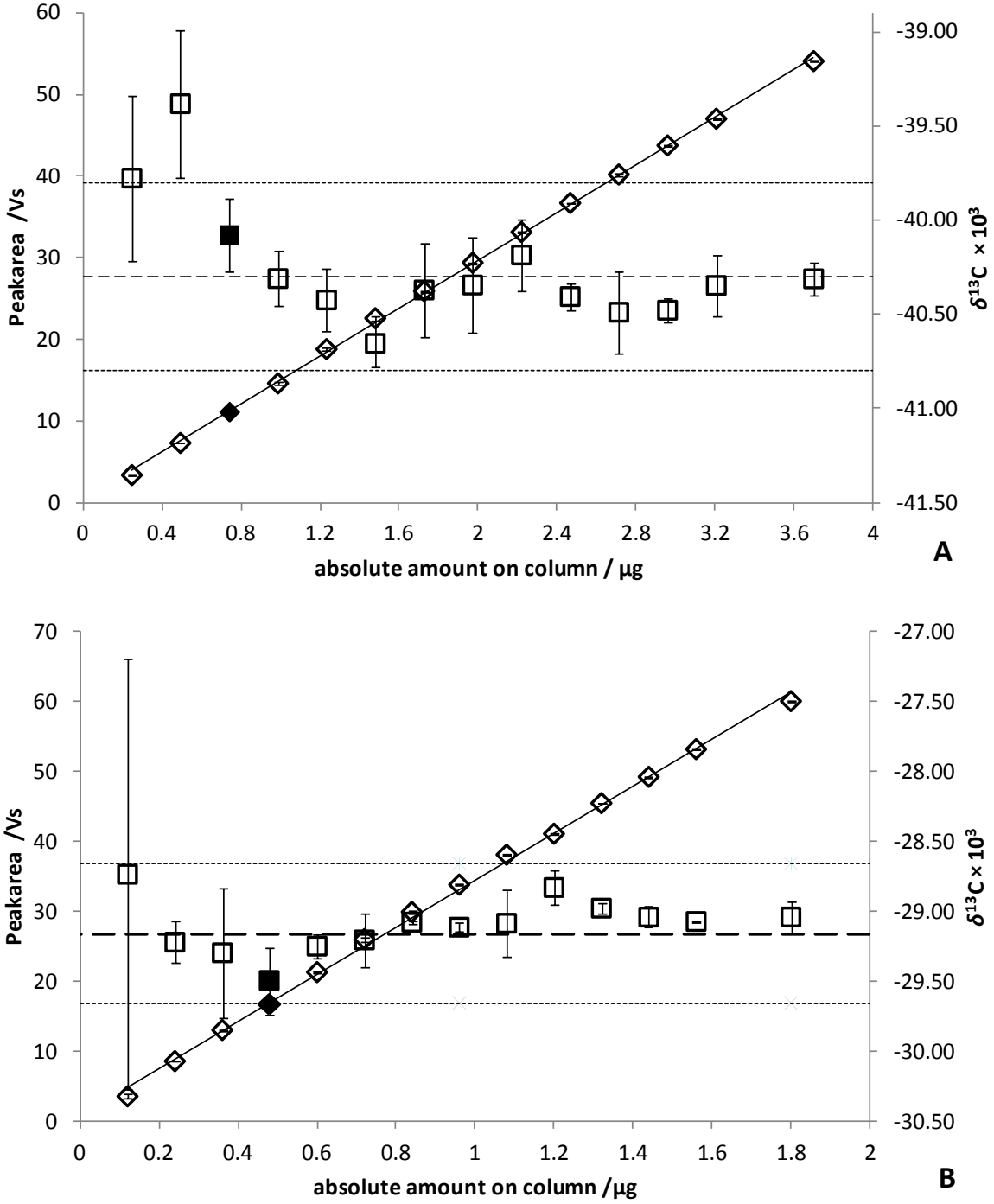

Figure 5.5 Calibration curves for AMPA (panel A) and glyphosate (panel B) on the PRP-X400 column. Diamonds correspond to peak areas of *m*/*z* 44 and squares to δ^{13}C values. The thick dashed horizontal line shows the EA-IRMS δ^{13}C value enclosed by a 0.5 ‰ confidence interval (light dashed lines). Points with a solid filling mark the detection limit.

5.3.3 Carbon isotope ratios of glyphosate from herbicide samples

δ^{13}C mainly depends both on i) the raw material and on ii) the industrial production processes used. For glyphosate, two main synthetic pathways are reported in the literature. The first is the alkyl ester pathway which requires glycine, dimethylphosphite, and paraformaldehyde as substrates.[31] The second way of producing glyphosate is to bind a phosphonomethyl group from phosphoric acid and formaldehyde to iminodiacetic acid hydrochloride and cleave one of the two carboxymethyl groups via oxidation.[31] Since in both pathways the glyphosate yield is not quantitative and numerous different raw materials are used, a broad range of δ^{13}C values can be expected.[31]

Results of the herbicide sample measurements are given in **Figure 5.6** and **Table 5.2**. The δ^{13}C values vary over a ~10 ‰ range. No δ^{13}C range could be attributed to a specific manufacturer. Of the 21 samples, ten were of the market leader for glyphosate herbicides. Its corresponding δ^{13}C values range between −26 ‰ and −34 ‰. The other tested products coming from 6 manufacturers revealed glyphosate with δ^{13}C values between −24 ‰ and −34 ‰. Source discrimination from a product to another might be possible if no degradation processes take place that ultimately alter the isotope ratio, and if the δ^{13}C values of the suspected sources significantly differ. At best, δ^{13}C values of glyphosate need to be combined with compound-specific isotope analysis of another element, for example ^{15}N/^{14}N ratios. However, LC-IRMS is restricted to carbon isotope compositions. The extension of the interface's capability to measure nitrogen isotopes would be very useful in this context.

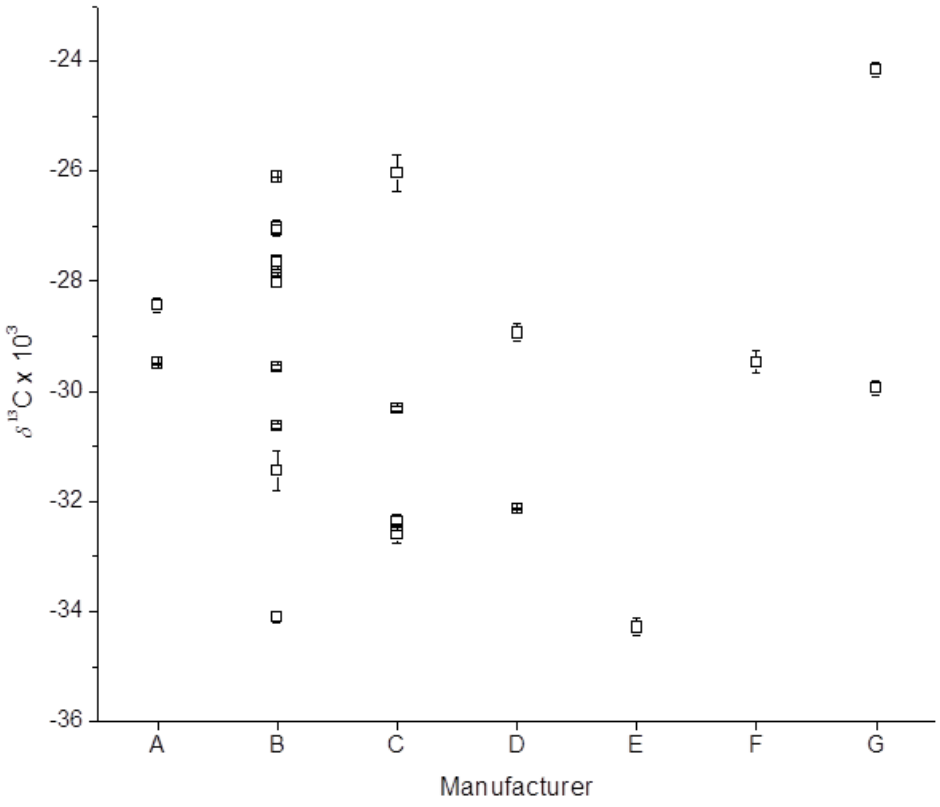

Figure 5.6 Distrubution of δ^{13}C values of glyphosate from commercial herbicide samples (N =21). Error bars indicate the standard deviation of triplicate measurements.

Table 5.2 δ ^{13}C values of glyphosate from the commercial herbicide samples

Manufacturer	δ ^{13}C × 10^3	
A	-29.50	±0.01
	-28.44	±0.13
B	-27.82	±0.03
	-34.10	±0.10
	-31.44	±0.36
	-30.64	±0.06
	-29.57	±0.05
	-28.01	±0.08
	-27.64	±0.09
	-27.08	±0.11
	-27.03	±0.14
	-26.11	±0.01
C	-32.59	±0.17
	-32.38	±0.15
	-30.31	±0.05
	-26.03	±0.33
D	-32.14	±0.02
	-28.94	±0.16
E	-34.29	±0.16
F	-29.47	±0.20
G	-24.15	±0.13
	-29.94	±0.13

For product authenticity, industry is highly interested in new methods for isotopic characterization mainly due to marketing of counterfeit products. These methods can be used for a quick screening of product authenticity without laborious offline purifications prior to EA-IRMS measurements. Although δ^{13}C values of different batches vary, δ^{13}C values of products with the same batch number from retained samples should be consistent and comparable. Using the Hypercarb column other matrix components might be used as isotopic authenticity markers as well. But for such an examination a much bigger dataset has to be generated.

5.4 Conclusion

We have extended the range of the reported methods for LC-IRMS to a new compound class which was not amenable to compound-specific isotope analysis before. Both methods developed in this work are complementary and can be used together in future investigations on glyphosate either in product authenticity or contaminant source identification. These methods also enable the investigation of degradation of glyphosate in the environment and constitute a first step for the tracking of chemical source(s) for AMPA. The characterization of the AMPA originated from other phosphonates should be studied as well as the fractionation during degradation.

Although we demonstrated a better performance for the Hypercarb column regarding resolution, the possibility of ion exchange separation method can be advantageous for some samples. For both methods equilibrium isotope effects for separation have been calculated. The calculated equilibrium isotope effects for separation indicate that adsorption of glyphosate in soil will not change its carbon isotope ratio.

References

1. Vereecken, H., Mobility and leaching of glyphosate: a review. *Pest Management Science* **2005,** *61* (12), 1139-1151.

2. Coupe, R. H.; Kalkhoff, S. J.; Capel, P. D.; Gregoire, C., Fate and transport of glyphosate and aminomethylphosphonic acid in surface waters of agricultural basins. *Pest Management Science* **2011,** *68* (1), 16-30.

3. Ermakova, I. T.; Shushkova, T. V.; Leont'evskii, A. A., Microbial degradation of organophosphonates by soil bacteria. *Microbiology* **2008,** *77* (5), 615-620.

4. Borggaard, O. K.; Gimsing, A. L., Fate of glyphosate in soil and the possibility of leaching to ground and surface waters: a review. *Pest Management Science* **2008,** *64* (4), 441-456.

5. Nowack, B., Environmental chemistry of phosphonates. *Water Research* **2003,** *37* (11), 2533-2546.

6. Singh, B. K.; Walker, A., Microbial degradation of organophosphorus compounds. *Fems Microbiology Reviews* **2006,** *30* (3), 428-471.

7. Schmidt, T. C.; Zwank, L.; Elsner, M.; Berg, M.; Meckenstock, R. U.; Haderlein, S. B., Compound-specific stable isotope analysis of organic contaminants in natural environments: a critical review of the state of the art, prospects, and future challenges. *Analytical and Bioanalytical Chemistry* **2004,** *378* (2), 283-300.

8. Elsner, M.; Jochmann, M. A.; Hofstetter, T. B.; Hunkeler, D.; Bernstein, A.; Schmidt, T. C.; Schimmelmann, A., Current challenges in compound-specific stable isotope analysis of environmental organic contaminants. *Analytical and Bioanalytical Chemistry* **2012,** *403* (9), 2471-2491.

9. Elsner, M., Stable isotope fractionation to investigate natural transformation mechanisms of organic contaminants: principles, prospects and limitations. *Journal of Environmental Monitoring* **2010,** *12* (11), 2005-2031.

10. Kujawinski, D. M.; Stephan, M.; Jochmann, M. A.; Krajenke, K.; Haas, J.; Schmidt, T. C., Stable carbon and hydrogen isotope analysis of methyl tert-butyl ether and tert-amyl methyl ether by purge and trap-gas chromatography-isotope ratio mass spectrometry: Method evaluation and application. *Journal of Environmental Monitoring* **2010,** *12* (1), 347-354.

11. Stalikas, C. D.; Konidari, C. N., Analytical methods to determine phosphonic and amino acid group-containing pesticides. *Journal of Chromatography A* **2001,** *907* (1-2), 1-19.

12. Reinnicke, S.; Bernstein, A.; Elsner, M., Small and Reproducible Isotope Effects during Methylation with Trimethylsulfonium Hydroxide (TMSH): A Convenient Derivatization Method for Isotope Analysis of Negatively Charged Molecules. *Analytical Chemistry* **2010,** *82* (5), 2013-2019.

13. Corr, L. T.; Berstan, R.; Evershed, R. P., Optimisation of derivatisation procedures for the determination of delta C-13 values of amino acids by gas chromatography/combustion/isotope ratio mass spectrometry. *Rapid Communications in Mass Spectrometry* **2007,** *21* (23), 3759-3771.

14. Krummen, M.; Hilkert, A. W.; Juchelka, D.; Duhr, A.; Schluter, H. J.; Pesch, R., A new concept for isotope ratio monitoring liquid chromatography/mass spectrometry. *Rapid Communications in Mass Spectrometry* **2004,** *18* (19), 2260-2266.

15. Dunn, P. J. H.; Honch, N. V.; Evershed, R. P., Comparison of liquid chromatography-isotope ratio mass spectrometry (LC/IRMS) and gas chromatography-combustion-isotope ratio mass spectrometry (GC/C/IRMS) for the determination of collagen amino acid delta(13) C values for palaeodietary and palaeoecological reconstruction. *Rapid Communications in Mass Spectrometry* **2011,** *25* (20), 2995-3011.

16. Godin, J.-P.; McCullagh, J. S. O., Review: Current applications and challenges for liquid chromatography coupled to isotope ratio mass spectrometry (LC/IRMS). *Rapid communications in mass spectrometry : RCM* **2011,** *25* (20), 3019-28.

17. Zhang, L.; Kujawinski, D. M.; Jochmann, M. A.; Schmidt, T. C., High-temperature reversed-phase liquid chromatography coupled to isotope ratio mass spectrometry. *Rapid Communications in Mass Spectrometry* **2011,** *25* (20), 2971–2981.

18. Heuer, V.; Elvert, M.; Tille, S.; Krummen, M.; Mollar, X. P.; Hmelo, L. R.; Hinrichs, K. U., Online delta C-13 analysis of volatile fatty acids in sediment/porewater systems by liquid chromatography-isotope ratio mass spectrometry. *Limnology and Oceanography-Methods* **2006,** *4*, 346-357.

19. McCullagh, J. S. O., Mixed-mode chromatography/isotope ratio mass spectrometry. *Rapid Communications in Mass Spectrometry* **2010,** *24* (5), 483-494.

20. Zhang, L.; Kujawinski, D. M.; Federherr, E.; Schmidt, T. C.; Jochmann, M. A., Caffeine in Your Drink: Natural or Synthetic? *Analytical Chemistry* **2012,** *84* (6), 2805-2810.

21. Winfield, T. W.; Bashe, W. J.; Baker, T. V., Determination Of Glyphosate In Drinking Water By Direct-Aqueous-Injection HPLC, Post-Column Derivatisation, And Fourescence Detection. 547, E. M., Ed. Environmental Monitoring Systems, Labratory Office of Research and Development, U.S. Environmental Protection Agency: Cincinnati, Ohio, 1990.

22. Werner, R. A.; Brand, W. A., Referencing strategies and techniques in stable isotope ratio analysis. *Rapid Communications in Mass Spectrometry* **2001,** *15* (7), 501-519.

23. Elsig, J.; Leuenberger, M. C., C-13 and O-18 fractionation effects on open splits and on the ion source in continuous flow isotope ratio mass spectrometry. *Rapid Communications in Mass Spectrometry* **2010,** *24* (10), 1419-1430.

24. Piez, K. A.; Eagle, H., C-14 Isotope Effect On The Ion-Exchange Chromatography Of Amino Acids. *Journal of the American Chemical Society* **1956,** *78* (20), 5284-5287.

25. Caimi, R. J.; Brenna, J. T., Quantitative evaluation of carbon isotopic fractionation during reversed-phase high-performance liquid chromatography. *Journal of Chromatography A* **1997,** *757* (1-2), 307-310.

26. Meier-Augenstein, W., Applied gas chromatography coupled to isotope ratio mass spectrometry. *Journal of Chromatography A* **1999,** *842* (1-2), 351-371.

27. Voskamp, M. Untersuchungen zur Sorption an Huminstoffen: Molekulargewicht und Kohlenstoff-Isotopenfraktionierung. University of Leipzig, Leipzig, 2005.

28. Ricci, M. P.; Merritt, D. A.; Freeman, K. H.; Hayes, J. M., Acquisition and Processing of Data for Isotope-Ratio-Monitoring Mass-Spectrometry. *Organic Geochemistry* **1994,** *21* (6-7), 561-571.

29. Jochmann, M. A.; Blessing, M.; Haderlein, S. B.; Schmidt, T. C., A new approach to determine method detection limits for compound-specific isotope analysis of volatile organic compounds. *Rapid Communications in Mass Spectrometry* **2006,** *20* (24), 3639-3648.

30. Kujawinski, D. M.; Zhang, L.; Schmidt, T. C.; Jochmann, M. A., When Other Separation Techniques Fail: Compound-Specific Carbon Isotope Ratio Analysis of Sulfonamide Containing Pharmaceuticals by High-Temperature-Liquid Chromatography-Isotope Ratio Mass Spectrometry. *Analytical Chemistry* **2012,** *84* (18), 7656-7663.

31. Dill, G. M.; Sammons, R. D.; Feng, P. C. C.; Kohn, F.; Kretzmer, K.; Mehrsheikh, A.; Bleeke, M.; Honegger, J. L.; Farmer, D.; Wright, D.; Haupfear, E. A., Glyphosate: Discovery, Development, Applications, and Properties. In *Glyphosate Resistance in Crops and Weeds*, Nandula, V. K., Ed. John Wiley & Sons, Inc.: 2010; pp 1-33.

6 Carbon isotope fractionation during degradation of glyphosate by manganese dioxide

Abstract

Glyphosate is one of the most widely used herbicides and its implication on the environment is debated. For many years it was believed that only sorption and biotic degradation govern the disappearance of glyphosate in the environment due to its resistance against hydrolysis. In the last decade the oxidation of glyphosate by manganese dioxide was found as a potential abiotic degradation pathway in the environment. However, the fact that all of these pathways produce non-specific metabolites challenges differentiating degradation routes in natural ecosystems.

This work presents the first isotopic study of a degradation reaction of this important herbicide. Suspensions of δ-MnO_2, or birnessite, were used to oxidize glyphosate at various temperatures and two concentrations. The appearance of sarcosine and aminomethylphosphonic acid during the reaction revealed two reaction pathways. The apparent kinetic isotope effect (*AKIE*) was calculated to be 1.011 at 20°C. Neither product appearance nor *AKIE* were significantly influenced by temperature or MnO_2 to glyphosate ratio. The latter points to electron transfer or bond cleavage as rate limiting step. This work also shows that it may also be possible to trace back the origin of AMPA to glyphosate in environmental samples under certain conditions.

6.1 Introduction

Oxides of transition metals are ubiquitous in soils. Since they are major constituents of soil, they can be partly responsible for the attenuation of organic pollutants of human origin. Various studies have shown the ability of metal hydroxides and oxides to degrade organic compounds either by photocatalysis or charge transfer induced cleavage. δ-MnO_2, or birnessite, is a frequently encountered manganese mineral in soils.[1] Although the main valence of manganese in this configuration is IV, it can also contain a certain fraction of lower valence manganese, since the oxygen-to-manganese ratio is often significantly lower than two.[2] It is proposed that after sorption, organic compounds reduce Mn(III) or Mn(IV) to yield Mn(II), which in turn can be reoxidized by molecular oxygen.[3] In that way, many micropollutants such as triclosan[4], chlorophene[4], sulfamethazine[5], aromatic amines[6-7] or carbamazepine[8] can be oxidized.

An oxidative cleavage of the popular herbicide glyphosate by manganese dioxide has been demonstrated in 2005 by Barrett and McBride.[9] It is proposed that glyphosate adsorbs to manganese via its phosphonate group and transfers an electron to Mn(III). This induces a splitting of glyphosate into sarcosine and eventually glycine and formic acid. The oxidation of glyphosate by manganese dioxide takes place under anoxic conditions as well, although the reaction rate is smaller.[9] Even when molecular oxygen is present, free Mn(II) does not react

with glyphosate to form phosphate and sarcosine, possibly because of the weak complex formation with glyphosate.[9]

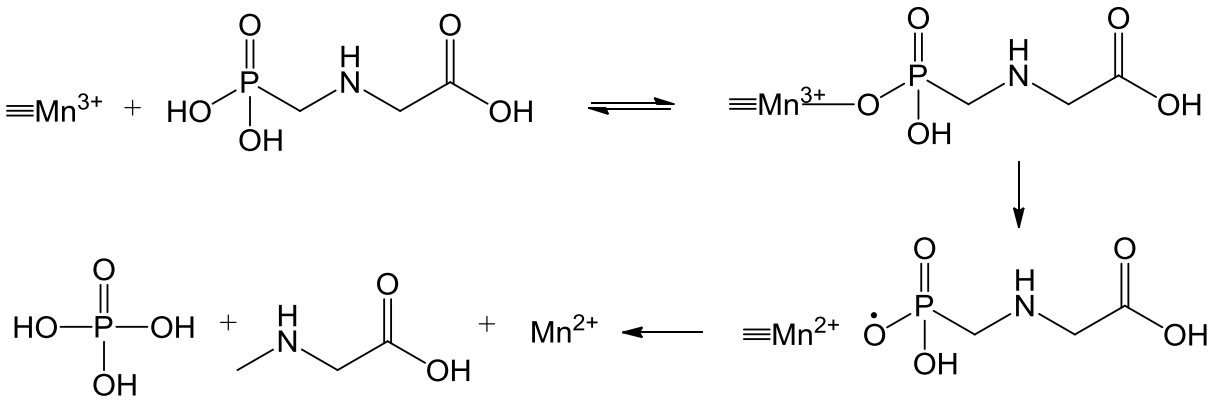

Figure 6.1 Proposed reaction scheme for the oxidative cleavage of glyphosate by birnessite (δ-MnO_2)after Barrett and McBride[9]

In contrast, no sarcosine was found when glyphosate was oxidized by thin films of birnessite electro-deposited on SnO_2, but aminomethylphosphonic acid (AMPA), formaldehyde, carbonate, phosphate, ammonia and nitrate have been found.[10]

Microorganisms transform glyphosate into sarcosine by a P-C lyase or into AMPA by glyphosate oxidoreductase.[11] Both compounds can only serve as a hint for glyphosate degradation in the environment since sarcosine is a common biological amino acid and AMPA can result from the decomposition of certain anthropogenic complexing agents.[12]

Hence, the examination of stable isotope ratios at natural abundance is nowadays a complementary tool to qualitative and quantitative analysis of degradation processes, especially when no specific metabolites are present. Stable isotope ratios, commonly reported in the *δ*-notation, can change during the course of a reaction. This change or isotopic fractionation can be expressed by the isotope enrichment factor ε, which is the difference of the *δ*-value between the reactant and the instantaneously formed product. If abiotic and biotic degradation involve different reaction mechanisms, it may be possible to distinguish them in the field, as in the case of the herbicides atrazine and isoproturon[13]. Although such enrichment factors have been determined for some relevant processes like hydrolyses, various dechlorination reactions and C-H bond oxidations, more controlled laboratory experiments are necessary to increase the reference data set for future investigations.

The aim of this work was to investigate if the oxidative decomposition of glyphosate by manganese dioxide is associated with a measureable isotope effect. Up to now no enrichment factors or kinetic isotope effect (*KIE*) values, respectively, have been published for this important herbicide or organophosphorous compounds in general. Recently, we have developed the first method to measure compound-specific carbon isotope ratios of glyphosate and its metabolite AMPA by liquid chromatography coupled to isotope ratio mass spectrometry (LC-IRMS).[14] Isotope enrichment factors from controlled laboratory experiments as presented herein can play a key role in understanding the fate of glyphosate in natural environments. Furthermore, degradation products will be identified and the origin of the fractionation discussed.

6.2 Experimental

6.2.1 Chemicals and Reagents

Glyphosate, sarcosine and AMPA were purchased from Sigma-Aldrich (Steinheim, Germany) in a purity of at least 99 %, sodium peroxodisulfate ($Na_2S_2O_8$), phosphoric acid (H_3PO_4) and monosodium phosphate (NaH_2PO_4) for eluent and reagent solutions were supplied by Fluka (Steinheim, Germany). Reagent solutions were degassed in an ultrasonic bath (Bandein Eletronic, Berlin, Germany) with a vacuum applied (Vacuubrand, Wertheim, Germany). Eluent and interface reagent solutions were continuously purged with Helium (purity 5.0, Air Liquide, Oberhausen, Germany) in order to avoid a regassing of CO_2.

6.2.2 LC-IRMS conditions

The LC-IRMS system has been described in Kujawinski el al.[14] In brief, the LC system consisted of a Rheos Allegro binary pump (Flux Instruments, Buchs, Switzerland) and a HTC PAL autosampler (CTC Analytics, Idstein, Germany). A Hypercarb column 100 × 4.6 mm, 3 µm particle size (Thermo Scientific, Langerwehe, Germany) was used to separate glyphosate from its degradation products. The eluent was a 2.5 mM NaH_2PO_4 adjusted to pH 1.9 with H_3PO_4. The flow rate was 300 µL min^{-1} in isocratic mode. The injected sample volume was 20 µL.

As described in our previous work, either an ion exchange or a porous graphitic carbon (PGC) column can be used to separate glyphosate.[14] Here, the PGC column was used, since it was impossible to separate glyphosate from its degradation products on the cation exchange column.

In order to fully separate AMPA from sarcosine but on the expense of a poor glyphosate peak, a sodium phosphate solution, 3 mM at pH 6 was used as eluent on the Hypercarb column as well. But this method has only been applied to a few samples of a degradation batch in which glyphosate had been fully degraded.

Via an LC-IsoLink (Thermo Scientific, Bremen, Germany) interface the HPLC was coupled to the Delta V Advantage (Thermo Scientific, Bremen, Germany) isotope ratio mass spectrometer (IRMS). The reagents to convert the HPLC effluent to CO_2 were phosphoric acid (1.5 M) and sodium peroxodisulfate (200 g L^{-1}). For all experiments flow rate of each reagent was 50 µL min^{-1}. The wet chemical oxidation was performed at a reactor temperature of 99.9 °C. The carrier gas flow of helium (Air Liquide, Oberhausen, purity 5.0) to transfer CO_2 to the IRMS was 2.3 mL min^{-1}. Several reference gas pulses of different amplitudes were used to monitor linearity and precision of the instrument.

Isodat 2.5 was used for data acquisition and $\delta^{13}C$ calculation based on the VPDB scale. All standard deviations were calculated from at least triplicate measurements.

6.2.3 MnO_2 preparation

Birnessite (δ-MnO_2) was prepared by slowly pouring 6 M HCl into a boiling solution of 1M $KMnO_4$. After 10 minutes of boiling, the mixture was filtered. The remaining solid was washed with pure water until the pH of the residue was neutral. The solid residue was dried

and stored over P_2O_5 as desiccant in an evacuated desiccator until further use. This procedure is according to the synthesis of synthetic birnessite used by McKenzie et al.[2].

6.2.4 Degradation experiments

For the degradation experiments 0.15 g or 0.3 g δ-MnO_2 were dissolved in 100 mL of a solution containing 1.5 mM glyphosate and 0.01 M sodium nitrate as background electrolyte. All experiments were conducted in 250-mL amber glass bottles at 20, 30, 40 and 50°C. The mixture was continuously stirred with a Teflon coated magnetic stir bar. The temperature was controlled with a water bath. Samples of 2 mL were withdrawn by a PP single-use syringe (5 mL, B.Braun Melsungen AG, Melsungen, Germany) and filtered by hydrophobic PTFE syringe filters of 0.22 µm pore size (BGB Analytik AG, Rheinfelden, Germany). The measurements were performed in triplicate immediately after sampling.

Methods of sterile working like addition of biocides or autoclaving were not used in order not to introduce extraneous compounds or significantly change the modification of the manganese dioxide. The absence of microbial growth was supported by chromatograms without indications of unresolved matrix anywhere.

6.2.5 Calculation of enrichment factors ε, AKIE and mass balances

Carbon isotope enrichment factors were calculated from a triplicate batch of degradation if not stated else.

Isotope enrichment factors ε were computed by the Rayleigh equation:

$$\ln\left(\frac{\delta^{13}C + 1}{\delta^{13}C_0 + 1}\right) = \varepsilon \cdot \ln\frac{c}{c_0}$$

Apparent kinetic isotope effect (AKIE) has been calculated according to the following equation:

$$AKIE = \frac{1}{\frac{n}{x}\,\varepsilon + 1}$$

Where n denotes the number of carbon atoms at the reactive positions and x the total number of carbon atoms.

The isotope balance was calculated from peak areas and $\delta^{13}C$ values from the three major product peaks and glyphosate:

$$\delta^{13}C_G^0 = \delta^{13}C_G^t \times \frac{A_G^t}{A_G^0} + \delta^{13}C_S^t \times \frac{A_S^t}{A_G^0} + \delta^{13}C_A^t \times \frac{A_A^t}{A_G^0} + \delta^{13}C_U^t \times \frac{A_U^t}{A_G^0}$$

Here, A is the peak area of glyphosate (subscript G), AMPA (subscript A), sarcosine (subscript S) and the unidentified product (subscript U) at different time t.

6.3 Results and discussion

6.3.1 Degradation products of glyphosate

In the LC-IRMS chromatograms three peaks other than glyphosate were observed (see **Figure 6.2**). A match with authentic standards revealed the expected product, sarcosine, but also AMPA, proving a second reaction mechanism taking place. In previous studies the formation of sarcosine has been concluded only from an increase in ortho-phosphate during the reaction, but a formation of AMPA could not be excluded due a randomly positive ninhydrin test.[9, 15] In another recent study no sarcosine could be detected although phosphate was found besides AMPA, formaldehyde, ammonia and nitrate.[10] Whether or not sarcosine is formed might be influenced by oxygen since in the case of nitrilotris (methyl phosphonic acid) (NTMP) oxidation by manganite suspensions (MnOOH) C-N bond cleavage is dominant under anoxic conditions, whereas C-N and C-P bond cleavage take place at similar rates when oxygen is present.[16]

The third product peak appearing in the chromatograms is likely glyoxalate resulting from the formation of AMPA. A coelution with other possible degradation products, formaldehyde, acetate, methylamine and carbonate[10], can be excluded as different chromatographic conditions (pH 6 and 3 mM $NaHPO_4$) did not resolve this peak. All three peaks appeared in all experiments regardless of reaction temperature or glyphosate/MnO_2 ratio.

Due to the low sensitivity of the LC-IRMS it cannot be excluded that other reaction products are formed to a small extent as well. Hence, the small bump at about 390 s in the chromatogram in might originate from further degradation of sarcosine, glyoxylate and AMPA. In fact, the reaction of MnO_2 with AMPA is about 20 times slower than with glyphosate[9], but there is no information on its reaction with sarcosine or glyoxylate published in literature.

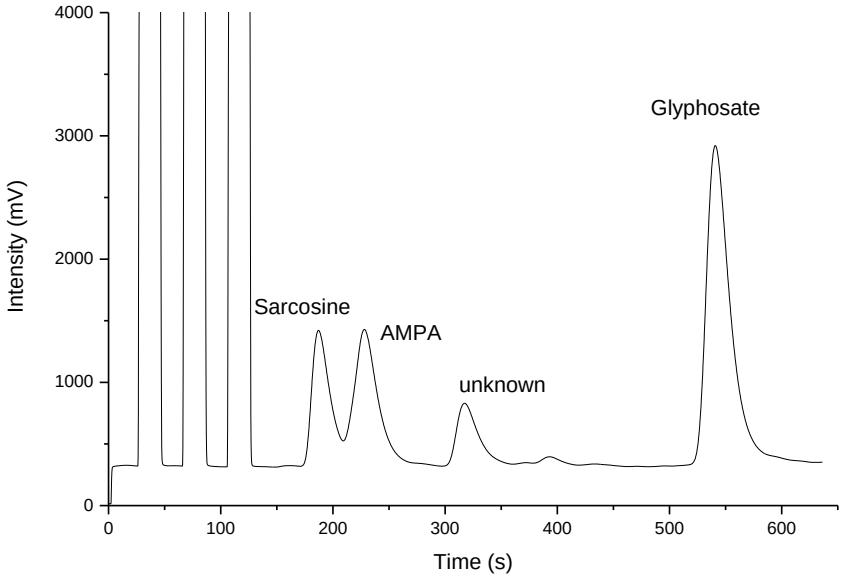

Figure 6.2 LC-IRMS chromatogram (m/z 44) of a degradation batch of 250 mgL^{-1} glyphosate and 1.5 gL^{-1} MnO_2 after 7 hours at 20°C.

6.3.2 Reaction kinetics and temperature dependency

It is assumed that the oxidation is very fast and the adsorption on the surface is the rate-determining step. As in the case of a transition-state complex or enzyme-substrate complex the reaction follows a second order rate law. Due to the reaction scheme of glyphosate reacting with Mn(III) proposed by Barrett and McBride.[9] (see **Figure 6.1**), a second-order rate law was chosen to fit the data (see **Figure 6.3** and **Figure 6.4**).[17] Furthermore, the reaction order of reaction at reactive surface sites can change with concentration of reactants.[18]

The observed second-order rate constants for this reaction can be taken from **Table 6.1**. The rate of sarcosine formation is comparable to the increase in ortho-phosphate described by Barrett and McBride[9] at a similar glyphosate/MnO_2 ratio, as the C-P cleavage forms sarcosine and phosphate. About 13% of the initial glyphosate is converted into sarcosine after seven hours.[9] The rate of phosphate formation and glyphosate elimination at 25°C in the work of Ndjeri et al. was close to the rate of sarcosine formation and glyphosate degradation in our study[10](see **Figure 6.6**) as well.

Activation energies derived from a linear regression of natural logarithmic rate constants and reciprocal temperatures (see **Figure 6.5**) differed between 1.5 g L^{-1} (32 $kJmol^{-1}$) and 3 g L^{-1} (87 $kJmol^{-1}$). This is either a result of the initial adsorption step, i.e. an equilibrium reaction, or points to a catalytic character of the manganese dioxide.

Looking at the sum of all peak areas in **Figure 6.6**, about 20% of the initial carbon is present as compounds which are not detectable, most likely due to strong adsorption to the MnO_2.

Table 6.1 Observed reaction rate constants (second order reaction) and activation energy

MnO_2 concentration	**20 °C k in $Lmol^{-1}s^{-1}$***	**30°C $Lmol^{-1}s^{-1}$***	**40°C $Lmol^{-1}s^{-1}$***	**Activation energy**
1.5 g L^{-1}	1.40(7) $\times10^{-2}$	2.06(7) $\times10^{-2}$	2.54(5) $\times10^{-2}$	31.99 kJ/mol
3 g L^{-1}	3.53(4) $\times10^{-2}$	0.105(2)	0.344(4)	86.83 kJ/mol

* Numbers in parenthesis show the standard deviation of three measurements

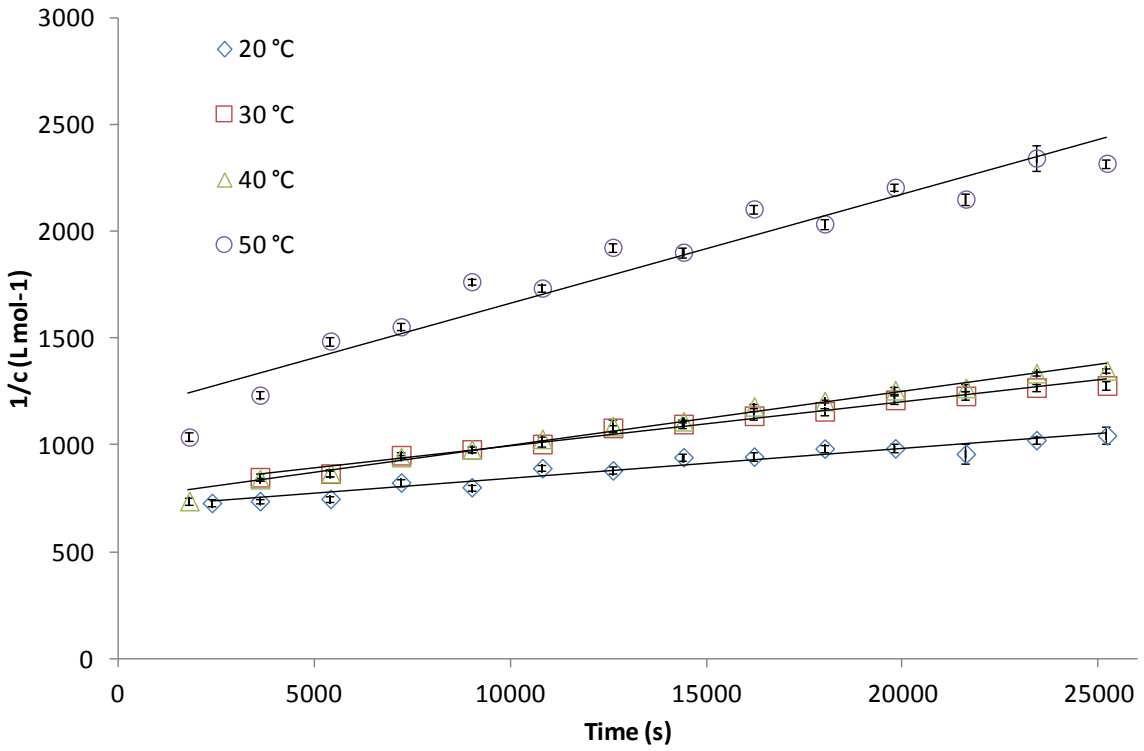

Figure 6.3 Reciprocal glyphosate concentration during degradation experiment with 1.5 g L^{-1} MnO_2

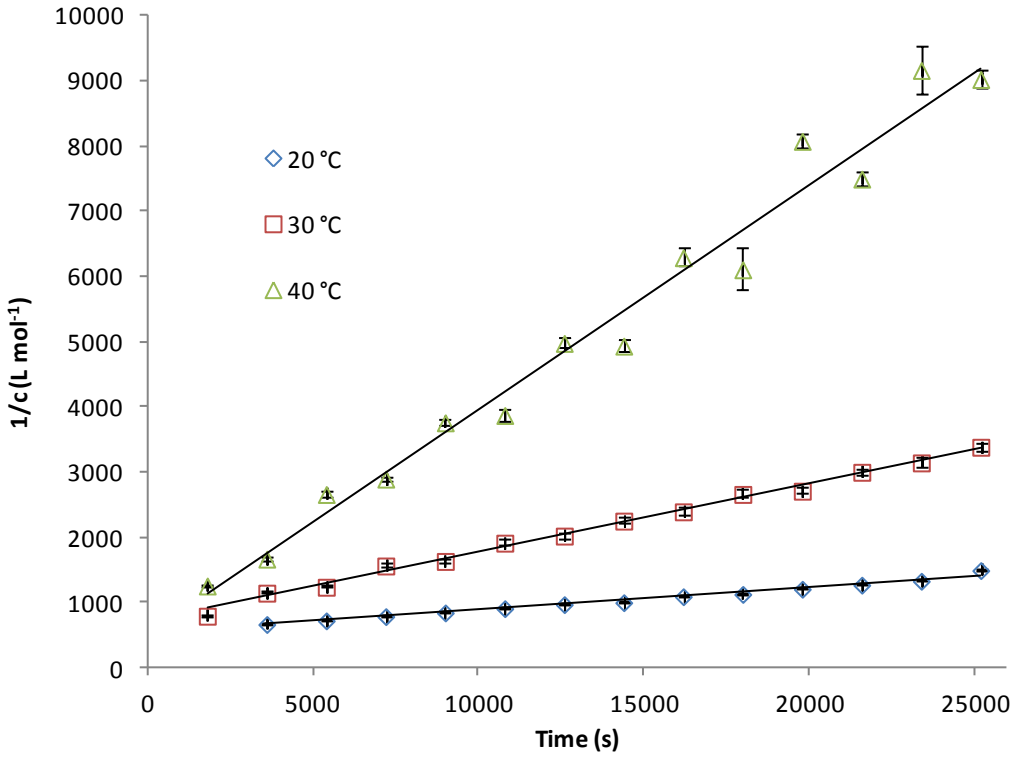

Figure 6.4 Glyphosate degradation experiment with 3 g L^{-1} MnO_2

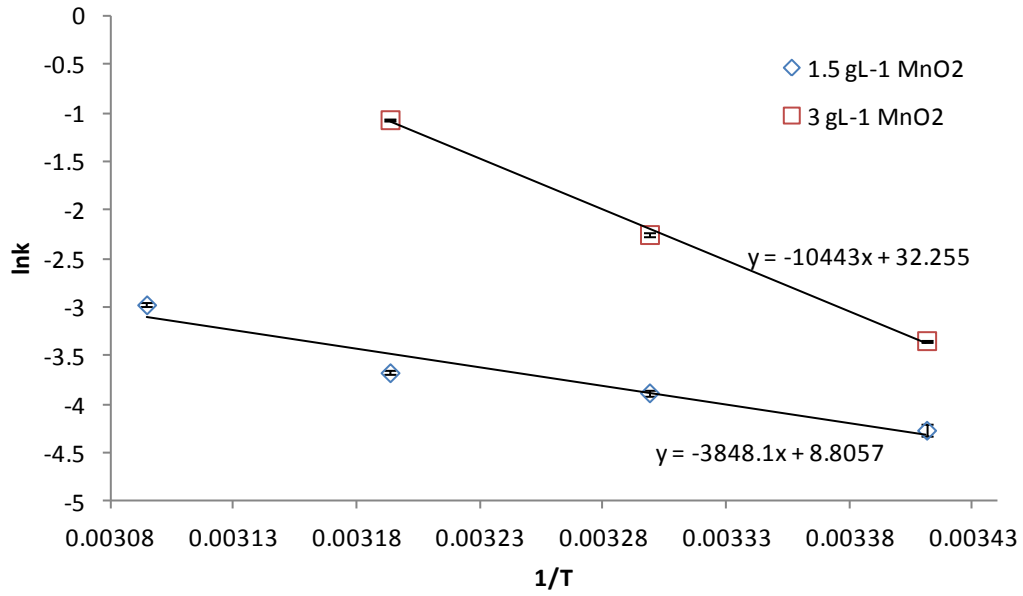

Figure 6.5 Arrhenius plot of the second-order rate constants

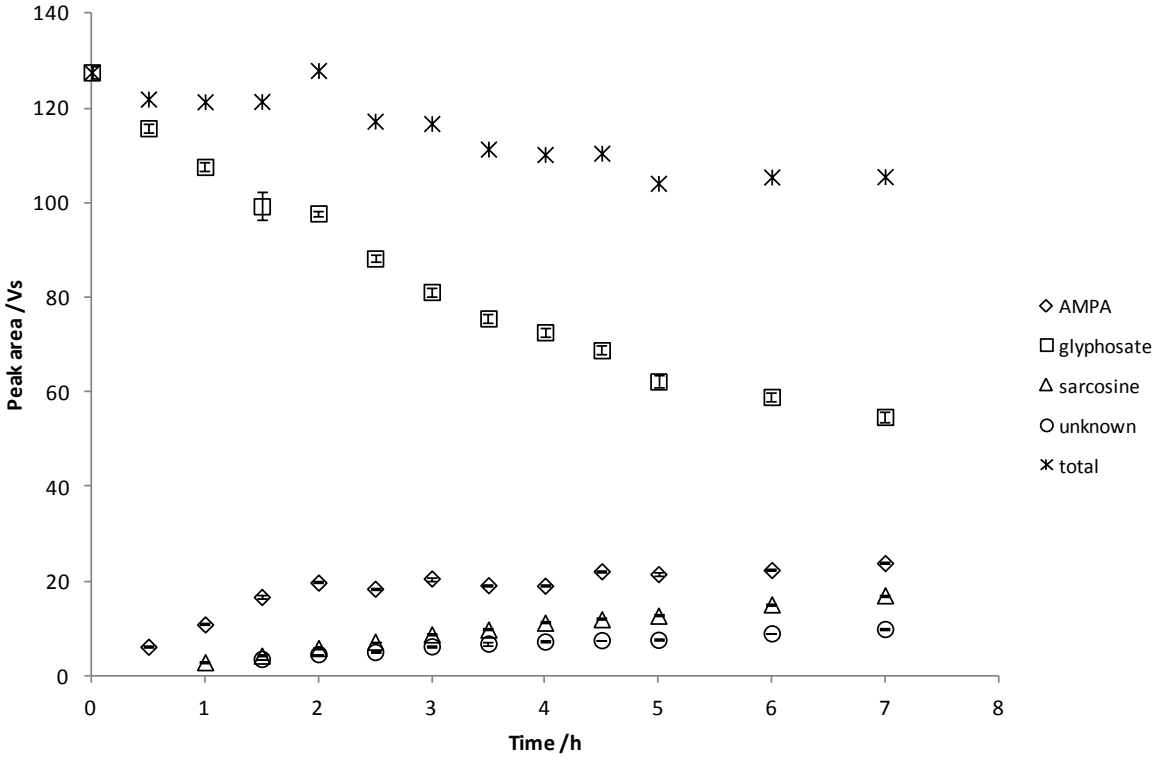

Figure 6.6 Peak areas (m/z 44) of glyphosate and products of its degradation by MnO_2 ($1.5gL^{-1}$) at 20°C

6.3.3 Carbon isotope enrichment during degradation

A relatively low carbon isotope enrichment factor ε of about -3.7(6) $\times 10^3$ has been found for the degradation of glyphosate by MnO_2. It was also quite variable with each experimental batch, although deviation of $\delta^{13}C$ values of glyphosate control standards was less than 0.5‰. Hence, the AKIE for a glyphosate oxidation on MnO_2 was 1.011. This value is lower than the AKIE of the oxidation of aromatic amines by MnO_2 which is in the range 1.018 to 1.022[7]. The AKIE was not temperature dependent in the range 20°C to 50°C (see **Figure 6.7** and **Table 6.2**).

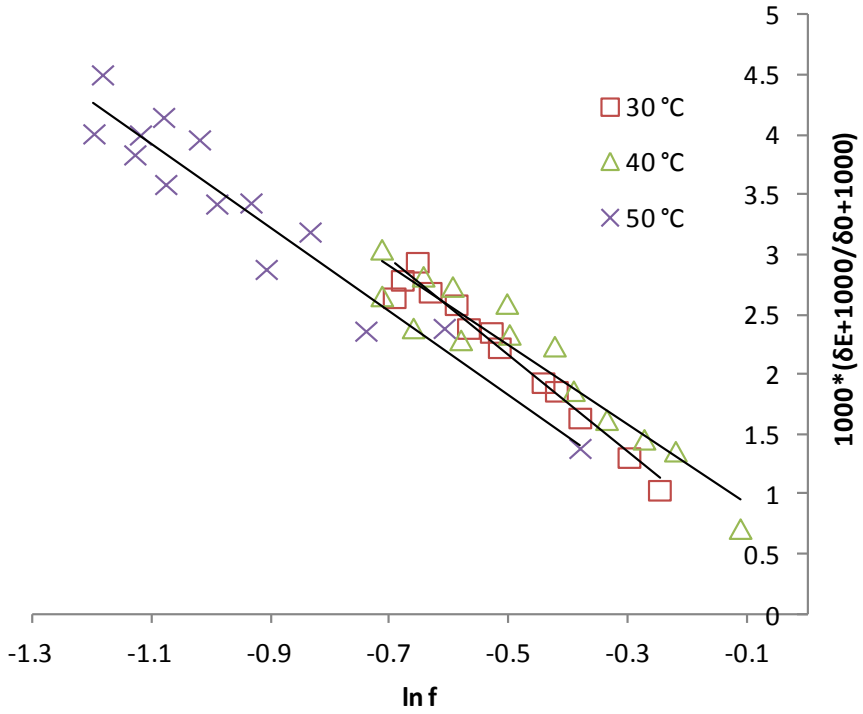

Figure 6.7 Rayleigh plot of glyphosate degradation with 1.5 gL^{-1} MnO_2

Table 6.2 Carbon isotope enrichment factors ε associated with glyphosate degradation by MnO_2

MnO_2 concentration	20 °C ε $\times 10^3$	30°C ε $\times 10^3$	40°C ε $\times 10^3$	50°C ε $\times 10^3$
1.5 gL^{-1}	-3.7	-4.2	-3.4	-3.3
3 gL^{-1}	-3.4	-3.8	-3.6	n.d.

Generally, it is supposed that the rate limiting step of the reaction governs an observable fractionation. Here, the initial step of complexation of the reactive manganese species by glyphosate is thought to be slower than its cleavage.[4, 9, 19] In case of the degradation of NTMP, the rate limiting step is the complex formation with the mineral bound manganese as well.[20] But the complexation of manganese by glyphosate is probably not responsible for the observed carbon isotope effect. There was no change of the carbon enrichment factor when the molar MnO_2/glyphosate ratio was doubled. Moreover, glyphosate adsorbs via its

phosphonate group on goethite (α-FeO(OH)) and manganite (γ-MnOOH) [21-22], which is likely to be the case for δ-MnO_2 as well. An observable secondary isotope effect on complexation can be ruled out. Furthermore, from chromatographic data presented in the previous chapter, it can be concluded that secondary or primary isotope effects on an anion exchange reaction via phosphonate group or carboxy group, respectively, are not measurable.[14] Thus, either the initial step of complexation is masking the isotope enrichment factor or it is not the rate-limiting step. In the case of oxidation of substituted anilines by MnO_2, electron transfer rather than the initial step of complexation is the rate-limiting step as nitrogen isotope fractionation does not change with MnO_2/reactant ratio as well.[17] On the other hand, carbon, hydrogen and nitrogen isotope analysis of substituted aromatic N-alkyl amines has shown that the rate-limiting step in MnO_2 degradation reactions is bond cleavage for many of these compounds.[23]

Looking closer into $\delta^{13}C$ values of the three main degradation products it may be concluded that the carbon AKIE of glyphosate can be a mixture of isotope effects associated with two reactions. In **Figure 6.8** $\delta^{13}C$ values of glyphosate, sarcosine, AMPA and the major unknown product, possibly glyoxylate, during the degradation can be seen. Although AMPA and sarcosine were not fully separated, their $\delta^{13}C$ values may be considered since they are consistent with $\delta^{13}C$ values measured with a LC method which allows a better separation but on the expense of the glyphosate peak (see **Chapter 6.2.2**).

Here, the $\delta^{13}C$ values of AMPA are of minor importance, since the carbon atom at the P-C position is not involved in the formation of AMPA or the secondary effects of an isotopic substitution are negligible, respectively. Thus, only $\delta^{13}C$ values of sarcosine and the unknown compound, probably glyoxylate, can give information on isotope effects of glyphosate degradation.

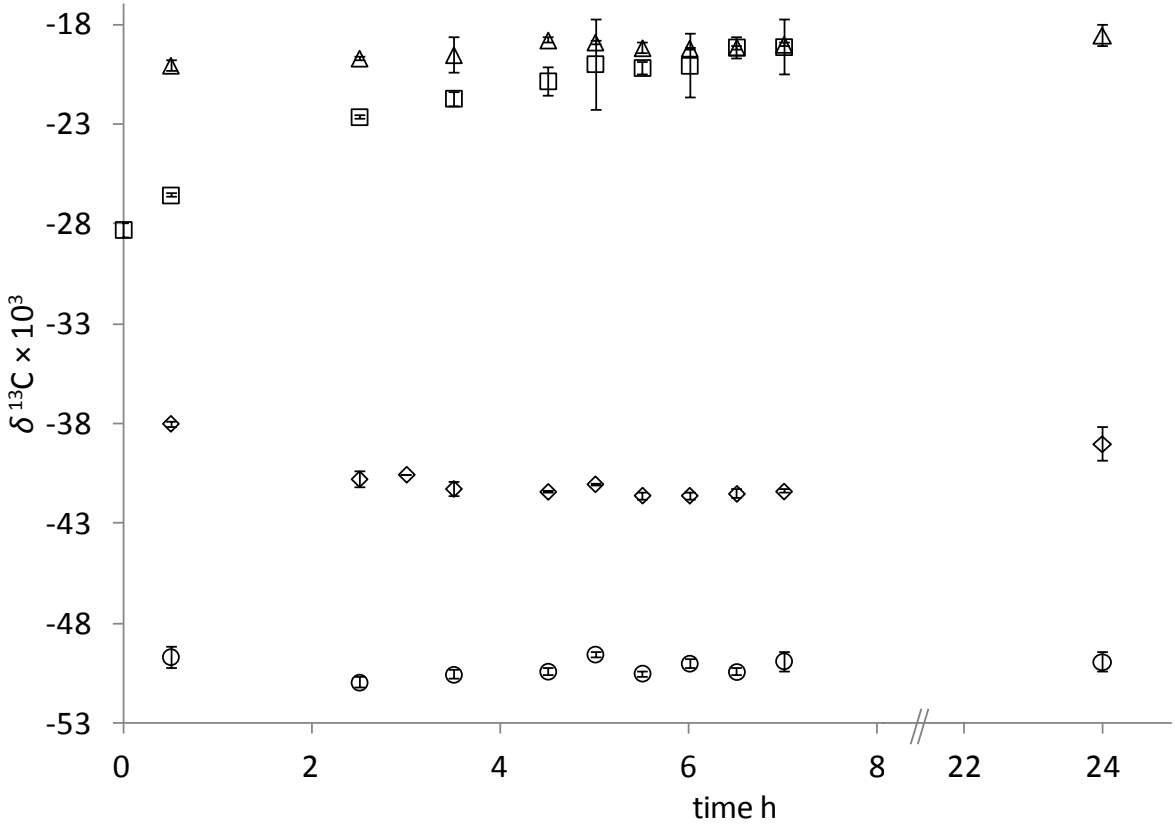

Figure 6.8 δ^{13}C values of glyphosate (squares), sarcosine (triangles), AMPA (diamonds) and the unidentified peak (circles) with experiment time. The concentration of MnO_2 was 3 gL^{-1} and the experiment was conducted at 40 °C. After 24 h glyphosate was not detected due advanced degradation. The last sample was measured with a different chromatographic method (see **Chapter 6.2.2**)

The δ^{13}C values of the unknown compound are more than 20 ‰ lower than the starting δ^{13}C value of glyphosate which can be an indicator of a strong fractionation during C-N cleavage, further degradation or during complex formation with MnO_2. Further processes associated with fractionation are supposable, since an isotopic mass balance after all glyphosate has reacted does not yield the starting δ^{13}C value of glyphosate, but is about 4 ‰ lower. The incomplete mass balance discussed in **Chapter 6.3.2** further supports this assumption.

This difference of δ^{13}C values cannot solely be attributed to different position-specific isotope ratios. Given that the only carbon atom of AMPA will not change its isotope ratio during C-N cleavage, since it is located at the other side of the molecule, its δ^{13}C value of about -39 ‰ can be regarded as a position-specific isotope ratio of glyphosate. Hence, in order to yield a "bulk" δ^{13}C value of about -28 ‰ of glyphosate, the unknown compound would need to have a δ^{13}C value of -23 ‰.

δ^{13}C values of sarcosine are 9 ‰ higher than the starting value of glyphosate and do not change during the reaction. The accuracy of the δ^{13}C value of sarcosine after 30 min reaction time cannot be assured due to a low peak area. Thus, the C-P cleavage will probably not cause the isotope effect. But more measurements on product isotope ratios are necessary, due to incomplete chromatographic separation of AMPA and sarcosine.

Maximum KIE have also been calculated from measured vibrational frequencies (see **Table 6.3**) published in literature[21, 24]. The assignment of absorption bands to a vibration of the P-C bond is difficult due to low intensity and spectral interferences with absorption of other groups, especially the phosphonic acid group[25]. Nevertheless, two frequencies for the P-C bond in glyphosate can be found in literature[21, 24-25]. Thus, the Streitwieser limit of a P-C bond cleavage calculated from the stretching vibration is 1.0065 at 20°C[26]. The maximum KIE for the cleavage of the C-N bond of glyphosate adsorbed to goethite was calculated to be lower with 1.0054. The AKIE determined here is higher than both values, thus other factors than zero point energy differences contribute to the observed isotope effect. Different mass moments of inertia of the isotopologues and symmetry differences should be further investigated. Here, a computational study would be useful in future research.

Table 6.3 Streitwieser limits for the cleavage of glyphosate to yield sarcosine or AMPA at 20°C

Bond	Vibrational frequency $\tilde{\nu}$	KIE	Species	Reference
P-C_1	936 cm^{-1}	1.0065	Free glyphosate in solution	24
N-C*	1041 cm^{-1}	1.0054	Glyphosate adsorbed to goethite	21

*no information on the position of the C-atom was given

6.3.4 Environmental importance

The oxidation of glyphosate by MnO_2 is associated with a moderately low isotope effect. The observed fractionation is a mixture of two cleavage reactions. The analysis of reaction products has shown that either sarcosine or the unknown product, which might be glyoxylate, are further degraded or adsorbed onto MnO_2. In order to further investigate this reaction, the oxidation of glyphosate by MnO_2 needs be conducted under anoxic conditions as probably only AMPA will be formed.

Since AMPA is probably not further degraded, its carbon isotope ratio can reflect the carbon isotope ratio of glyphosate at the P-C position. Hence, glyphosate could be identified as the chemical source of AMPA in environmental samples by a comparison of its $\delta^{13}C$ value with the $\delta^{13}C$ value the P-C position of the remaining glyphosate, assuming that other processes such as microbial conversion do not have an influence on $\delta^{13}C$ values of AMPA. Therefore, a method for position-specific isotope ratios of glyphosate needs to be developed.

The rate-limiting step of this reaction is probably not complexation of glyphosate on MnO_2 but electron transfer or bond cleavage, since a change of MnO_2 concentration did not change the carbon enrichment factor. The observed change in rate constant with MnO_2 concentration is rather an effect of available active sites or Mn(III) since it is a second order reaction.

References

1. Post, J. E., Manganese oxide minerals: crystal structures and economic and environmental significance. *Proceedings of the National Academy of Sciences of the United States of America* **1999,** *96* (7), 3447-54.

2. McKenzie, R. M., The Synthesis of Birnessite, Cryptomelane, and some other Oxides and Hydroxides of Manganese. *Mineralogical Magazine* **1971,** *38* (296), 493-502.

3. Stone, A. T., Reductive Dissolution of Manganese(III/IV) Oxides by Substituted Phenols. *Environmental Science & Technology* **1987,** *21* (10), 979-988.

4. Zhang, H. C.; Huang, C. H., Oxidative transformation of triclosan and chlorophene by manganese oxides. *Environmental Science & Technology* **2003,** *37* (11), 2421-2430.

5. Gao, J.; Hedman, C.; Liu, C.; Guo, T.; Pedersen, J. A., Transformation of Sulfamethazine by Manganese Oxide in Aqueous Solution. *Environmental Science & Technology* **2012,** *46* (5), 2642-2651.

6. Skarpeli-Liati, M.; Jiskra, M.; Turgeon, A.; Garr, A. N.; Arnold, W. A.; Cramer, C. J.; Schwarzenbach, R. P.; Hofstetter, T. B., Using Nitrogen Isotope Fractionation to Assess the Oxidation of Substituted Anilines by Manganese Oxide. *Environmental Science & Technology* **2011,** *45* (13), 5596-5604.

7. Skarpeli-Liati, M.; Pati, S. G.; Bolotin, J.; Eustis, S. N.; Hofstetter, T. B., Carbon, Hydrogen, and Nitrogen Isotope Fractionation Associated with Oxidative Transformation of Substituted Aromatic N-Alkyl Amines. *Environmental Science & Technology* **2012,** *46* (13), 7189-7198.

8. He, Y.; Xu, J.; Zhang, Y.; Guo, C.; Li, L.; Wang, Y., Oxidative transformation of carbamazepine by manganese oxides. *Environmental Science and Pollution Research* **2012,** *19* (9), 4206-4213.

9. Barrett, K. A.; McBride, M. B., Oxidative degradation of glyphosate and aminomethylphosphonate by manganese oxide. *Environmental Science & Technology* **2005,** *39* (23), 9223-9228.

10. Ndjeri, M.; Pensel, A.; Peulon, S.; Haldys, V.; Desmazières, B.; Chaussé, A., Degradation of glyphosate and AMPA (amino methylphosphonic acid) solutions by thin films of birnessite electrodeposited: A new design of material for remediation processes? *Colloids and Surfaces A: Physicochemical and Engineering Aspects* **2013**.

11. Singh, B. K.; Walker, A., Microbial degradation of organophosphorus compounds. *Fems Microbiology Reviews* **2006,** *30* (3), 428-471.

12. Nowack, B., Environmental chemistry of phosphonates. *Water Research* **2003,** *37* (11), 2533-2546.

13. Elsner, M., Stable isotope fractionation to investigate natural transformation mechanisms of organic contaminants: principles, prospects and limitations. *Journal of Environmental Monitoring* **2010,** *12* (11), 2005-2031.

14. Kujawinski, D. M.; Wolbert, J. B.; Zhang, L.; Jochmann, M. A.; Widory, D.; Baran, N.; Schmidt, T. C., Carbon isotope ratio measurements of glyphosate and AMPA by liquid chromatography coupled to isotope ratio mass spectrometry. *Analytical and bioanalytical chemistry* **2013,** *405* (9), 2869-78.

15. Aisha, U.; Qamruzzaman; Rafiquee, M. Z. A., Kinetics of Reduction of Colloidal MnO2 by Glyphosate in Aqueous and Micellar Media. *International Journal of Inorganic Chemistry* **2011,** *2011* (Article ID 243519), 6.

16. Nowack, B.; Stone, A. T., Manganese-catalyzed degradation of phosphonic acids. *Environmental Chemistry Letters* **2003,** *1* (1), 24-31.

17. Skarpeli-Liati, M.; Jiskra, M.; Turgeon, A.; Garr, A. N.; Arnold, W. A.; Cramer, C. J.; Schwarzenbach, R. P.; Hofstetter, T. B., Using nitrogen isotope fractionation to assess the oxidation of substituted anilines by manganese oxide. *Environmental Science & Technology* **2011,** *45* (13), 5596-604.

18. Schwarzenbach, R. P.; Gschwend, P. M.; Imboden, D. M., *Environmental Organic Chemistry*. 2 ed.; Wiley-Interscience: 2003.

19. Wang, D. J.; Shin, J. Y.; Cheney, M. A.; Sposito, G.; Spiro, T. G., Manganese dioxide as a catalyst for oxygen-independent atrazine dealkylation. *Environmental Science & Technology* **1999,** *33* (18), 3160-3165.

20. Nowack, B.; Stone, A. T., Degradation of nitrilotris(methylenephosphonic acid) and related (amino)phosphonate chelating agents in the presence of manganese and molecular oxygen. *Environmental Science & Technology* **2000,** *34* (22), 4759-4765.

21. Tribe, L.; Kwon, K. D.; Trout, C. C.; Kubicki, J. D., Molecular orbital theory study on surface complex structures of glyphosate on goethite: Calculation of vibrational frequencies. *Environmental Science & Technology* **2006,** *40* (12), 3836-3841.

22. Ramstedt, M.; Norgren, C.; Shchukarev, A.; Sjoberg, S.; Persson, P., Co-adsorption of cadmium(II) and glyphosate at the water-manganite (gamma-MnOOH) interface. *J. Colloid Interface Sci.* **2005,** *285* (2), 493-501.

23. Skarpeli-Liati, M.; Pati, S. G.; Bolotin, J.; Eustis, S. N.; Hofstetter, T. B., Carbon, hydrogen, and nitrogen isotope fractionation associated with oxidative transformation of substituted aromatic N-alkyl amines. *Environmental Science & Technology* **2012,** *46* (13), 7189-98.

24. Sheals, J.; Persson, P.; Hedman, B., IR and EXAFS spectroscopic studies of glyphosate protonation and copper(II) complexes of glyphosate in aqueous solution. *Inorganic chemistry* **2001,** *40* (17), 4302-9.

25. Leslie, C. T., *Interpretation of the infrared spectra of organophosphorus compounds*. Heyden: London 1974.

26. Cook, P. F., *Enzyme mechanism from isotope effects*. Boca Raton [u.a.] : CRC Press: Boca Raton, 1991.

7 Preliminary Work on the Determination of Position-specific Carbon Isotope Ratios of Glyphosate by NMR spectroscopy and a Manganese-catalyzed Enzyme Reaction followed by LC-IRMS

Abstract

The analysis of overall isotope ratios of a molecule can be a very powerful tool in the identification of chemical reaction pathways or identification of the botanical origin and authenticity of a substance. Nevertheless, in some cases a position-specific isotope ratio determination is superior to conventional compound-specific isotope ratio analysis.

The aim of the following work was to develop a method to determine position-specific carbon isotope ratios of glyphosate at the carbon adjacent to phosphorous. In this context methods of nuclear magnetic resonance and an enzymatic cleavage reaction of glyphosate mediated by divalent manganese prior to LC-IRMS measurements were checked for their suitability and accuracy. It was shown that the ^{13}C satellite lines of P and H cannot be used in this purpose mainly due to non-linear response of the detector. The enzymatic reaction chosen in order to obtain a one-carbon fragment of glyphosate did not yield the expected result. Further experiments on reaction conditions are necessary.

7.1 Introduction

Although chemical reactions associated with a measureable isotope effect generally include the cleavage of a single bond, they are usually traced by a determination of isotope ratios of the whole molecule. In the case of bigger molecules, the change in isotope ratio during a reaction can be masked due to “dilution” by other non-reactive atoms. Thus, KIE need to be corrected for the amount of the element atoms of interest (apparent kinetic isotope effect AKIE).

Isotope ratios at specific positions can also help in authenticity control of various chemical products. Since isotope ratios can be different from one position to another, additional information can be obtained to clearly identify an original product.[1-2]

Although nuclear magnetic resonance spectroscopy (NMR) can determine isotope ratios at each position of the molecule, it has some drawbacks which limit the application for stable isotope analysis. In the case of carbon, a high signal to noise ratio of about at least 1000:1 needs to be obtained.[3] This means long scan times and very high concentrations of the target compound are required if the isotope has a low natural abundance. For some analytes the solubility in a suitable solvent might be too low or viscosity increases leading to line

broadening. The lines of all carbon positions need to be clearly resolved from adjacent matrix lines.

The other way to determine the position-specific $\delta^{13}C$ value is to quantitatively cleave glyphosate and analyze the fragments. As long as each bond cleavage is associated with only one mechanism, i.e. no disproportionation, and the reaction is quantitative, $\delta^{13}C$ values of the fragments correspond to position-specific isotope ratios.[4] Hence, the reaction does not even need to be free of an isotope effect.

An enzymatic cleavage of glyphosate has been proposed by Pizzul et al.[5] They used a manganese peroxidase (MnP) that catalyzes the oxidation of Mn(II) to Mn(III). The formed Mn(III) is reduced by organic compounds, in this case glyphosate, to Mn(II). This enzyme is extracted from white rot fungi (*Nematoloma frowardii*) that use it to non-selectively decompose lignin.[6] This enzyme has already been used to degrade organic compounds like adamsite.[7-8] Pizzul et al.[5] found that the only product resulting from this cleavage reaction of glyphosate is AMPA. At certain conditions this reaction is quantitative and thus can be used to determine the $\delta^{13}C$ value at this position.

The aim of the following experiments was to evaluate the applicability of (i) an enzymatic reaction to form a simple one-carbon molecule which can be analyzed by compound-specific isotope ratio analysis and (ii) the use of NMR to determine the isotope ratio of the carbon atom adjacent to phosphorous. Since the carbon atom of interest is bound to phosphorous and hydrogen, the carbon satellite lines of these elements were chosen to calculate isotope ratios.[9] The carbon satellite lines can be observed easily during NMR experiments. Additionally, it was checked if isotope ratio analysis of glyphosate can be done by ^{13}C-NMR.

A suitable method to determine the carbon isotope ratio of glyphosate at the P-C position might be useful to identify an original product. Since AMPA is also one the metabolites of glyphosate in nature but can be a result of the degradation of other phosphonates as well, such a method might even help to allocate its source in the environment.

7.2 Experimental

7.2.1 Chemicals and Reagents

Glyphosate, AMPA and D_2O (99.99 atom %) were bought from Sigma-Aldrich (Steinheim, Germany). Sodium peroxodisulfate ($Na_2S_2O_8$), $MnSO_4$, sodium citrate, phosphoric acid (H_3PO_4) and monosodium phosphate (NaH_2PO_4) for eluent and reagent solutions for LC-IRMS were purchased from Fluka (Steinheim, Germany). Manganese peroxidase (Manganese-Peroxidase EC 1.11.1.13, from *Nematoloma frowardii*) was supplied by Jena Bioscience (Jena, Germany).

7.2.2 Enzyme reaction

Enzyme reactions were performed similar to Pizzul et al.[5] The reaction batch contained 10 mM $MnSO_4$, 250 mM citrate buffer adjusted to pH 4.5 with NaOH, 0.05 mM H_2O_2 and 1 U/mL manganese peroxidase. The reaction started with the addition of glyphosate stock solution to a final concentration of 300 mg/L. The solution was kept in a water bath at 35°C. At each sampling interval, 200 µL were withdrawn and heated in a water bath at 90°C for 5 min to deactivate the enzyme. A mixture without enzyme served as control and standards of glyphosate (250 mgL^{-1}) and AMPA (350 mgL^{-1}) were measured along with the samples in order to verify peak identity and LC-IRMS performance.

The solution was injected onto the Hypercarb column with sodium phosphate, 3 mM at pH 6, as eluent (see **Chapter 6.2.2)**. The HPLC system consisted of a HTC PAL autosampler (Axel Semrau, Sprockhövel, Germany), a Rheos Allegro binary pump (Flux Instruments, Buchs, Switzerland), a HT-HPLC 200 column oven (SIM Scientific Instruments Manufacturer GmbH, Oberhausen, Germany). The separation was performed at 30°C. After 20 min the column was heated to 70 °C for 30 min in order to elute citrate from the buffer and possibly also the enzyme. The LC-IRMS interface conditions can be taken from **Chapter 6.2.2**.

7.2.3 NMR

NMR experiments were performed with a Bruker Avance DRX instrument with Topspin 2.5 software which was used to perform relaxation time determination, Fourier transformation, background correction and peak integration. Authentic standards of glyphosate and AMPA were dissolved in D_2O in 8" thin wall NMR tube made of borosilicate glass (P/N 528-PP-8, Wilmad-LabGlass, Rototec-Spintec GmbH, Griesheim, Germany) at concentrations of 16.42 and 9.24 % (w), respectively. Scans were performed in intervals of ten times the relaxation time as recommended by Caytan et al.[10] ^{13}C-NMR spectra were recorded with a standard decoupling of H.

Table 7.1 Basic parameters for isotope ratio determinations by NMR

	Frequency /MHz	Acquisition time /s	Scan number	Free induction decay size
^{31}P	200	4.22	640	65536
^{1}H	500	5.5	640	65536
^{13}C	125	2.2	640	131072

The calculation scheme of carbon isotope ratios from the triplet signal in ^{31}P and ^{1}H-NMR can be taken from.

$$R_i = \frac{PA_{sat}}{PA_{cent}} = \frac{^{13}C}{^{12}C}$$

PA_{sat} is the summarized peak area of the ^{13}C satellite lines at the specific position and PA_{cent} means the same for the center line representing the ^{12}C atom.

In case of ^{13}C NMR, isotope ratios were calculated from the following equation:

$$R_i = R_{bulk} \times \frac{PA_i}{PA_{total}}$$

Here, R_{bulk} is the $^{13}C/^{12}C$ ratio of the whole molecule determined by IRMS and PA_i and PA_{total} the peak areas of carbon at the specific position i and the total peak area of all carbon atoms in the molecule, respectively. The assignment of the signal lines to the individual carbon atoms is given **Table 7.2**.

Table 7.2 Signal assignment for individual carbon atom positions

Chemical shift /ppm	^{31}P-NMR	^{13}C-NMR	^{1}H-NMR
C_1 ($P\text{-}CH_2$)	8.5 – 9.5 ppm (sat+center line)	45ppm (d)	n.a.
C_2 (CH_2)	-	52ppm (d)	n.a.
C_3 (COOH)	-	172 (s)	n.a.
AMPA	11-12 ppm (sat+center line)	-	

7.3 Results

7.3.1 NMR

The evaluation of peak areas of carbon satellite lines of phosphorous by ^{31}P-NMR gave calculation of δ^{13}C values of -17 and -142 ‰ (see **Table 7.3**). The last value is beyond the natural variation of carbon isotopes, thus it can be concluded that it is not accurate. AMPA was measured along as a standard for accuracy of the method as it only has one carbon atom and its δ ^{13}C value has been determined by EA-IRMS in **Chapter 5**. Here, the calculated δ^{13}C value of -192 ‰ was not accurate as well. ^{13}C-NMR and ^{1}H-NMR have also shown too low δ^{13}C values.

Although many steps during acquisition and processing of the NMR signal such as length of the frequency induced decay signal and Fourier-transformation parameters influence the peak area in the spectrum, it is mainly the non-linearity of the detector which causes the wrong δ^{13}C values obtained here.[9] The determination of δ^{13}C values from satellite lines has been shown for isotope ratios of lead.[11] But lead isotopes are more abundant in nature than carbon, thus it is easier to compare peak areas of satellites with the center line.

Furthermore, peaks in NMR have the shape of a Lorentzian function (see **Figure 7.1**). Thus, it is difficult to subtract the background and deconvolute the satellite lines from the center line. Additionally, due to the phase correction which is performed after the Fourier transformation, the satellite peaks and the centerline are not symmetrical which can also lead to biased peak areas.[12]

Table 7.3 Results of δ^{13}C determination by NMR

	Glyphosate $\delta^{13}C_{P\text{-}C}$ ‰	AMPA δ^{13}C ‰
^{13}C determined by EA-IRMS (see **Chapter 5**)	Not applicable	-40.3
^{13}C-NMR	-680 ±4	Not applicable*
^{31}P-NMR: ^{13}C-Satellites	-17 and -142	-192 ±14
^{1}H-NMR: ^{13}C-Satellites	Too many interferences	-137 ±30

*^{13}C-NMR is not applicable to AMPA since it only has one carbon atom

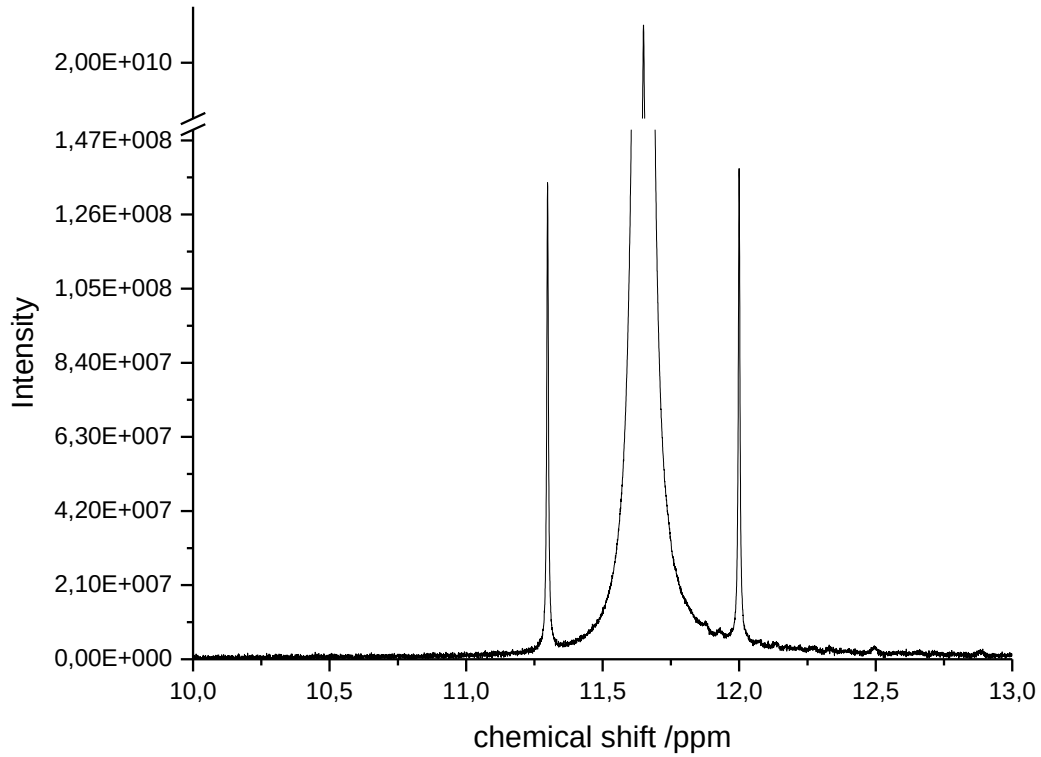

Figure 7.1 Partial ^{31}P NMR spectrum of an AMPA solution. Adjacent to the center line, the two small carbon satellite lines of ^{13}C can be seen.

7.3.2 Manganese peroxidase

The chromatographic method was suitable to separate AMPA and glyphosate from matrix components. Sodium acetate buffer used in the work of Pizzul et al.[5] was replaced by sodium citrate since it was not possible to resolve the analytes from acetate. Citrate has a quite strong retention on the Hypercarb column [13], thus, the temperature of the column was increased to 70°C to purge the column after each sample run. Low baselines together with repeatable retention times confirmed the successful removal of citrate from the column.

Nevertheless, the enzymatic cleavage of glyphosate was not reproducible, although the reactivity of the enzyme was not affected. As can be seen in **Figure 7.2,** the peak area of glyphosate does not change even after almost two days of reaction. Citrate might form very strong complexes with Mn(II) or Mn(III) so that glyphosate cleavage is not taking place.

Basically, the replacement of acetate with citrate should not inhibit the oxidation reaction of glyphosate. In the natural catalytic cycle of MnP, carboxylic acids such as malate, lactate and tartrate stabilize the formed Mn(III) by chelation and also act as redox-mediators.[6]

The identity of the unknown peak at 550s should be investigated as its peak area increases with time. There is probably a more feasible reaction of a matrix component from the enzyme powder than glyphosate cleavage taking place. Although glyphosate peaks are not decreasing

with reaction time, AMPA is formed. Thus, it also has to be checked if there is no coelution with other substances and the target compounds.

Further experiments on reaction conditions such as variation of buffer type and Mn(II) or enzyme concentration might be useful as the concentrations used during this work have been increased relative to Pizzul et al.[5] since more glyphosate in the reaction mixture was needed due to the high detection limits of the LC-IRMS.

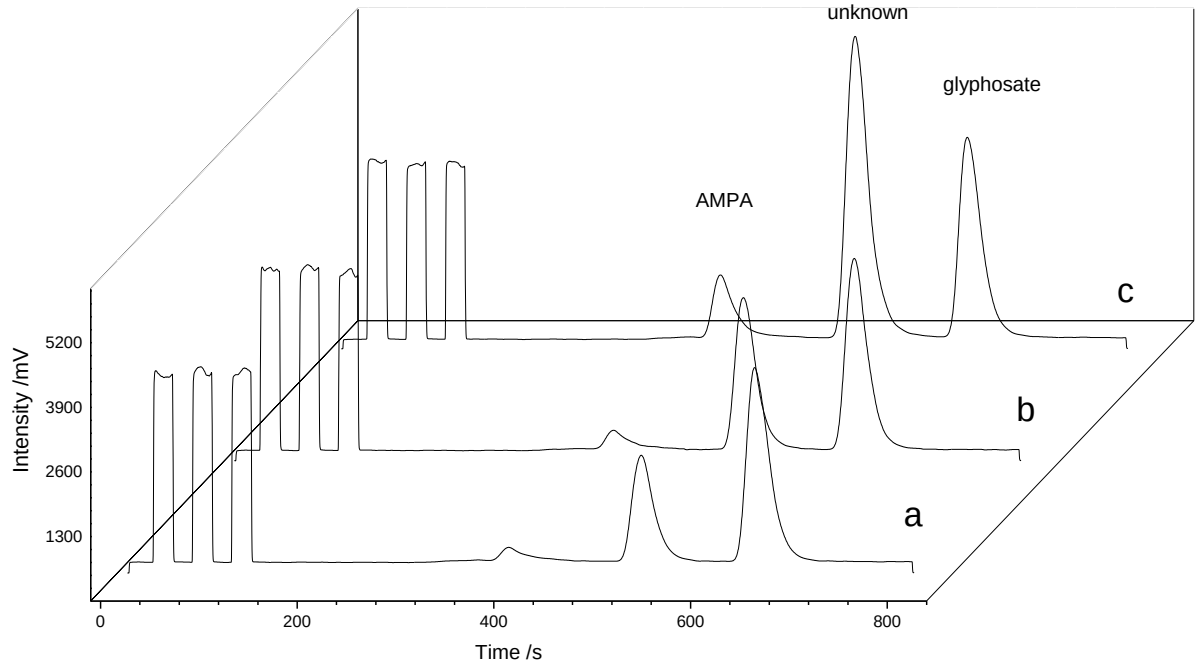

Figure 7.2 Chromatograms of the reaction mixture after 21 (a), 28 (b) and 46 h (c). Glyphosate peak areas of m/z 44 trace are 104 Vs, 102 Vs and 105 Vs after 21, 28 and 46 h, respectively.

7.4 Conclusion

Position-specific isotope ratios of glyphosate may be of interest for product identification as well as for degradation studies of this compound. In particular, the analysis of the carbon atom adjacent to phosphorous might help to identify an original agricultural product or distinguish the source of AMPA in the environment.

From the two methods investigated here, only the enzymatic cleavage might be of further use in order to determine carbon isotope ratios at the P-C position of glyphosate, since reaction conditions are easier to adjust than instrumental properties in NMR. Moreover, sample throughput is much lower in NMR than in LC-IRMS, which is an important factor in environmental research as well as in routine analysis.

References

1. Ogrinc, N.; Kosir, I. J.; Spangenberg, J. E.; Kidric, J., The application of NMR and MS methods for detection of adulteration of wine, fruit juices, and olive oil. A review. *Anal Bioanal Chem* **2003,** *376* (4), 424-30.

2. Thomas, F.; Randet, C.; Gilbert, A.; Silvestre, V.; Jamin, E.; Akoka, S.; Remaud, G.; Segebarth, N.; Guillou, C., Improved characterization of the botanical origin of sugar by carbon-13 SNIF-NMR applied to ethanol. *Journal of agricultural and food chemistry* **2010,** *58* (22), 11580-5.

3. Tenailleau, E.; Akoka, S., Adiabatic 1H decoupling scheme for very accurate intensity measurements in 13C NMR. *Journal of magnetic resonance* **2007,** *185* (1), 50-8.

4. Breider, F.; Hunkeler, D., Position-specific carbon isotope analysis of trichloroacetic acid by gas chromatography/isotope ratio mass spectrometry. *Rapid Communications in Mass Spectrometry* **2011,** *25* (24), 3659-3665.

5. Pizzul, L.; Castillo, M. d. P.; Stenstrom, J., Degradation of glyphosate and other pesticides by ligninolytic enzymes. *Biodegradation* **2009,** *20* (6), 751-759.

6. Hofrichter, M., Review: lignin conversion by manganese peroxidase (MnP). *Enzyme and Microbial Technology* **2002,** *30* (4), 454-466.

7. Haas, R.; Scheibner, K.; Hofrichter, M., Enzymatische Umsetzung von Arsenkampfstoffen durch das Pilzenzym Mangan-Peroxidase. *UWSF - Z Umweltchem Okotox* **2003,** *15* (4), 224-226.

8. Haas, R.; Tsivunchyk, O.; Steinbach, K.; von Low, E.; Scheibner, K.; Hofrichter, M., Conversion of adamsite (phenarsarzin chloride) by fungal manganese peroxidase. *Applied Microbiology and Biotechnology* **2004,** *63* (5), 564-566.

9. Fujiwara, S.; Arata, Y.; Ozawa, H.; Kunugi, M., NMR Satellites as a Probe for Chemical Investigations. *Pure Appl. Chem.* **1972,** *32* (No. 1-4), 117-122.

10. Caytan, E.; Remaud, G. S.; Tenailleau, E.; Akoka, S., Precise and accurate quantitative (13)C NMR with reduced experimental time. *Talanta* **2007,** *71* (3), 1016-21.

11. Fujiwara, S.; Ogimura, Y.; Nagashima, K., Determination of Lead-207 by Nuclear Magnetic Resonance. *Instrumentation Science & Technology* **1968,** *1* (1), 21-32.

12. Martin, G. J.; Akoka, S.; Martin, M. L., SNIF-NMR—Part 1: Principles. *Modern Magnetic Resonance* **2006**, 1651-1658.

13. Godin, J. P.; Hopfgartner, G.; Fay, L., Temperature-programmed high-performance liquid chromatography coupled to isotope ratio mass spectrometry. *Analytical Chemistry* **2008,** *80* (18), 7144-7152.

8 General Conclusions and Outlook

In the work presented here analytical methods for the isotopic analysis of sulfonamide drugs and trimethoprim as well as the herbicide glyphosate and its degradation product aminomethylphosphonic acid were developed and applied to selected degradation processes relevant in the environment and product characterization.

Stable isotope ratios of many compounds, which are of high interest for commercial product authenticity control or environmental research, cannot be determined due to a lack of liquid chromatographic methods feasible for LC-IRMS. In this regard, the main challenge is the exclusion of organic modifiers in the mobile phase that are used to elute compounds in HPLC using conventional detection techniques.

Here, we have shown that high temperature liquid chromatography is a valuable separation technique for moderately polar compounds like sulfonamides and trimethoprim to be analyzed by LC-IRMS. The analysis of pharmaceutical samples of sulfamethoxazole and trimethoprim has shown the potential applicability of HTLC-IRMS in product authenticity control. For the first time the carbon isotope enrichment factor of a degradation reaction, i.e. direct photolysis, of a sulfonamide has been reported. The low enrichment factor ε_C of 0.7 ‰ and the identified photolysis products point to a small secondary carbon isotope effect. In the future, it should be investigated how far the observed isotope effect is dependent on pH, irradiation wavelength and water matrix in order to assess if photolysis reactions of sulfonamide pharmaceuticals in surface waters can be traced by isotope ratios.

Photolysis represents an important research area in environmental organic chemistry, where many questions regarding the nature of observed isotope effects are not fully understood as well as reaction pathways not confirmed yet. LC-IRMS offers the possibility to record isotope ratios of photolysis products as well. This may help to answer the question why sometimes a normal, sometimes an inverse isotope effect occurs. An interesting topic can be the comparison of fractionation factors of five-ring with six-ring-membered sulfonamides, as the latter extrude SO_2 during UV irradiation. It can be worked out if the resulting SO_2 can be extracted and measured for its sulfur isotope ratio by EA-IRMS.

In this work, several chromatographic methods to determine carbon isotope ratios of glyphosate and AMPA have been developed. It was emphasized that in the context of LC-IRMS it can be helpful to resort to a complementary separation method depending on the matrix components. Although a cation exchange method was applicable to most commercial herbicide samples of glyphosate, it was not suitable for the measurement of glyphosate from MnO_2 degradation experiments. In that case a reversed phase chromatography on porous graphitic carbon yielded the best results.

The fractionation factors of glyphosate and AMPA for three separation modes, i.e. cation and anion exchange and reversed phase, calculated from chromatographic data suggest that processes like ion exchange or van-der-Waals interactions with soil will not alter their isotopic carbon signature. Thus, if degradation of glyphosate will be studied from real world samples these processes can be neglected evaluating isotopic data at natural abundance.

A first step towards degradation experiments has been performed in the second last chapter of this work. The glyphosate degradation by MnO_2 has revealed a moderate fractionation factor. The AKIE is in this case 1.011 and reflects a mixture of C-P and N-C bond cleavage. In order to separately investigate these reactions, different experimental conditions should be tested. It is known that only C-N bond cleavage takes place at anoxic conditions. Furthermore, the effect of metal cations like Cu^{2+} or Fe^{3+} on the degradation should be elaborated since glyphosate is a good complexing agent. In that way, the formation of sarcosine possibly can be suppressed and only the fractionation of the N-C bond cleavage measured.

It has also been shown that the oxidation of glyphosate does not influence $\delta^{13}C$ values of AMPA. Hence, it may be possible to trace the origin of AMPA in natural samples assuming that biotic transformation will not change $\delta^{13}C$ values of AMPA. For that purpose position-specific isotope ratios of glyphosate need to be determined. Thus, the aim of the last chapter of this work was to investigate if a $\delta^{13}C$ value at the P-C position can be determined by satellite lines from NMR measurements or from an enzymatic cleavage followed by LC-IRMS measurement of the fragments. Unfortunately, it was not possible to determine precise and accurate $\delta^{13}C$ values of glyphosate at this position. Future experiments on this topic should be performed on variations of the reaction conditions of the enzymatic cleavage.

Besides these, more degradation experiments for glyphosate and AMPA such as biotic degradation by soil microorganisms should be investigated.

Although this work brought more insights to the chemical and physical behavior of the studied compounds, each chapter in this work also emphasized the need for complementary instruments to couple LC to IRMS in order to measure other elements than carbon as well. Many parts of this work would have benefited a lot from the possibility to measure compound-specific nitrogen isotope ratios.

The photolysis of sulfamethoxazole studied in this work leads to a formation of products originating from an S-N bond cleavage. It may be possible to differentiate S-N and N-C bond cleavage from nitrogen isotope ratios of the parent substance.

The coupling of LC with a method to measure compound-specific nitrogen isotope ratios would be very valuable for studying glyphosate degradation. The formation of either sarcosine or AMPA could be traced by nitrogen isotope ratios of glyphosate. Most probably this fractionation is a much more sensitive indicator of glyphosate degradation than carbon, since a carbon-nitrogen bond is broken to yield AMPA and there is only one nitrogen atom present in glyphosate. But here, the role of pH needs to be carefully considered due to a potential nitrogen isotope effect associated with pH speciation as it is the case for aniline.[1]

The measurements of pharmaceuticals and glyphosate samples have revealed that products of different manufacturers cannot be distinguished solely by carbon isotope ratios of a single compound. Additional information on nitrogen isotope ratios or even position-specific isotope ratios might improve the applicability of the methods for product authenticity. Especially, the authenticity of herbicide formulations containing glyphosate could be of interest for companies since it is one of the most frequently used herbicides. Given that new interface systems are compatible, the chromatographic methods developed in this work could also be used for nitrogen isotope analysis because the eluents did not contain nitrogen additives.

Hence, it is recommended to improve the sensitivity of existing complementary interface systems like the chemical reaction interface. This system can be used in combination with reversed phase chromatography using organic modifiers and nitrogen isotope ratios can be measured as well. Although these systems were prone to fractionation and the components were difficult to service and therefore this system never got commercialized, the same holds true for the commercial wet oxidation interfaces used in this work.

References

1. Skarpeli-Liati, M.; Turgeon, A.; Garr, A. N.; Arnold, W. A.; Cramer, C. J.; Hofstetter, T. B., pH-dependent equilibrium isotope fractionation associated with the compound specific nitrogen and carbon isotope analysis of substituted anilines by SPME-GC/IRMS. *Anal Chem* **2011,** *83* (5), 1641-8.

9 Appendix

9.1 Calibration lines of SMX photolysis products

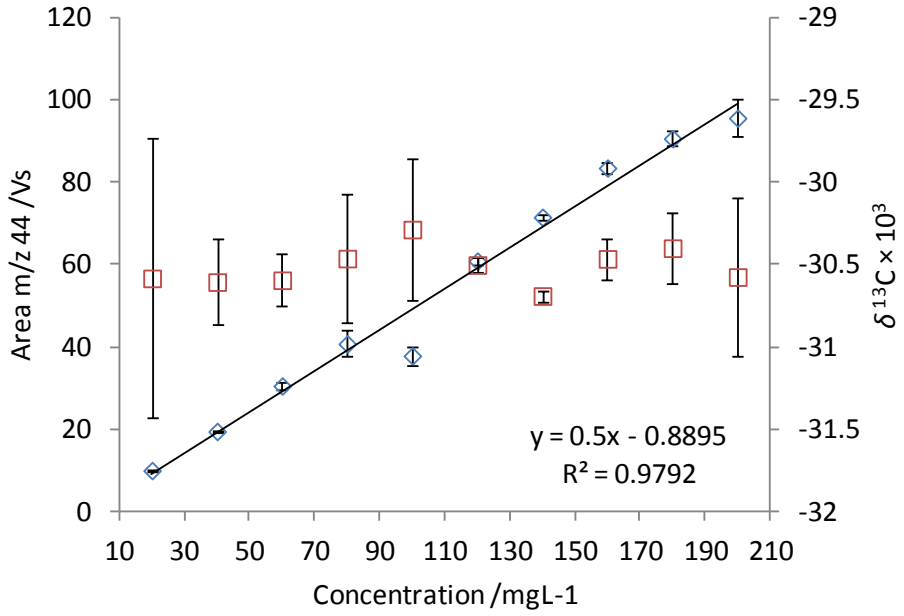

Figure 9.1 Calibration line of sulfamethoxazole. The blue squares correspond to peak area, while red boxes symbolize $\delta^{13}C$ values. The lowest amount to determine reliable $\delta^{13}C$ was 40 mg L^{-1} or peak areas of about 20 Vs.

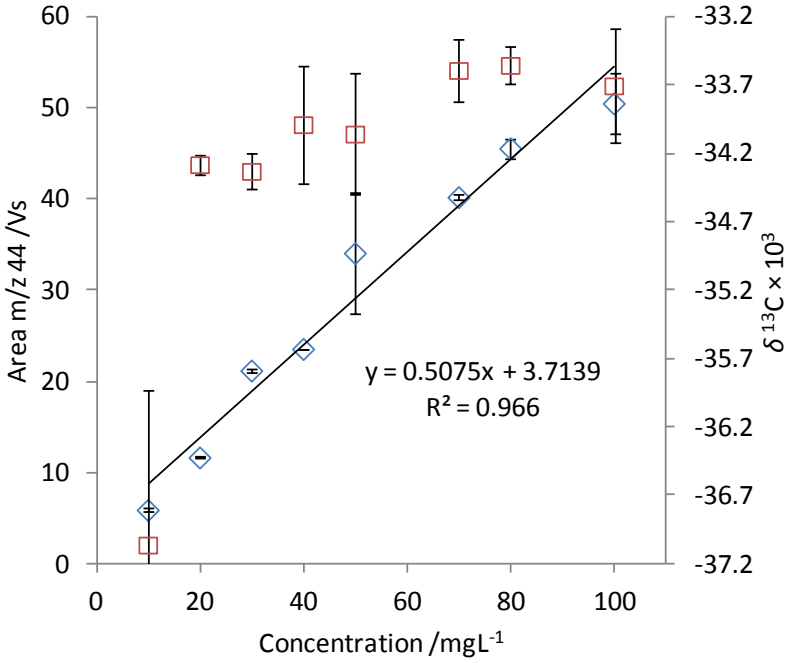

Figure 9.2 Calibration line of 3-amino-5-methylisoxazole. The blue squares correspond to peak area, while red boxes symbolize $\delta^{13}C$ values. The detection limit was 20 mg L^{-1} or about 10 Vs, respectively.

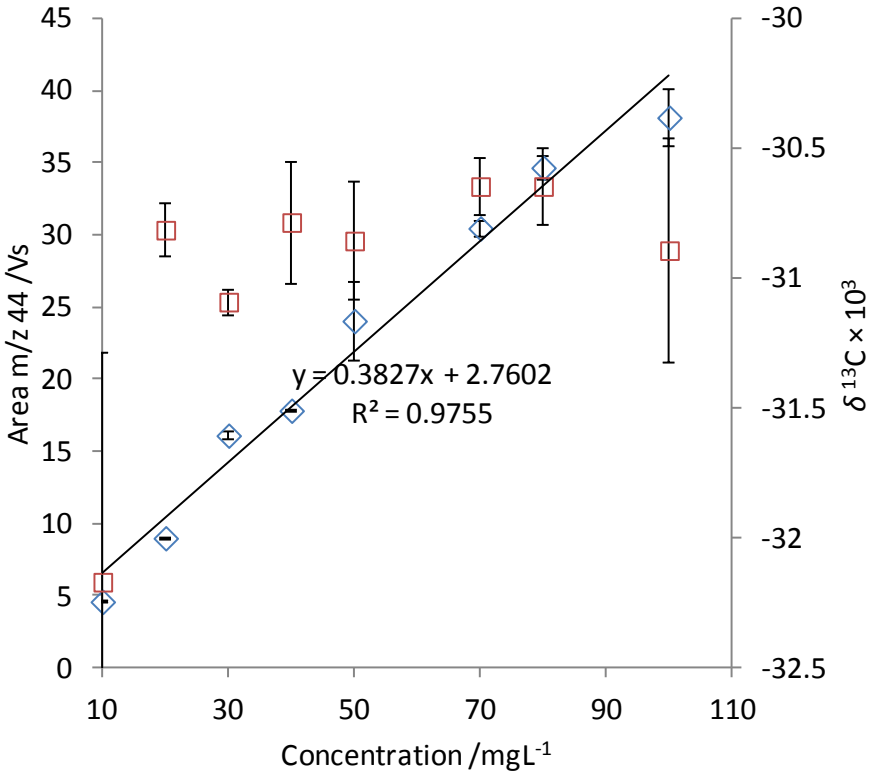

Figure 9.3 Calibration of sulfanilamide. The blue squares correspond to peak area, while red boxes symbolize δ ^{13}C values. The detection limit was 20 mg L^{-1} or about 10 Vs, respectively.

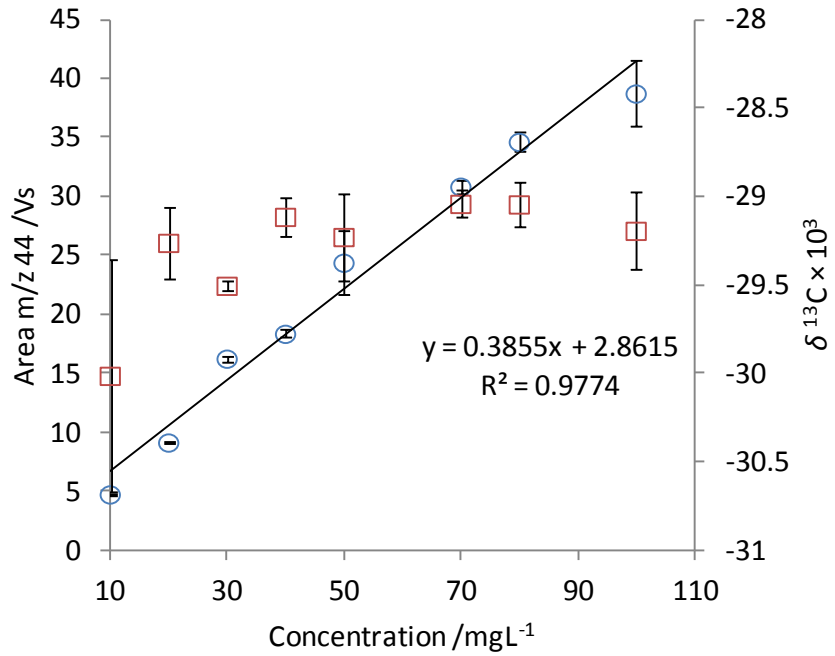

Figure 9.4 Calibration of sulfanilic acid. The blue circles correspond to peak area, while red boxes symbolize δ ^{13}C values. The detection limit was 20 mg L^{-1} or about 10 Vs, respectively.

9.2 List of abbreviations

α	fractionation factor
AKIE	apparent kinetic isotope effect
AM	3-amino-5-methylisoxazole
AMPA	aminomethylphosphonic acid
BSIA	bulk stable isotope analysis
CRDS	cavity ring down spectroscopy
CRI	chemical reaction interface
CSIA	compound-specific stable isotope analysis
EA	elemental analyzer
ε	enrichment factor
EPA	US Environmental Protection Agency
FIA	flow injection analysis
HPLC	high performance liquid chromatography
HTLC	high temperature liquid chromatography
IAEA	International Atomic Energy Agency
IRMM	Institute for Reference Measurements and Materials
IRMS	isotope ratio mass spectrometry
KIE	kinetic isotope effect
LC	liquid chromatography
LPIA	limits of precise isotope analysis
MCPA	2-methyl-4-chlorophenoxyacetic acid
MDL	method detection limits
MMC	mixed-mode chromatography
MMI	mass moments of inertia
MnP	manganese peroxidase
NIST	National Institute of Standards
NMR	nuclear magnetic resonance spectroscopy
NTMP	nitrilotris(methylenephosphonic acid)
PDB	Pee Dee Belemnite
PGC	porous graphitic carbon
RP	reversed phase
RP-LC	reversed phase liquid chromatography
SA	sulfanilic acid

SAM	sulfanilamide
SIRA	stable isotope ratio analysis
SMX	sulfamethoxazole
SNIF-NMR	site-specific natural isotopic fractionation- nuclear magnetic resonance spectroscopy
TOC	total organic carbon
VPDB	Vienna Pee Dee Belemnite
ZPE	zero point energy

9.3 Publication list

1. L. Zhang, **D. M. Kujawinski**, E. Federherr, M.A. Jochmann, T. C. Schmidt. (2014). "Carbon Isotope Ratio Analysis of Steroids by High-Temperature Liquid Chromatography-Isotope Ratio Mass Spectrometry Liquid Chromatography-Isotope Ratio Mass Spectrometry" Analytical Chemistry 86: 2297−2302

2. **D. M**. **Kujawinski**, J.B. Wolbert, L. Zhang, M.A. Jochmann, D. Widory, N. Baran, T. C. Schmidt. (2013). "Carbon isotope ratio measurements of glyphosate and AMPA by liquid chromatography coupled to isotope ratio mass spectrometry" Analytical and Bioanalytical Chemistry 405: 2869-2878

3. **D. M**. **Kujawinski,** L. Zhang, M.A. Jochmann, T. C. Schmidt. (2012). "When Other Separation Techniques Fail: Compound-Specific Carbon Isotope Ratio Analysis of Sulfonamide Containing Pharmaceuticals by High-Temperature-Liquid Chromatography-Isotope Ratio Mass Spectrometry." Analytical Chemistry 84(18): 7656-7663.

4. L. Zhang, **D. M. Kujawinski**, E. Federherr, M.A. Jochmann, T. C. Schmidt. (2012). "Caffeine in Your Drink: Natural or Synthetic?" Analytical Chemistry 84(6): 2805-2810

5. L. Zhang, **D. M. Kujawinski**, M.A. Jochmann, T. C. Schmidt. (2011). "High-temperature reversed-phase liquid chromatography coupled to isotope ratio mass spectrometry." Rapid Communications in Mass Spectrometry 25(20): 2971–2981

6. **D. M. Kujawinski**, M. Stephan, M. A. Jochmann, K. Krajenke, J. Haas, T. C. Schmidt (2010) "Stable Carbon and Hydrogen Isotope Analysis of Methyl Tert-Butyl Ether and Tert-Amyl Methyl Ether by Purge and Trap-Gas Chromatography-Isotope Ratio Mass Spectrometry: Method Evaluation and Application"
Journal of Environmental Monitoring 12 (1), 347-354

7. T. Teutenberg, S. Wiese, M.A. Jochmann, **D.M. Kujawinski**, L. Zhang, T.C. Schmidt, B. Fischer, H. Bettermann:
Kopplungsverfahren zur Authentizitätskontrolle: Neuartige Kombination innovativer Detektionstechniken auf Basis der Isotopenmassenspektrometrie und Ramanspektroskopie
GIT Labor-Fachzeitschrift 2010, S. 182-185

Oral Presentation

1. **D.M. Kujawinski**:
„Carbon Stable Isotope Analysis of Sulfonamides and Trimethoprim by High Temperature – LC–IRMS"
Oxford University, LC-IRMS User's Meeting, 24.11.2010

Poster Presentations

1. **D.M. Kujawinski**, M. Stephan, M.A. Jochmann, T. C. Schmidt:
Stable Isotope Analysis of fuel oxygenates by Purge and Trap-Gas Chromatography-Isotope Ratio Mass Spectrometry: Method Evaluation and Application
Bremen, 18th International Mass Spectrometry Conference (IMSC 2009), 30.08–04.09.2009

2. **D.M. Kujawinski**, L. Zhang, M.A. Jochmann, T. C. Schmidt:
   Carbon Stable Isotope Analysis of Sulfonamides by online High Temperature - High Performance Liquid Chromatography - Isotope Ratio Mass Spectrometry
   Arnhem, BASIS Benelux IRMS Users Group Meeting 2010, 15–16.04.2010
3. **D.M. Kujawinski**, L. Zhang, M.A. Jochmann, T. C. Schmidt:
   Carbon Stable Isotope Analysis of Sulfonamides by online High Temperature - High Performance Liquid Chromatography - Isotope Ratio Mass Spectrometry
   Amsterdam, Fifth International Symposium on Isotopomers (ISI 2010), 21–25.06.2010
4. **D.M. Kujawinski**, L. Zhang, M.A. Jochmann, T. C. Schmidt:
   Compound-specific Carbon Isotope Ratio Determination of Sulfonamides by online High Temperature Liquid Chromatography Isotope Ratio Mass Spectrometry
   Zurich, ANAKON 2011, 23–25.03.2011
5. **D.M. Kujawinski**, D. Widory, L. Zhang, M.A. Jochmann, T. C. Schmidt:
   Determination of Compound-specific Carbon Isotope Compositions (δ 13C) of Glyphosate and Aminomethylphosphonic acid (AMPA) by Liquid Chromatography Coupled to Isotope Ratio Mass Spectrometry
   München, Analytica 2012, 17–20.04.2012
6. **D.M. Kujawinski**, J.B. Wolbert, D. Widory, L. Zhang, M.A. Jochmann, T. C. Schmidt:
   Determination of Compound-specific Carbon Isotope Compositions (δ 13C) of Glyphosate and Aminomethylphosphonic acid (AMPA) by Liquid Chromatography Coupled to Isotope Ratio Mass Spectrometry
   Leipzig, Jesium 2012, 02–07.09.2012
7. **D.M. Kujawinski**, J.B. Wolbert, L. Zhang, M.A. Jochmann, T. C. Schmidt:
   Position-specific Carbon Isotope Ratio Determination (δ ^{13}C) of Glyphosate by a Manganese Catalyzed Enzyme Reaction and subsequent LC-IRMS
   Essen, ANAKON 2013, 03–07.03.2013

9.4 Curriculum vitae

Der Lebenslauf ist in der Online-Version aus Gründen des Datenschutzes nicht enthalten.

9.5 Erklärung

Hiermit versichere ich, dass ich die vorliegende Arbeit mit dem Titel

„Liquid Chromatography coupled to Isotope Ratio Mass Spectrometry of Selected Polar Compounds"

selbst verfasst und keine außer den angegebenen Hilfsmitteln und Quellen benutzt habe, und dass die Arbeit in dieser oder ähnlicher Form noch bei keiner anderen Universität eingereicht wurde.

Essen, im Juli 2014

9.6 Acknowledgements

I cordially thank Prof. Torsten Schmidt for his supervision of this work and valuable comments on this manuscript and Prof. Oliver Schmitz for his efforts as second assessor of this work.

I also thank Dr. Maik Jochmann for his support and various discussions throughout the last years. Furthermore, I sincerely thank Manuel Stephan, Jens Laaks and especially Lijun Zhang for the good cooperation and mutual assistance in the lab. I thank Benjamin Wolbert, Joris Buiter and Eugen Federherr for their excellent input to this dissertation. I also thank the other members of the stable isotope lab, Kamil Michalski and Marcel Schulte, for their support and company. For this, I also thank the whole department of Instrumental Analytical Chemistry.

I thank Prof. Christian Meyer and Manfred Zähres for their effort in all NMR measurements and support. I also gratefully acknowledge the financial support of the AiF.

Last, I thank my family and friends for their endless encouragement.